Vehicle Dynamics Modeling for Electric Vehicles

Laura J Prange

A thesis

submitted in partial fulfillment of the

requirements for the degree of

Master of Science in Mechanical Engineering

University of Washington

2017

Committee:

Brian Fabien, Chair

Steve Shen

Joseph Garbini

Program Authorized to Offer Degree:

Mechanical Engineering

University of Washington

Abstract

Vehicle Dynamics Modeling for Electric Vehicles

Laura J Prange

Chair of the Supervisory Committee:
Professor Brian Fabien
Department of Mechanical Engineering

Electric vehicles have become more popular in the last few decades due to governmental regulations and environmental awareness. This increased demand has allowed manufacturers to explore new methods of controlling vehicle motion. One technique called torque vectoring allows independent electric motors to output different torques without the use of a mechanical differential. This process necessitates the use of a robust dynamic model of vehicle motion to better predict how a car will respond to changes in torque and to control the stability of the vehicle. This thesis presents equations of motion for two-wheel and four-wheel models of a vehicle and applies them to lane changes, turns, and vehicle roll. The models can be applied to a vehicle with torque vectoring capabilities to aid in the creation of a controls algorithm.

TABLE OF CONTENTS

LIST OF FIGURES

LIST OF TABLES

ACKNOWLEDGEMENTS

I would not have been able to complete my thesis without the help of Professor Fabien. He has given me critical feedback on difficult aspects of the dynamics models and patiently guided me along the way to finishing my work. His support, enthusiasm, and background in dynamics modeling have allowed me to achieve the level of understanding that I sought out in a master's degree.

Also, I would like to thank Professor Shen for the class on vibrations and dynamics in the fall of 2015. It gave me the fundamental background I needed in order to start my thesis work. Thank you both to Professor Shen and Professor Garbini for serving on the review committee.

The EcoCAR team at the University of Washington was helpful and encouraging throughout my experience as a master's student. No matter how much work team leads or students had to do in order to prepare for a competition, there was always someone to help answer my questions.

A special thanks to the sponsors of the EcoCAR program, especially General Motors, for answering questions about vehicle modeling.

Chapter 1. INTRODUCTION

Increasing interest in electric vehicles has encouraged manufacturers to experiment with new technologies and ideas. This section will cover the basics of a differential, briefly describe why electric vehicles gained popularity, and introduce the topic of torque vectoring to highlight the need for a vehicle dynamics model that can be used to increase the stability of the vehicle.

1.1 MECHANICAL DIFFERENTIALS

Mechanical differentials are used to give the inner and outer wheels of a vehicle different torque values. Different torque values are needed because the inner and outer wheels move at different speeds as a car turns around a corner. For example, the inner wheel travels in a circle with a smaller radius than the outer wheel when the car is making a turn. The mechanical differential consists of a series of gears and elements to allow for equal torque for straight paths and unequal torque for curved paths. However, mechanical differentials do not always distribute torque in an ideal manner. If the road conditions are icy or otherwise undesirable, torque distribution from the mechanical differential could cause the vehicle to behave erratically. With independent electric motors, torque vectoring becomes an important method to improve vehicle handling (Husain, 2003).

1.2 BRIEF HISTORY OF ELECTRIC VEHICLES

The average vehicle consumer may consider electric vehicles to be a recent invention. However, electric vehicles were around since the late 1800's. One interesting electric vehicle was produced by Krieger Company in 1897 which had a maximum speed of 15 miles per hour and a 50 mile per charge rate. Even though electric vehicles were available, they were not as popular because

electricity was difficult to access in rural areas. Electric vehicles became popular again when oil prices increased in the 1970's as the government began promoting the technology. The push to create electric vehicles continued into the 1990's as air quality standards began requiring vehicle manufacturers to sell zero-emission vehicles (Husain, 2003).

1.3 TORQUE VECTORING

There are various methods of controlling the torque values given to each wheel in the process of torque vectoring, but the method described here is purely an electrical one. Consider a vehicle with two electric motors which drive two wheels independently. In order to move in a straight-line path, there needs to be a controls algorithm to send signals between the motors and make the wheels move in harmony. This system has several advantages. Although the system may seem unstable at first, it has the capability to be more stable than a traditional vehicle with a mechanical differential. For example, road surface sensors can be added to the front of the test vehicle to allow the electric vehicle to sense a change in road condition and relay the information to a controls algorithm, which can give the rear wheels independent responses. This can cause the system to follow a more accurate path. An additional factor in favor of an electric torque vectoring system is that frictional clutches can be avoided, and less energy will be wasted as heat (Kato and Sawase, 2012).

Chapter 2. TWO-WHEEL MODEL OF A VEHICLE

Torque vectoring is an appropriate method to control vehicle stability in difficult handling situations if a robust dynamics model is used to predict how the car will react to different torque values. This section goes over the two-wheel model of a vehicle, also known as the bicycle model, to predict how a car would handle in a turn.

2.1 BASICS OF A TWO-WHEEL MODEL

The simplest way to model a vehicle is to assume that the two front tires behave roughly the same and condense the effect of the two tires into one modeled tire. The rear tires can be treated in a similar fashion. This gives a vehicle with one tire in the front and one in the rear. This model involves several assumptions. First, it does not look at the rolling aspects of a vehicle, which makes the model different from a true representation of a two-wheeled object such as a bicycle or motorcycle. Second, the model assumes that there is no effect to the motion of the vehicle due to vibration of the suspension. In reality, suspension is extremely important in determining how the car will behave and makes a big impact on rider comfort. The two-wheel model does not consider the effect of aerodynamic forces. The model assumes a constant forward velocity is maintained by the vehicle. Lastly, the model assumes tires behave linearly. Tire modeling is one of the most difficult elements to add to a vehicle model, because the interaction between the road surface and the tire involves many factors such as roughness, tire pressure, contact surface, tire type, and more.

A depiction of the simplification made in modeling a four-wheeled vehicle as a two-wheeled vehicle is shown in Fig 2.1.

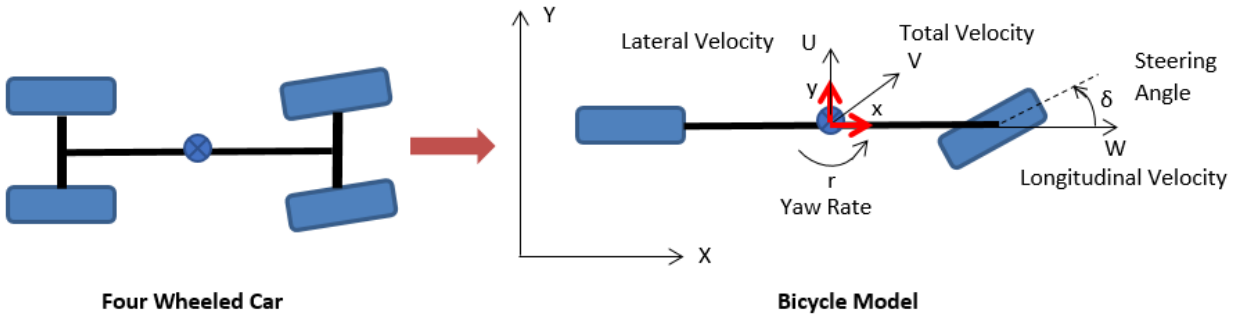

Figure 2.1 Bicycle Model

The two-wheel model is called a two-degree-of-freedom model because there are two state variables needed to describe its motion: the lateral velocity U and the yawing velocity r. A steering input of δ is applied to the front wheel. The small angle assumption is commonly used throughout the two-wheel model. The steering angle is assumed to be a small angle so that the longitudinal velocity of the car, called W, is approximately equal to the total velocity V of the car.

There are several variables used in the two-wheel model, and they are shown in Table 2.1.

Table 2.1 Two-Wheel Model Symbols

Term	Symbol
Lateral velocity	U
Longitudinal velocity along length of car	W
Total velocity of car	V
Vehicle slip angle, body slip angle	β
Front slip angle	α_f
Rear slip angle	α_r
Front tire cornering stiffness	$C_{\alpha f}$
Rear tire cornering stiffness	$C_{\alpha r}$
Yawing velocity	r
Steering angle	δ
Ackermann steering angle	δ_A
Length of wheelbase	L
Distance from front of car to center of gravity	a
Distance from rear of car to center of gravity	b
Radius of path curvature	R
Angle of Rotation	θ
Center of Gravity	CG

These variables will be explained in more detail as they appear in the derivation of the two-wheel model.

2.2 CIRCULAR MOTION

First consider an object moving in a circular path as shown in Fig. 2.2. The longitudinal velocity is $\vec{v}$ and the position vector from the center of the turn to the vehicle is $\vec{r}$.

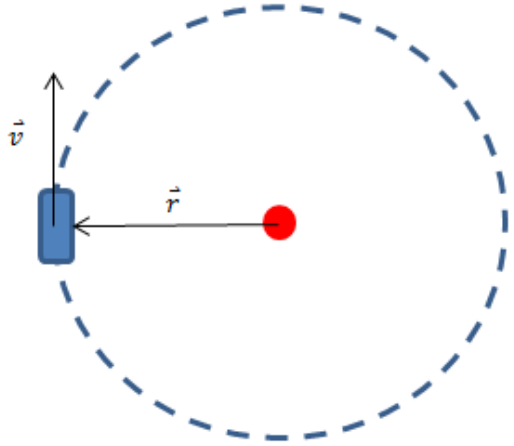

Figure 2.2 Vehicle in Circular Path

When a vehicle moves around a turn, it will have lateral acceleration towards the center of rotation due to the change in direction of the velocity vector according to Eqn. 2.1:

$$\vec{a} = \frac{d\vec{V}}{dt} = \frac{V^2}{R} \tag{2.1}$$

This equation can be derived by looking at instantaneous changes in velocity and location (Serway and Jewett, 2010). This equation shows that the circular path taken by the car is defined by the radius of the turn. However, the radius is not enough to define the location of the vehicle. To fully represent the motion of the vehicle, a coordinate system must be chosen. Two coordinate systems will be used in the two-wheel model. One will be fixed to the center of gravity of the car called the body-centered coordinate system. The other coordinate system will be the global coordinate system. These two coordinate systems can be related to one another by the angle of rotation,

denoted as θ. Refer to Fig. 2.3 to see the relationship. The distance from the center of the turn to the center of gravity of the vehicle is R, the global coordinates are X and Y, the body-centered coordinates are x and y, and the yaw rate of the vehicle is r.

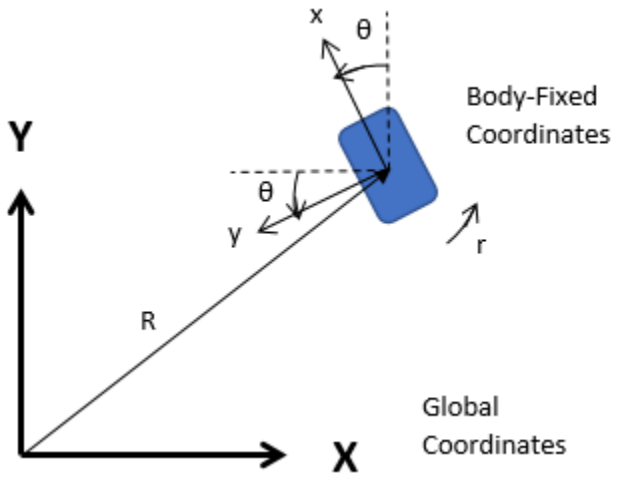

Figure 2.3 Global and Body-Centered Coordinate Systems

$$X = -U\cos\theta - V\sin\theta \tag{2.2}$$

$$Y = V\cos\theta - U\sin\theta \tag{2.3}$$

The relationship between the global and body-centered coordinate systems is shown in Eqns. 2.2 and 2.3. These can be found by noticing the small displacement θ shown in Fig. 2.3.

2.3 VEHICLE STEERING

Vehicle steering is a complex subject, although it may seem simple at first. The geometry of the turn varies depending on the speed and can be further complicated by adding in the effect of suspension components. However, there is useful information to be gained from a simple model. In assuming that the vehicle can be modeled as a two-wheeled vehicle, it is implied that the inner and outer radii of the tires are approximately the same as shown in Fig. 2.4. When a vehicle is in a turn, the center of gravity may not always be aligned by a perpendicular line to the center of the turn. In general, the tangent point is defined as the point on the vehicle where a perpendicular line

can be drawn from the car body to the center of the turn. The body slip angle (also known as the vehicle slip angle, attitude angle, or vehicle side slip angle) is defined by SAE standard J670 as the inverse tangent of the lateral velocity divided by the longitudinal velocity.

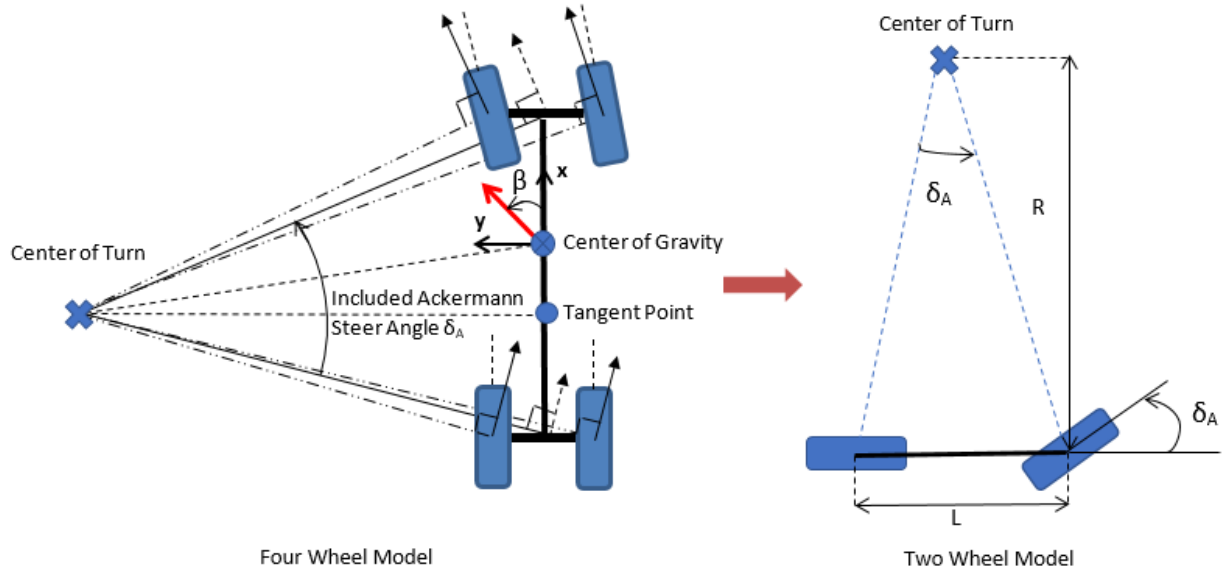

Figure 2.4 Four-Wheel Model to Two-Wheel Model

The tires deflect as they roll, and this deflection is characterized by the slip angle of the tire. The slip angle is defined as the angle from a line along the length of a tire to the tire velocity vector. Note that the body slip angle and tire slip angle have unusual names – they do not represent the loss of friction between the tire and the road surface. Instead, they represent where the velocity vector of the car or tire points.

Tire slip angles are important for representing centripetal forces acting on the vehicle. Tire slip angles are a measure of how much a tire deflects from a straight-line path. The tire can be thought of as a spring that deflects laterally and whose stiffness can be described by either the front or rear tire stiffness denoted as $C_{\alpha f}$ or $C_{\alpha r}$. Like any spring, when small forces are applied, the spring will deflect a small amount. For a passenger vehicle, this deflection becomes negligible as the centripetal acceleration decreases. Around 35 miles per hour and below, the centripetal

acceleration is small enough to cause negligible impact on tire deflection. At low speeds, the lateral forces are due to the turning of the front tire and not due to the tire deflection. This also means that the rear axle becomes the tangent point in a turn, because the tires in the rear are assumed to deflect very little and there is no steering angle applied. In this situation, the steering angle is called the Ackermann steering angle as shown in Fig. 2.5 (Milliken, 1995).

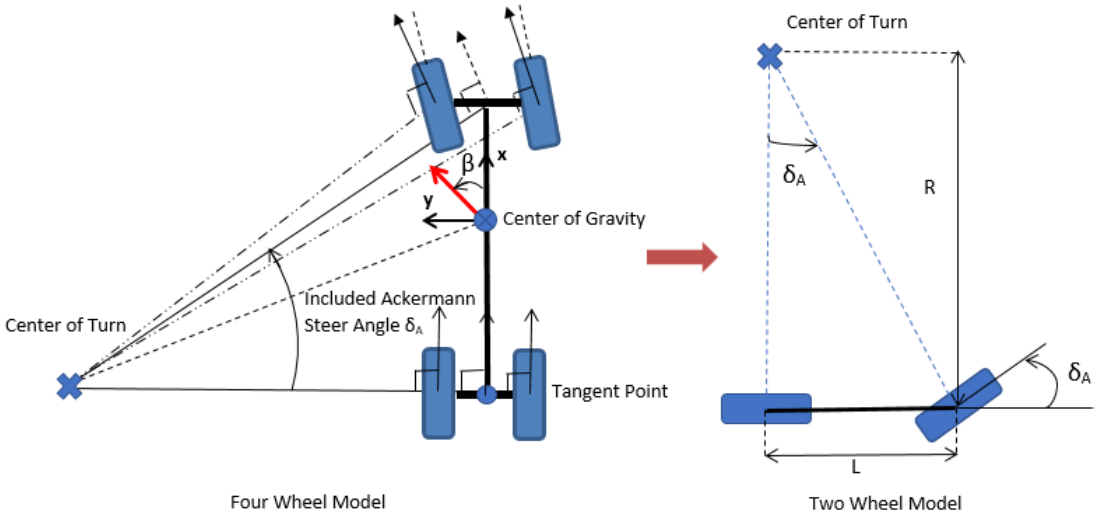

Figure 2.5 Low-Speed Ackermann Steering Angle

The Ackermann steering angle can be solved for using the geometry of the turn (see Fig. 2.6).

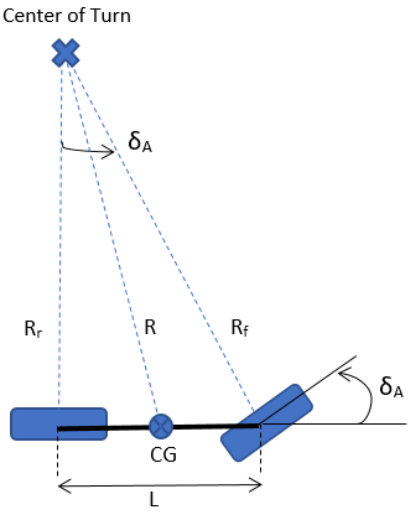

Figure 2.6 Ackermann Steering Angle

The equation for finding the Ackermann steering angle is given by Eqn. 2.4.

$$tan\ \delta_A = \frac{L}{R_r} \approx \frac{L}{R} \tag{2.4}$$

Using the small angle approximation, the resulting Eqn. 2.5 is derived.

$$\delta_A = L/R \tag{2.5}$$

Since the front wheel has a steering angle applied to it, the front wheel makes a different turn than the rear wheel. The front and rear wheels travel in circular paths of different radii. This difference is called off-tracking. Let the front wheel's turn radius be R_f and the rear turn radius be R_r. Equations 2.6 and 2.7 show how to calculate the turn radii using the small angle assumption.

$$\sin \delta_A = \frac{L}{R_f} \ \therefore\ R_f = \frac{L}{\sin \delta_A} \tag{2.6}$$

$$\tan \delta_A = \frac{L}{R_r} \ \therefore\ R_r = \frac{L}{\tan \delta_A} \tag{2.7}$$

The off-tracking of the vehicle is the difference between Eqns. 2.6 and 2.7. The result is shown in Eqn. 2.8.

$$R_{OF} = R_f - R_r = \frac{L}{\sin \delta_A} - \frac{L}{\tan \delta_A} \tag{2.8}$$

As an example, consider a car with a length of 2.77 meters in a tight four-meter radius turn. This gives an off-tracking of about one meter. This means that in a tight turn, even if the front wheels are able to navigate around the curb the rear tires may not because they travel in a circle that is one meter less than the front.

The body slip angles can be found in a similar manner. Consider Fig. 2.7, which shows the body slip angles of a car turning at low speed. Due to the low speed, the slip angles will be negligible and the rear axle will be in line with the turn. This means that the body slip angle will be zero in the back of the car. The body slip angle at the center of the car is given by Eqn. 2.9 and the body slip angle at the front of the car is given by Eqn. 2.10.

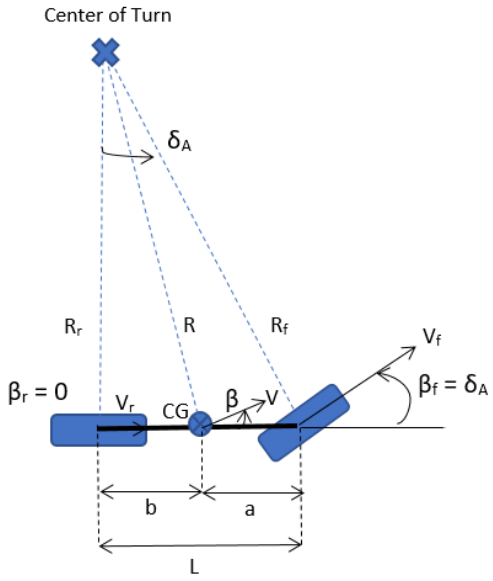

Figure 2.7 Body Slip Angles at Low Speed

$$\beta = \tan^{-1}\frac{b}{R_r} \approx \frac{b}{R} = \frac{b}{L}\delta_A \tag{2.9}$$

$$\beta_f = \sin^{-1}\frac{L}{a} \approx \frac{L}{R} = \delta_A \tag{2.10}$$

At higher velocities, the tires begin to deflect and generate lateral forces. The slip angles cause lateral forces on the tires, which in turn makes the tangent point move away from the rear axle (see Fig. 2.8). The geometry of the turn can be used to relate the steering angle to the Ackermann steering angle and the body slip angles of the vehicle (see Fig. 2.9). Notice that there is an added angle γ in the equation for the Ackermann steering angle because the center of gravity is not the tangent point. There are special cases when the center of gravity will be the tangent point. For a vehicle moving at a speed of about ten meters per second in a thirty-meter turn, the center of gravity will more closely act as the tangent point (Dixon, 2009). When the tangent point becomes the center of gravity, equations for the Ackermann steering angle become easier to determine. This simplified view is shown in Fig. 2.10. Although the tangent point will move along the length of the car during various maneuvers and at different points in time, generally speaking the tangent

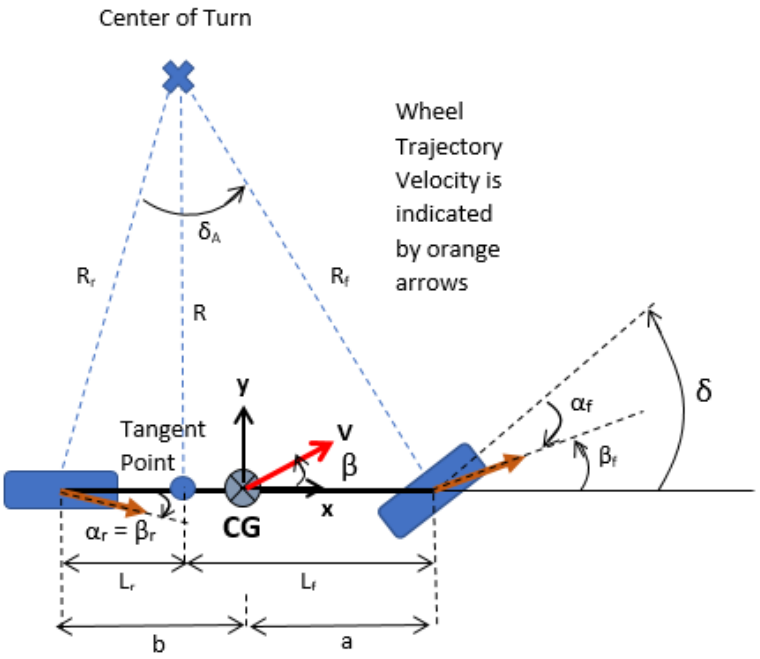

Figure 2.8 Tangent Point Moving to Center of Gravity

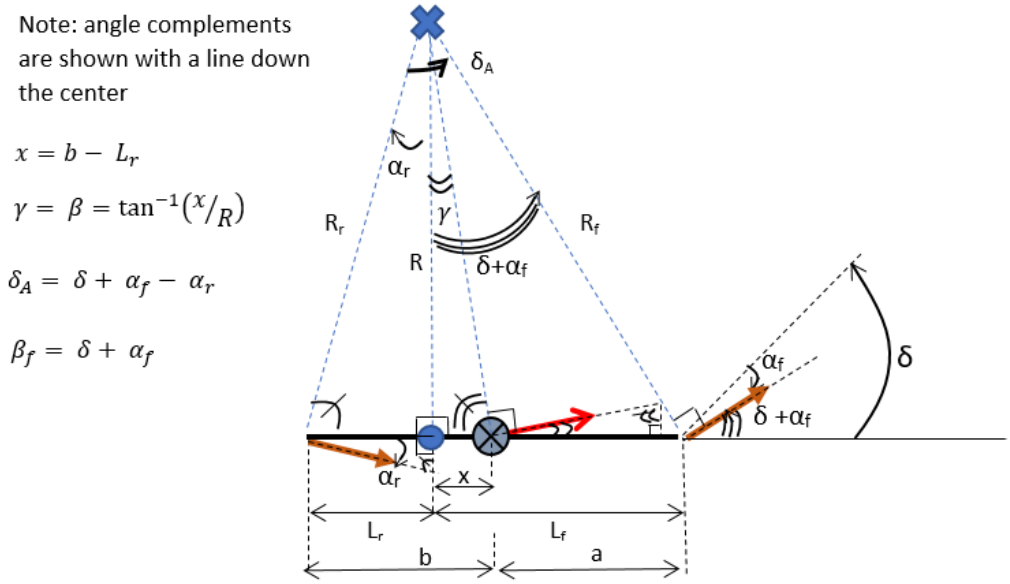

Figure 2.9 Geometric Relationships for Ackermann Steering Angle

point is assumed to be the center of gravity. It is assumed that the distance translated by the tangent point along the length of the vehicle is small in comparison to the total length of the vehicle while at speeds greater than about 35 miles per hour.

Note: angle complements are shown with a line down the center

$\gamma = \beta = 0$

$\delta_A = \delta + \alpha_f - \alpha_r$

$\beta_f = \delta + \alpha_f$

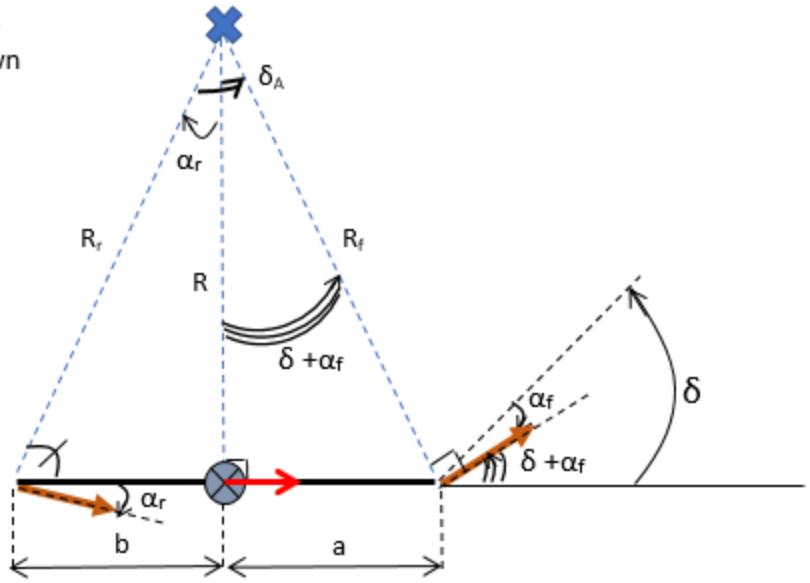

Figure 2.10 Simplified Geometric Relationships for Steering

2.4 CORNERING

The center of gravity is used as a reference point in creating the two-wheel model. Vehicles will have centers of gravity in different locations, and this can affect how the car maneuvers. The placement of the center of gravity is especially important in a turn. Neutral steer, understeer, and oversteer are terms used to describe cars with centers of gravity in the middle, front, or back of the car. Note that the following sections will make simplifications that are not always applicable, especially when determining stability. The center of gravity is an important factor in determining stability of a vehicle, but it is not the primary factor. These models focus on the effect of slip angles and steering angles on the vehicle. Camber angles describe a tilting of the wheel face away from the car body, and are used in some racing vehicles. Camber angles will not be discussed, as slip angles are generally twenty times the magnitude of camber angles in common vehicle dynamics (Blundell and Harty, 2004).

2.4.1 Neutral Steer

A neutrally-steered car is one that has a center of gravity in the middle of the vehicle (see Fig. 2.11). For now, consider the cornering coefficients $C_{\alpha f}$ and $C_{\alpha r}$ of the front and rear tires to be the same. Assume that the lateral force on the tire is linearly related to the slip angle. The lateral force will be modeled as the slip angle times the cornering coefficient. To write the equations of motion for the vehicle, assume that the small angle assumption can be used.

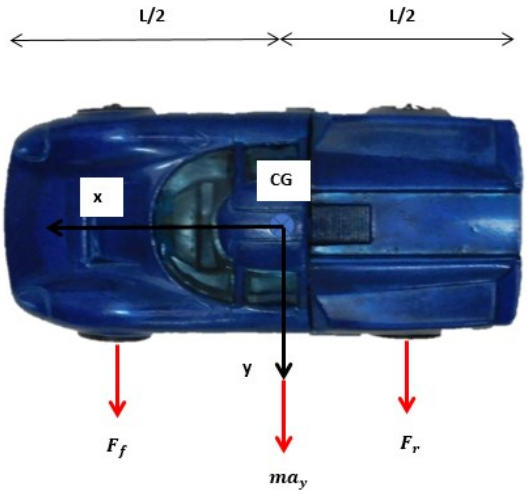

Figure 2.11 Neutral Steer Car

This means that sufficiently small steering angles are applied to the vehicle and the slip angles are small. Normally, most drivers will experience slip angles of about three degrees or less, so the small angle assumption will work well in most situations (Dixon, 2009). It is also assumed that the car is in steady-state cornering, so that pitching or rolling is not considered. Figure 2.12 shows a neutrally-steered vehicle as it maneuvers a turn. The sum of the forces in the y-direction is shown in Eqn. 2.11 and the moment balance about the z-axis (pointing out of the paper) is shown in Eqn. 2.12.

$$\sum F_y = ma: \ -C_{\alpha r}\alpha_r - C_{\alpha f}\alpha_f = (m)(V^2/R) \tag{2.11}$$

$$\sum M_{z-axis} = 0: \quad C_{\alpha f}\alpha_f a = C_{\alpha r}\alpha_r b \tag{2.12}$$

The sign of the lateral forces in Eqn. 2.11 may be confusing at first. Note that the sign of the slip angle is determined using the right-hand rule according to section 7.4.2 of SAE J670. This means that the slip angles will be negative as shown in Fig. 2.12. To have lateral forces that pull the vehicle into the center of the turn, there must be a negative sign multiplied to the cornering stiffness and slip angle.

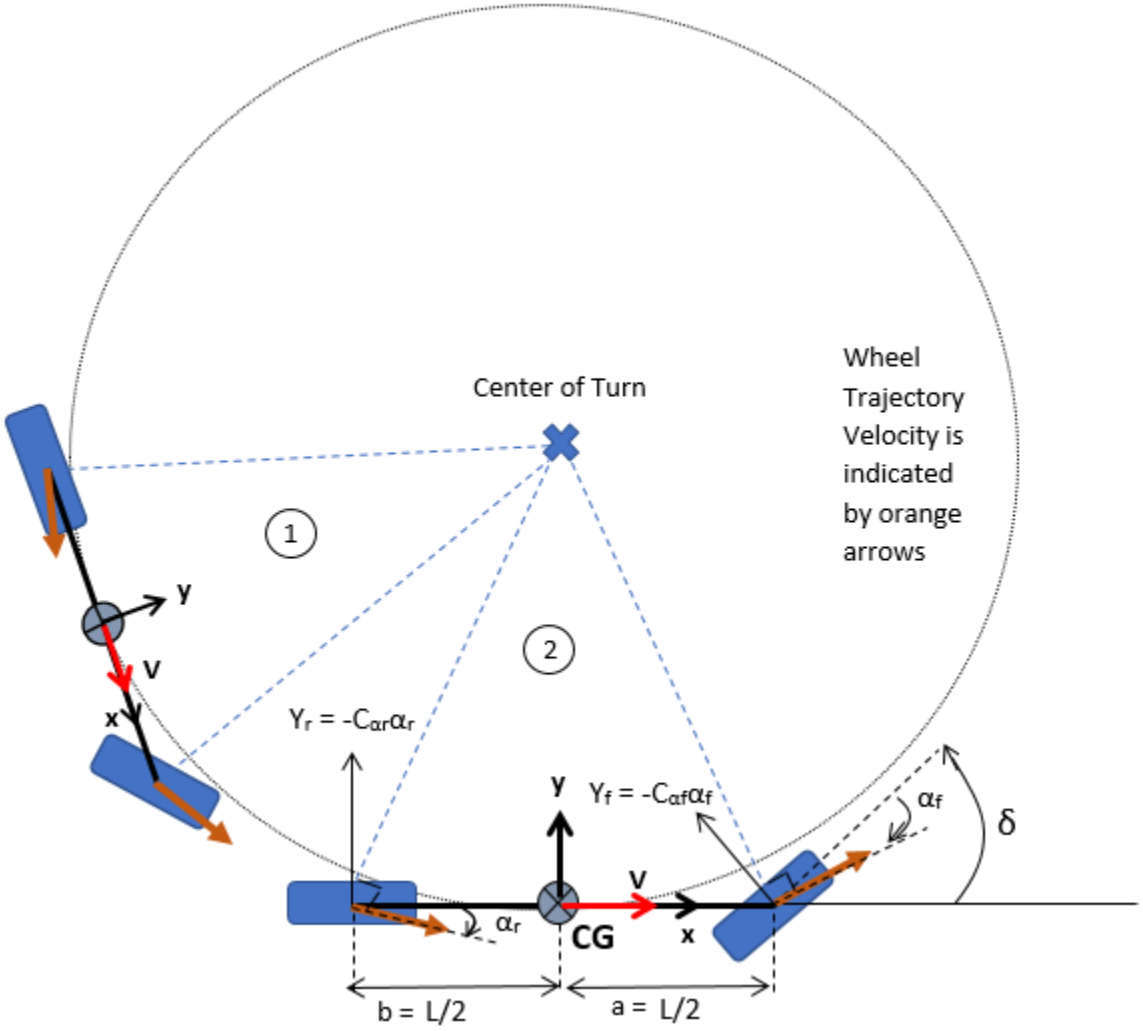

Figure 2.12 Neutral Steer Car Path Diagram

The sum of the moments equation shows that the slip angles are equal because the cornering coefficients are equal and the distance from the back of the car to the center of gravity is equal to

the distance from the front of the car to the center of gravity. Also, note that the Ackermann steering angle is equal to the steering angle δ because the slip angles are equal in magnitude. From the sum of the forces in the y-direction, the slip angles are shown to increase as the lateral acceleration increases.

Although neutral steer cars are simple to look at and analyze, few cars on the market are perfectly neutral steer. Often, vehicles are slightly understeered or oversteered, depending on the cornering characteristics required.

2.4.2 Understeer

An understeer vehicle is one that has a center of gravity towards the front of the vehicle. As an example, consider a vehicle with a center of gravity located one-third of the total length of the car from the front (see Fig. 2.13).

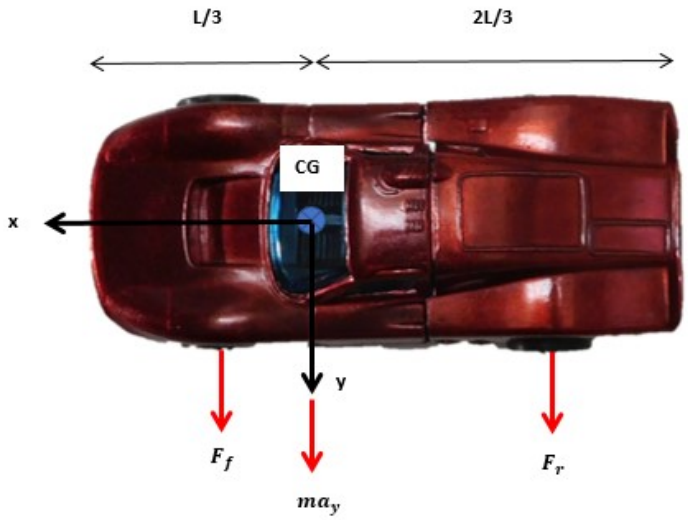

Figure 2.13 Understeer Car Model

As with the previous section on neutrally-steered vehicles, assume that the cornering stiffness is equal in the front and rear tires of the car. The sum of the forces in the y-direction is shown by Eqn. 2.13 and the sum of the moments in the z-direction is shown in Eqn. 2.14.

$$\sum F_y = ma_y:\ ma_y = F_f + F_r \tag{2.13}$$

$$\sum M_{z-axis} = 0:\ F_f\left(\frac{1}{3}\right)L = F_r\left(\frac{2}{3}\right)L \tag{2.14}$$

Equations 2.13 and 2.14 can be used to find relationships between the front and rear slip angles. Rearranging the equations and solving for the lateral forces gives Eqns. 2.15 and 2.16.

$$F_f = \left(\frac{2}{3}\right)ma_y = -C_{\alpha f}\alpha_f \tag{2.15}$$

$$F_r = \left(\frac{1}{3}\right)ma_y = -C_{\alpha r}\alpha_r \tag{2.16}$$

Equations 2.15 and 2.16 show that the magnitude of the front slip angle is two times the magnitude of the rear slip angle. To visualize the slip angles more clearly, see Fig. 2.14. The larger front slip angle means that the front tire takes on a larger lateral load than the rear. The slip angles are similar to the steering angle, because both direct the car in a particular direction. Since the slip angles are not equal in magnitude, the steering angle will have to change in order to keep the vehicle on its intended path. Refer to Fig. 2.10 for the background on the derivation of Eqn. 2.17.

$$\delta = \delta_A + \alpha_r - \alpha_f \tag{2.17}$$

After substituting the values of the front and rear slip angles, the steering angle of the understeered vehicle is given in Eqn. 2.18.

$$\delta = \delta_A + \alpha_r - 2\alpha_r = \delta_A - \alpha_r < \delta_A \tag{2.18}$$

Equation 2.18 shows that the steering angle must be less than the Ackermann steering angle. In other words, the steering angle needed to keep an understeered car on a path of fixed radius is less than the steering angle needed to keep a neutrally-steered vehicle on a fixed path.

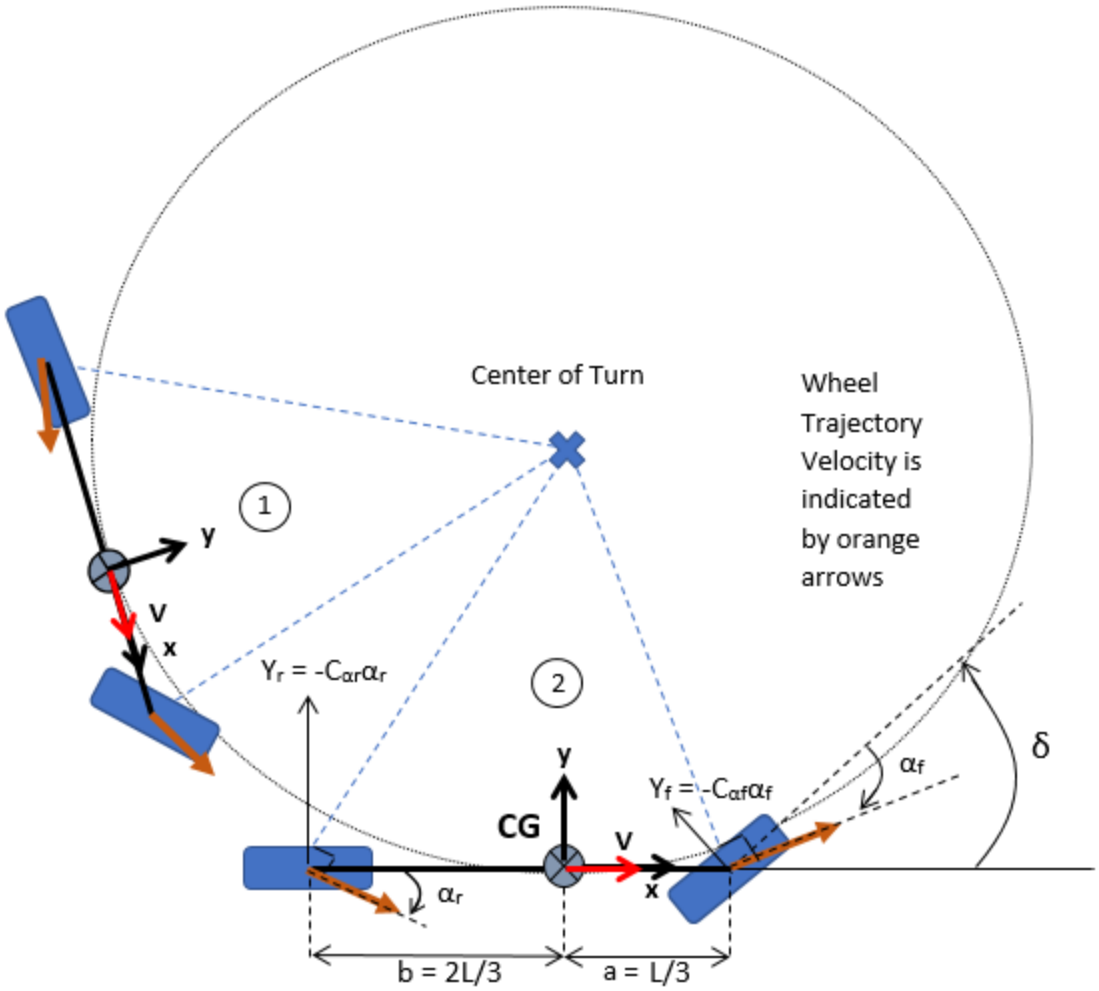

Figure 2.14 Understeer Car Path

2.4.3 Oversteer

An oversteer vehicle has a center of gravity in the rear of the car. For example, consider a vehicle with a center of gravity located two-thirds of the total body length from the front of the car (see Fig. 2.15). The sum of the forces in the y-direction and the sum of the moments about the z-axis is shown in Eqns. 2.19 and 2.20.

$$\sum F_y = ma_y: \; ma_y = F_f + F_r \tag{2.19}$$

$$\sum M_{z-axis} = 0: \; F_f\left(\frac{2}{3}\right)L = \; F_r\left(\frac{1}{3}\right)L \tag{2.20}$$

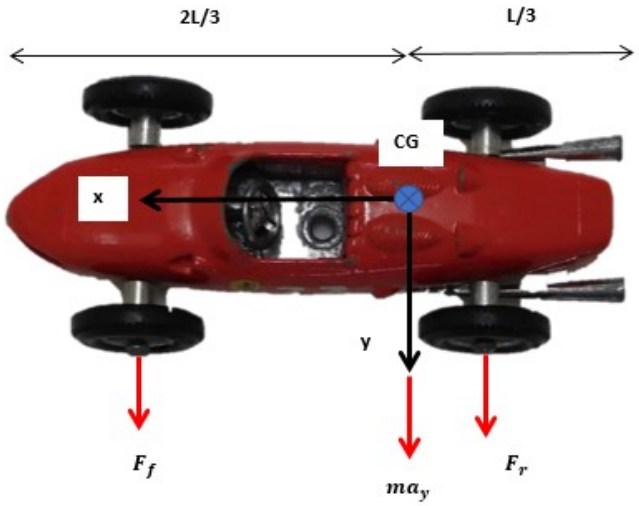

Figure 2.15 Oversteer Car Model

In this case, the rear wheel takes on a larger force than the front wheel, as seen by rearranging Eqns. 2.19 and 2.20 to get Eqns. 2.21 and 2.22.

$$F_f = \left(\frac{1}{3}\right)ma_y = \; -C_{\alpha f}\alpha_f \tag{2.21}$$

$$F_r = \left(\frac{2}{3}\right)ma_y = \; -C_{\alpha r}\alpha_r \tag{2.22}$$

The rear slip angle is two times the front slip angle. The steering angle will have to change to accommodate the difference in magnitude between the front and rear slip angles. The new steering angle is given by Eqn. 2.23.

$$\delta = \delta_A + \alpha_r - \frac{1}{2}\alpha_r = \; \delta_A + \frac{1}{2}\alpha_r > \; \delta_A \tag{2.23}$$

Figure 2.16 shows the oversteered car along a curved path, and the associated slip angles as well as the steering angle (Milliken, 1995).

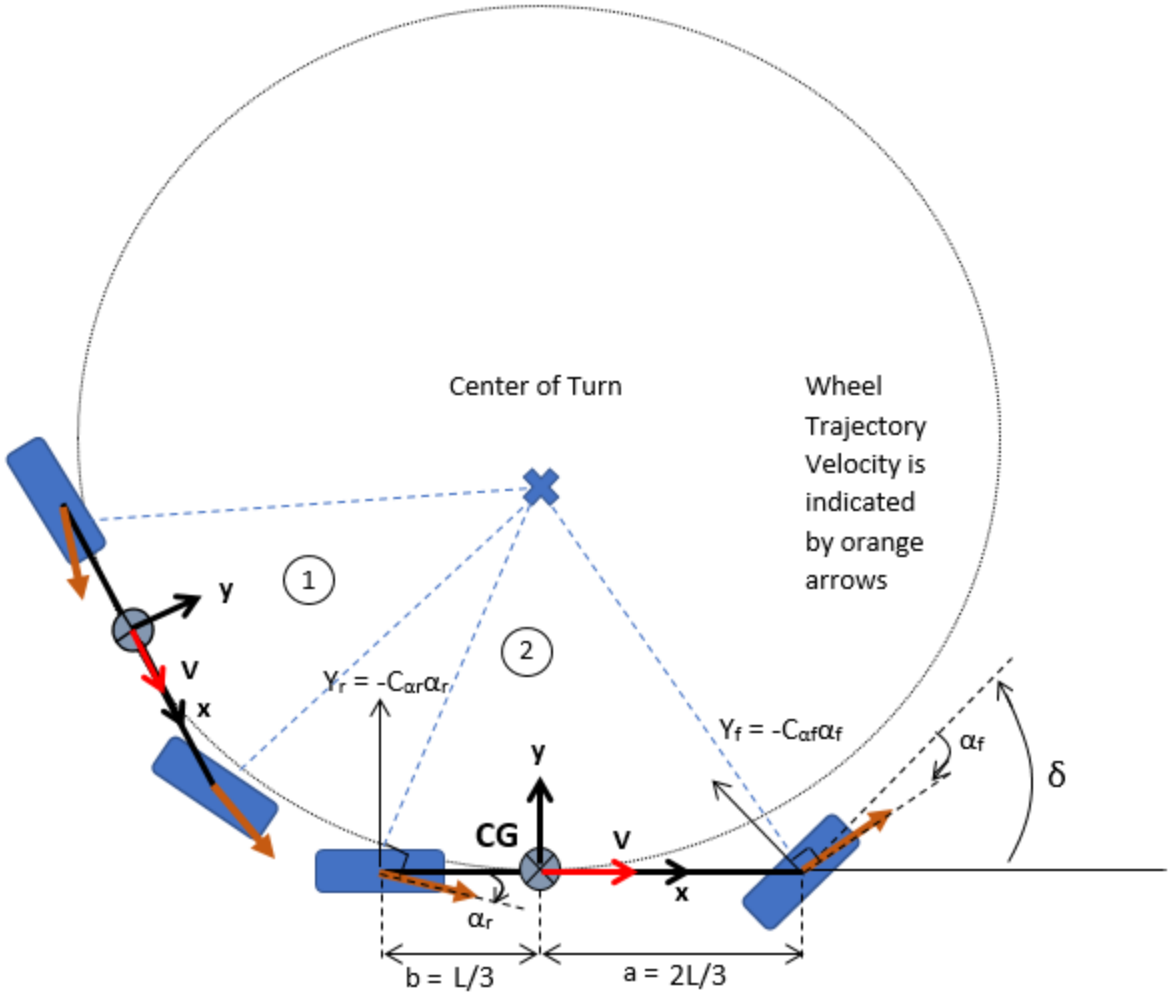

Figure 2.16 Oversteer Car Path

2.5 ACCELERATION PERFORMANCE

The differences in location of the center of gravity affect the steering angle to keep a vehicle on a straight-line path. The placement of the center of gravity can also affect the acceleration performance of a vehicle.

2.5.1 Oversteer Car Acceleration Performance

Consider a vehicle as shown in Fig. 2.17 with a total longitudinal length of L which experiences an acceleration a_x in the x-direction. Assume the center of gravity is one-twelfth of the length L.

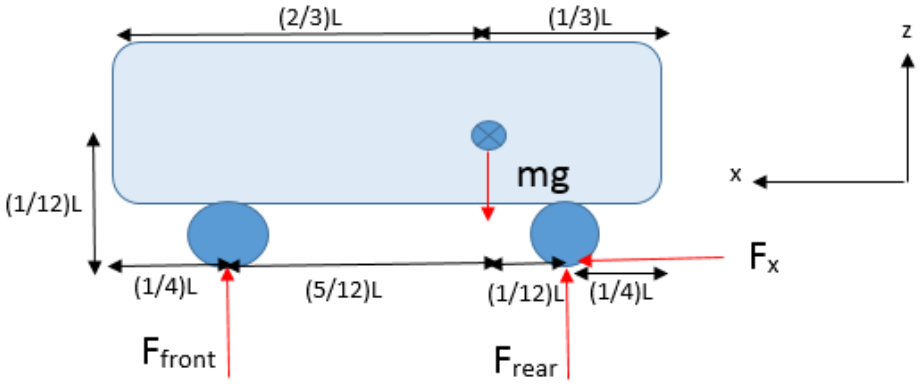

Figure 2.17 Theoretical Oversteer Car

The frictional force F_x acting on the tire in the x-direction are assumed to be equal to a coefficient of friction times the normal force on the tire. The effect of aerodynamic forces will be ignored. The equations for the sum of the forces in the z-direction, sum of the moments about the y-axis, and the sum of the forces in the x-direction are shown in Eqns. 2.24, 2.25, and 2.26.

$$\sum F_z = mg: \quad F_f + F_r = mg \tag{2.24}$$

$$\sum M_{y-axis} = 0: \quad -F_f\left(\frac{5}{12}L\right) + F_r\left(\frac{L}{12}\right) - F_x\left(\frac{L}{12}\right) = 0 \tag{2.25}$$

$$\sum F_x = ma_x: \quad F_x = ma_x \tag{2.26}$$

The equation for the force due to friction on the rear tire is modeled as shown in Eqn. 2.27.

$$F_x = \mu F_r \tag{2.27}$$

These equations can be rearranged to solve for the acceleration in the x-direction (see Eqn. 2.28).

$$a_x = \frac{30g}{6-\mu} - 5g \tag{2.28}$$

This result will be compared with the acceleration of an understeered car in the next section.

2.5.2 Understeer Car Acceleration Performance

The model of the understeered car is shown in Fig. 2.18.

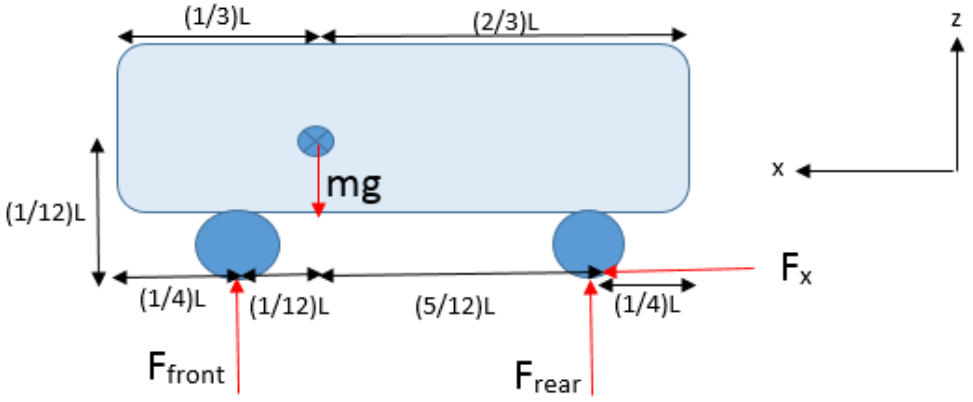

Figure 2.18 Theoretical Understeer Car

The frictional force F_x acting on the tire in the x-direction are assumed to be equal to a coefficient of friction times the normal force on the tire. The effect of aerodynamic forces is ignored. The equations of motion for the sum of the forces in the z-direction, sum of the moments about the y-axis, the sum of the forces in the x-direction, and the equation for the frictional force on the rear tire is shown in Eqns. 2.29, 2.30, 2.31, and 2.32.

$$\sum F_z = mg: \quad F_f + F_r = mg \tag{2.29}$$

$$\sum M_{y-axis} = 0: \quad -F_f\left(\frac{1}{12}L\right) + F_r\left(\frac{5}{12}L\right) - F_x\left(\frac{L}{12}\right) = 0 \tag{2.30}$$

$$\sum F_x = ma_x: \quad F_x = ma_x \tag{2.31}$$

$$F_x = \mu F_r \tag{2.32}$$

This gives an acceleration in the x-direction as shown in Eqn. 2.33.

$$a_x = \frac{6g}{6-\mu} - g \tag{2.33}$$

The acceleration for the understeered car is five times less than that of the oversteered vehicle. This helps explain why some sports cars, such as the test vehicle used in this thesis, are oversteered. It allows the vehicle to accelerate more quickly because the weight is closer to the torque-driven

tires. It may seem odd at first that the relationship between the two equations for acceleration is based on a factor of five. However, this is just due to the set-up of the problem. If the car had not been split so that the distance to the center of gravity from the front was five-twelfths, then the factor between the accelerations of the oversteer and understeer vehicles would have been different.

2.6 FULL TWO-WHEEL MODEL

These simple situations have been helpful for understanding the basics of vehicle motion. However, to understand the stability of a vehicle when going into a turn or during a lane change, equations of motion to describe the yaw rate and lateral velocity need to be derived. To do this, the velocities of the tires must be known in detail. See Fig. 2.19 for a complete diagram of the tire velocities.

At the center of gravity of each tire, there is a velocity vector due to the forward motion of the car called V, the lateral motion called U, and the rotational effect of the yaw rate r. The equations for the lateral velocity vectors of the front and rear tire are given in Eqns. 2.34 and 2.35.

$$\text{front lateral velocity} = U + ar \tag{2.34}$$

$$\text{rear lateral velocity} = U - br \tag{2.35}$$

Now the equations for the body slip angle and the tire slip angles can be determined. The body slip angle is defined by SAE J670 as shown in Eqn. 2.36. The small angle assumption is applied.

$$\beta = tan^{-1}\frac{U}{V} \approx \frac{U}{V} \tag{2.36}$$

The slip angles for the front and rear tires are shown in Eqns. 2.37 and 2.38. They are derived using Fig. 2.19.

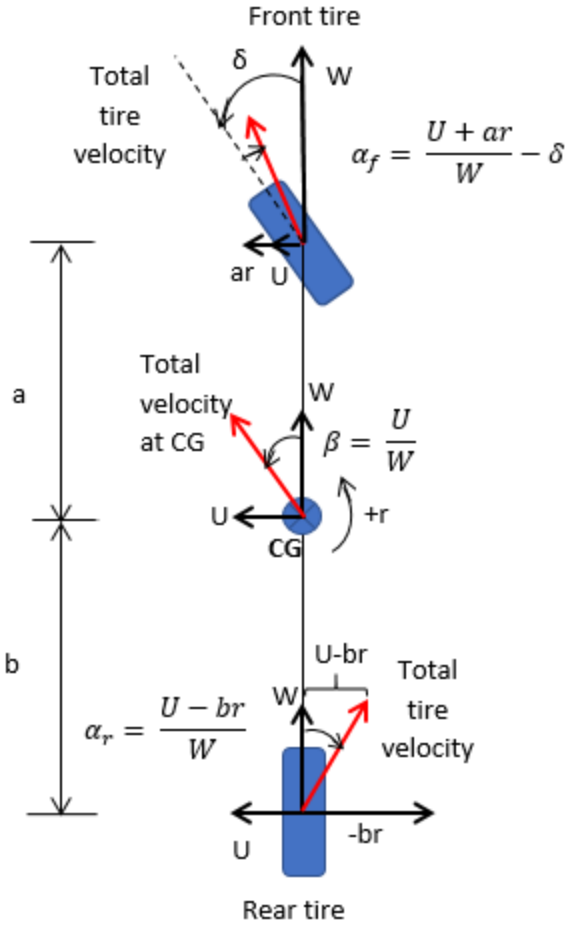

Figure 2.19 Velocity Vector Diagram

$$\alpha_r = tan^{-1}\frac{U - br}{V} \approx \frac{U - br}{V} \approx \frac{U}{V} - \frac{br}{V} \approx \beta - \frac{br}{V} \tag{2.37}$$

$$\alpha_f = tan^{-1}\left(\frac{U + ar}{V} - \delta\right) \approx \frac{U + ar}{V} - \delta \approx \frac{U}{V} + \frac{ar}{V} - \delta \approx \beta + \frac{ar}{V} - \delta \tag{2.38}$$

The lateral acceleration of the vehicle is given by Eqn. 2.39.

$$a_y = \dot{U} + r \times V \tag{2.39}$$

Equation 2.39 can be rewritten using the body slip angle, which is given by Eqn. 2.36, as $U \approx \beta V$. The derivative of this equation is $\dot{U} \approx \dot{\beta} V$. The lateral acceleration with the body slip angle is given by Eqn. 2.40.

$$a_y = \dot{\beta}V + Vr = V(r + \dot{\beta}) \tag{2.40}$$

The equations of motion can be written by viewing Fig. 2.12, 2.14, or 2.16.

$$\sum F_y = ma_y: \ -C_{\alpha r}\alpha_r - C_{\alpha f}\alpha_f = m\big(V(r + \dot{\beta})\big) \tag{2.41}$$

$$\sum M_{z-axis} = I_z\dot{r}: \ -C_{\alpha f}\alpha_f a + C_{\alpha r}\alpha_r b = I_z\dot{r} \tag{2.42}$$

The lateral forces in Eqns. 2.41 and 2.42 can be expanded by writing the slip angles in terms of vehicle velocities from Eqns. 2.37 and 2.38. The expanded versions of the lateral forces are shown in Eqns. 2.43 and 2.44.

$$F_f = -C_{\alpha f}\,\alpha_f = -C_{\alpha f}\left(\beta + \frac{ar}{V} - \delta\right) = -C_{\alpha f}\beta - C_{\alpha f}\frac{ar}{V} + C_{\alpha f}\delta \tag{2.43}$$

$$F_r = -C_{\alpha r}\alpha_r = -C_{\alpha r}\left(\beta - \frac{br}{V}\right) = -C_{\alpha r}\beta + C_{\alpha r}\frac{br}{V} \tag{2.44}$$

The sum of Eqns. 2.43 and 2.44 is the total force in the y-direction. This is given in Eqn. 2.45.

$$F = F_r + F_f = \beta\big(-C_{\alpha r} - C_{\alpha f}\big) + \frac{r}{V}\big(-aC_{\alpha f} + bC_{\alpha r}\big) + C_{\alpha f}\delta \tag{2.45}$$

The expanded versions of the lateral forces can be used to expand the sum of the moments about the z-axis (see Eqn. 2.46).

$$\begin{aligned} M = M_f + M_r &= F_f a - F_r b \\ &= \beta\big(bC_{\alpha r} - aC_{\alpha f}\big) + \frac{r}{V}\big(-a^2C_{\alpha f} - b^2C_{\alpha r}\big) + aC_{\alpha f}\delta \end{aligned} \tag{2.46}$$

These equations can be thought of as a series of partial derivatives with respect to β, δ, and r. These derivatives can be individually labeled and re-named to make the equation of motion more compact. Also, they help users conceptualize the changing of a variable. According to Milliken, this idea of using partial derivatives is common in the aeronautical industry (1995). For Eqn. 2.45, partial derivatives of the lateral force components are written in Eqns. 2.47, 2.48, and 2.49.

$$\frac{\partial F}{\partial \beta} = F_\beta = -(C_{\alpha r} + C_{\alpha f}) \tag{2.47}$$

$$\frac{\partial F}{\partial r} = F_r = \frac{-1}{V}(aC_{\alpha f} - bC_{\alpha r}) \tag{2.48}$$

$$\frac{\partial F}{\partial \delta} = F_\delta = C_f \tag{2.49}$$

Using Eqns. 2.47, 2.48, and 2.49 in Eqn. 2.45 yields Eqn. 2.50.

$$F = \beta F_\beta + rF_r + \delta F_\delta \tag{2.50}$$

The partial derivatives can make the relationship between the lateral force and changes in the variables clear. The F_δ term can be thought of as the control term. The steering angle will have a larger effect on the lateral forces as the cornering stiffness increases. In other words, a stiffer spring will output a larger force for the same amount of deflection compared to a less stiff spring.

The F_β is the damping term because it reduces the body angle as cornering stiffness in either tire increases. The body angle is approximately the lateral velocity divided by the longitudinal velocity. As the lateral velocity increases, the F_β term becomes more negative and reduces the lateral force. In other words, the damping term opposes an increase in lateral force per change in lateral velocity.

The F_r term is the forcing term. It is the rate of change between the lateral force and the yaw rate. As the difference between the moments caused by the lateral forces and the front and rear tires increases, so does the F_r term and the yaw rate. This can be physically explained by imagining a car that has lost traction in the rear wheels. In this case, the difference between the moment caused by the front and rear tires will be large, the yaw rate will increase, and the car will spin. Note that this term decreases as velocity decreases. If the car had begun losing traction in the rear wheels, but it was only going ten miles per hour, it would spin less than a car going fifty miles per hour.

The partial derivatives of the moment equation are shown in Eqns. 2.51, 2.52, and 2.53.

$$\frac{\partial M}{\partial \beta} = M_\beta = \left(bC_{\alpha r} - aC_{\alpha f}\right) \tag{2.51}$$

$$\frac{\partial M}{\partial r} = M_r = \frac{1}{V}\left(-a^2 C_{\alpha f} - b^2 C_{\alpha r}\right) \tag{2.52}$$

$$\frac{\partial M}{\partial \delta} = M_\delta = aC_{\alpha f} \tag{2.53}$$

Equation 2.46 can be rewritten in terms of the moment partial derivatives presented in Eqns. 2.51, 2.52, and 2.53 (see Eqn. 2.54).

$$M = \beta M_\beta + rM_r + \delta M_\delta \tag{2.54}$$

Like the partial derivatives for the lateral forces, the partial derivatives of the moment equation have special meaning. The M_δ term is the control term because it can change the direction of the car from an input from the driver via the steering angle. Notice that M_δ is more sensitive to changes in the steering angle than F_δ by a factor of a, the length from the front of the car to the center of gravity.

M_β is the moment stability term. M_β is the rate at which the moment balance changes with β. When the moment at the front tire is greater than the moment at the rear tire, the car is oversteered and the entire term is negative. For an oversteered car, to increase the magnitude of the M_β term for tires of equal stiffness, the center of mass is shifted farther forward to increase the length a. This causes the slip angle β to decrease, and the longitudinal velocity vector will increase as the lateral velocity decreases. In the understeer case where b is greater than a, M_β is positive. As the car becomes more understeered, a change in the moments will cause the lateral velocity to increase as β increases.

M_r is the moment damping term. It increases in magnitude whenever the moment created by either the front or rear tire increases. The term is always negative, meaning that it opposes a change in the yaw rate for a given change in the moments. It decreases as the velocity decreases, and it increases as the length of the vehicle increases. The partial derivatives are used to rewrite Eqns. 2.41 and 2.42 (see Eqns. 2.55 and 2.56).

$$m\big(V(r+\dot{\beta})\big) = \beta F_\beta + rF_r + \delta F_\delta \tag{2.55}$$

$$I_z\dot{r} = \beta M_\beta + rM_r + \delta M_\delta \tag{2.56}$$

These equations will help determine the stability of the car, as seen in the next section.

2.7 Stability of a Two-Wheel Model in a Steady-State Turn

Consider a vehicle that is traveling in a circular path. The rate of change of the angle of rotation will be considered constant in this model, since the car is assumed to be following a curve of constant radius. This gives the relationship shown in Eqn. 2.57.

$$r = V/R \tag{2.57}$$

This model assumes that the car will have a constant longitudinal speed. This means that the car will have a constant yaw rate, and that $\dot{r}$ and $\dot{\beta}$ will be zero. The model assumes the steering input is a constant value. Applying these assumptions to Eqns. 2.55 and 2.56 gives Eqns. 2.58 and 2.59.

$$mV\left(\frac{V}{R}\right) = \beta F_\beta + \left(\frac{V}{R}\right)F_r + \delta F_\delta \tag{2.58}$$

$$0 = \beta M_\beta + \left(\frac{V}{R}\right)M_r + \delta M_\delta \tag{2.59}$$

In a steady-state turn, it is interesting to see the relationship between the curvature of the path (1/R) and the steering angle. Rearranging Eqns. 2.58 and 2.59 yields the relationship (see Eqn. 2.60).

$$\frac{M_\delta F_\beta - F_\delta M_\beta}{V\left(-mVM_\beta - M_r F_\beta + M_\beta F_r\right)} = \frac{1/R}{\delta} \tag{2.60}$$

This equation can be simplified by rearranging the partial derivatives (see Eqn. 2.61).

$$\frac{1/R}{\delta} = \frac{1/L}{1 + KV^2} \tag{2.61}$$

The K value in Eqn. 2.61 is called the stability factor. The stability factor is defined by Eqn. 2.62 (Milliken, 1995).

$$K = \left(\frac{1}{L}\right)\frac{-mM_\beta}{M_\delta F_\beta - F_\delta M_\beta} \tag{2.62}$$

By substituting in the values of the partial derivatives defined by Eqns. 2.47, 2.48, 2.49, 2.51, 2.52, and 2.53, the stability factor can be reduced into physical terms (see Eqn. 2.63).

$$K = \left(\frac{1}{L}\right)\frac{m\left(bC_{\alpha r} - aC_{\alpha f}\right)}{LC_{\alpha f}C_{\alpha r}} \tag{2.63}$$

Equation 2.61 can be rearranged to obtain a function for the steering angle δ (see Eqn. 2.64).

$$\delta = \frac{L}{R} + \frac{LKV^2}{R} \tag{2.64}$$

Figure 2.20 shows a graph Eqn. 2.64. Recall from Eqn. 2.1 that the lateral acceleration of a vehicle in a constant turn is equal to the longitudinal speed squared divided by the radius of the turn. This means that Fig. 2.20 shows the change in lateral acceleration of the car with respect to the steering angle. This graph shows that an oversteered vehicle will have a lateral acceleration that changes sign as the steering angle increases. This effect is seen through counter-steering. In racing vehicles, sometimes drivers will reverse the direction of the steering wheel in order to go through a turn more quickly. This is not seen with understeered vehicles, which need increasing steering angles in order to achieve higher lateral accelerations.

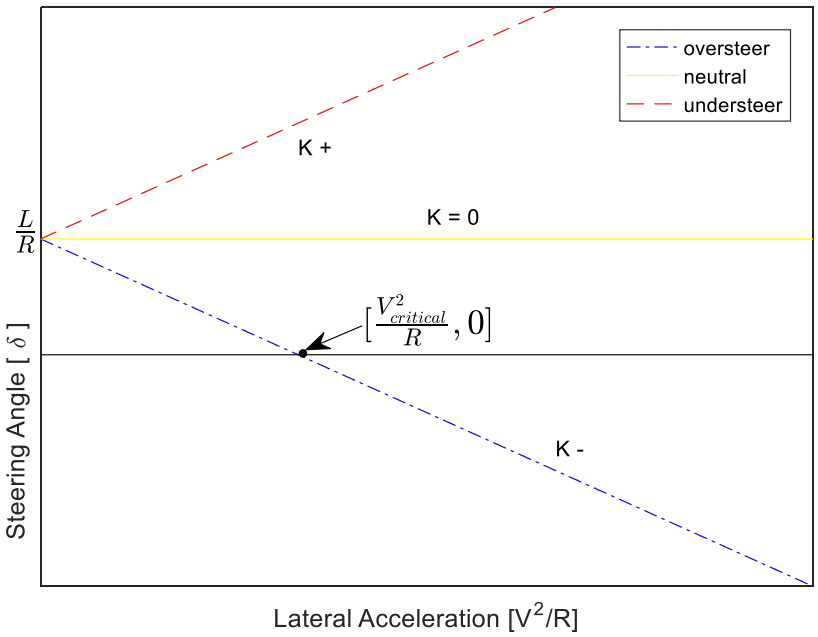

Figure 2.20 Steering Angle versus Lateral Acceleration Response

The point at which the steering angle of an oversteered vehicle changes from a positive value to a negative value is called the critical speed. The critical speed can be calculated using Eqn. 2.64 by setting the steering angle equal to zero (see Eqn. 2.65).

$$V_{crit} = \sqrt{\frac{-1}{K}} \tag{2.65}$$

Note that the critical velocity will not be an imaginary number, because the value of K is negative for oversteered vehicles. The stability factor provides the best method to determine the stability of a vehicle, because it can numerically quantify whether a vehicle is oversteered or understeered. This is important because an oversteered vehicle, past its critical velocity, is tending toward an unstable handling scenario.

Notice that the graph of steering angle versus lateral acceleration response starts at a value equal to the length of the car divided by the radius of the turn. This is equal to the Ackermann steering angle defined by Eqn. 2.10. The car is constrained to the geometry of the turn, which

means that the lowest acceleration the vehicle can achieve is at low speed, which satisfies the Ackermann steering conditions. As the lateral acceleration increases, the steering angle must increase beyond the Ackermann steering angle.

Another informative gain function to analyze is the response of the yaw rate to changes in the steering angle. Recall from Eqn. 2.57 that the yaw rate is equal to the longitudinal velocity divided by the radius of the turn. This means that Eqn. 2.61 can be multiplied by the longitudinal velocity of the vehicle to get a relationship between yaw rate and steering angle (see Eqn. 2.66).

$$\frac{V/_R}{\delta} = \frac{V/_L}{1 + KV^2} \tag{2.66}$$

Equation 2.66 is graphed in Fig. 2.21.

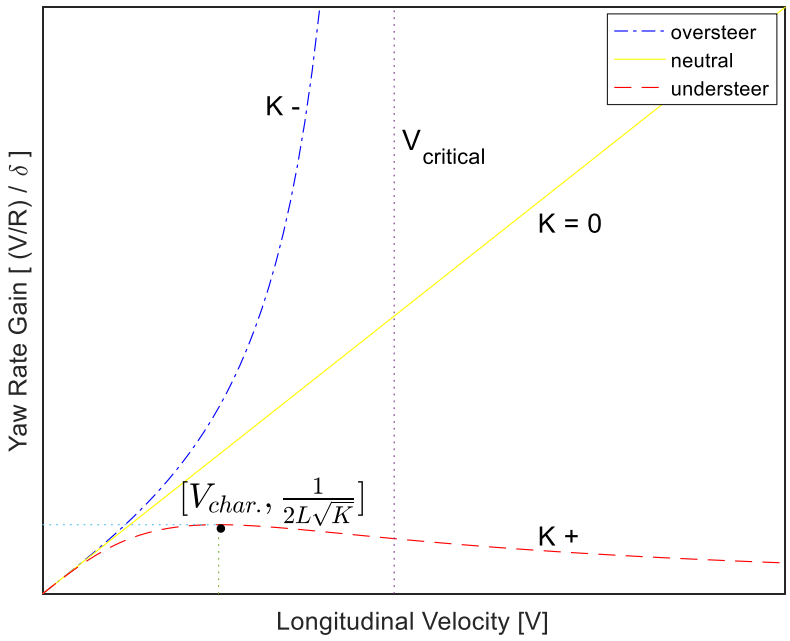

Figure 2.21 Yaw Rate versus Steering Angle Response

There are several important features to Fig. 2.21. First, note that for a positive value of K, there is a maximum yaw rate gain that is achieved but not exceeded. This means that an understeered vehicle has a limit to how fast it can change its angle of rotation. This maximum value is called the characteristic speed of an understeered vehicle, and can be calculated by finding the derivative

of the yaw rate gain equation and setting it equal to zero. First, divide the top and bottom by V (see Eqn. 2.67).

$$\frac{V/R}{\delta} = \frac{1/L}{\frac{1}{V} + KV} \tag{2.67}$$

Take the derivative and set it equal to zero (see Eqn. 2.68).

$$\frac{d}{dV}\left(\frac{V/R}{\delta}\right) = \frac{-1}{L}\left[\frac{1}{V} + KV\right]^{-2}\left[\frac{-1}{V^2} + K\right] = \frac{\frac{1}{V^2} - K}{L\left[\frac{1}{V^2} + 2K + K^2V^2\right]} = 0 \tag{2.68}$$

This gives $\frac{1}{V^2} - K = 0$, which can be re-arranged to solve for the characteristic velocity shown in Eqn. 2.69.

$$V_{characteristic} = \sqrt{\frac{1}{K}} \tag{2.69}$$

Note that the characteristic velocity will not be an imaginary number because the stability factor for an understeered vehicle is positive. The value of the yaw rate gain at this characteristic velocity can be found by substituting the result into Eqn. 2.67 as shown in Eqn. 2.70.

$$\frac{V/R}{\delta}(V_{characteristic}) = \frac{\sqrt{\frac{1}{K}}/L}{1 + K\left(\sqrt{\frac{1}{K}}\right)^2} = \frac{1}{2L\sqrt{K}} \tag{2.70}$$

Equations 2.69 and 2.70 show that at the characteristic speed, there is a maximum yaw rate gain that is a function of the length of the vehicle and the stability factor K. It is interesting to note that the yaw rate gain decreases as the length of the car decreases. This makes physical sense, because it is easier to picture a small sports car moving around a turn quickly rather than a long limo.

Granted this example involves two vehicles which have very different masses, but it gives a general sense of the relationship between rotation angle and car length.

The oversteered vehicle has a vertical asymptote equal to the critical velocity. This can be calculated by setting the denominator of the yaw rate gain equation equal to zero, which will give the same result as in Eqn. 2.65. The asymptote clearly shows that the vehicle will become unstable at the critical velocity, because it will begin to spin at continuously increasing rates. Physically, if an oversteered vehicle makes a turn too quickly and increases the yaw rate rapidly, it could approach this critical velocity and spin out.

One other gain equation that is useful in determining vehicle stability is the lateral acceleration versus steering angle. This gain equation can be found by multiplying the yaw rate gain equation by the longitudinal velocity of the vehicle (see Eqn. 2.71).

$$\frac{V^2/R}{\delta} = \frac{V^2/L}{1 + KV^2} \tag{2.71}$$

The lateral acceleration gain equation will have an asymptote equal to the critical velocity. This can be found by setting the denominator of Eqn. 2.71 equal to zero. A graph of the lateral acceleration gain equation is shown in Fig. 2.22.

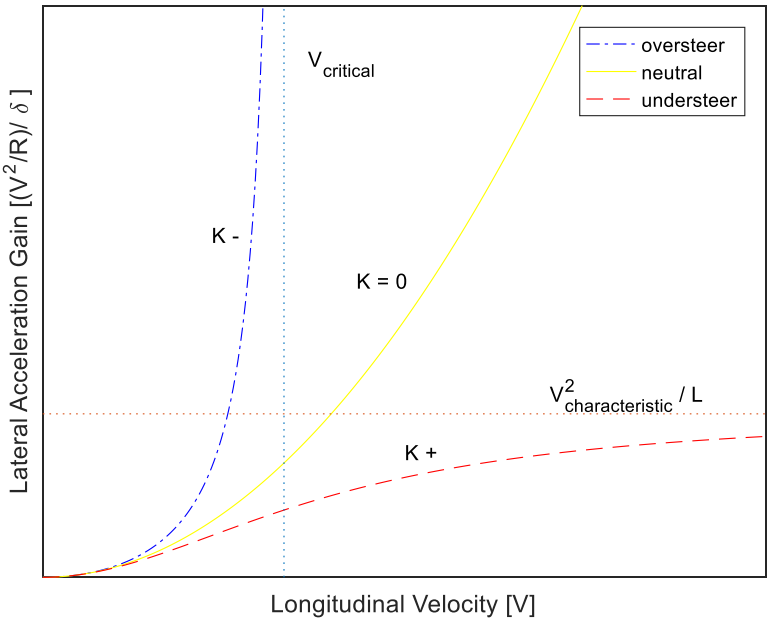

Figure 2.22 Lateral Acceleration versus Steering Angle Response

The understeered vehicle will approach a horizontal asymptote. The horizontal asymptote can be found using the limit of the lateral acceleration gain equation after using L'Hospital's Rule twice by taking the derivative with respect to V of the numerator and denominator (see Eqn. 2.72).

$$\lim_{V\to\infty}\frac{V^2/L}{1+KV^2}=\lim_{V\to\infty}\frac{2V/L}{1+2KV}=\lim_{V\to\infty}\frac{2/L}{2K}=\frac{1}{KL}=\left(\sqrt{\frac{1}{K}}\right)^2\frac{1}{L}=\frac{V^2{}_{characteristic}}{L} \quad (2.72)$$

This horizontal asymptote means that an understeered vehicle will not be able to laterally accelerate as quickly as an oversteered vehicle. This makes the vehicle more stable in a turn, but also limits the ability of an understeered vehicle to be a competitive car in racing. However, it is very suitable for passenger vehicles. Many passenger vehicles are understeered to increase the turning stability of the car (Karnopp and Margolis, 2008).

2.8 CONSTANT STEERING AND CONSTANT SPEED INPUT SIMULATION

The two-wheel model is fairly simple to simulate, but defining the simulation parameters can prove more difficult. As with any engineering parameter, it can be found experimentally or theoretically.

Both approaches will be taken to find the cornering stiffness of the front and rear tire of a neutrally-steered vehicle. The results for each method are compared afterwards.

2.8.1 Experimental Determination of Cornering Stiffness

The first step in determining the cornering stiffness is to calibrate the vehicle and the accelerometer. The first input to calibrate is the steering angle. In most cars, the rotation of the steering wheel does not have a one-to-one ratio of output to the tires. In fact, the steering wheel can rotate more that ninety degrees, but tires will generally rotate a total of forty-five degrees or less.

Vehicle manufacturers will have much more exact methods for determining the ratio than the procedure described here, but it is appropriate for a rough estimate. First, the front wheels of the car are aligned so that the face of the tire is in line with the body of the car. Tape is placed on the ground to mark the straight condition of the tires. Next, the tires are rotated and the steering angle rotation is recorded. The actual angle of rotation of the tires is measured by placing a piece of tape on the ground along the edge of the rotated tire. A protractor is used to measure the angle between the two pieces of marking tape. The relationship between tire angle and steering wheel angle is measured twice and is shown in Table 2.2.

Table 2.2 Tire to Steering Wheel Ratio

Steering Wheel Angle	Tire Angle	Ratio of Wheel/Tire Angle
323	14	23.1
392	28	14
Average		18.5

Table 2.2 shows that the steering wheel will move 18.5 times that of the tire angle. This ratio will be used in determining the steering angle in further calculations.

The mass of the car can be determined by driving the vehicle onto a set of scales. It is important to determine the weight on the front tires and the rear tires, because this information is used to calculate where the center of gravity is located on the vehicle. To find the center of gravity, set up a free-body diagram as shown in Fig. 2.17. Solve for the location of the center of gravity (defined by the lengths a and b) using a sum of the moments and sum of the forces in the y-direction to get Eqns. 2.73 and 2.74. Note that the vehicle length can usually be found online at the vehicle manufacturer's website or a rough estimate can be found using a tape measure.

$$a = \frac{LF_{rear}}{mg} \tag{2.73}$$

$$b = \frac{LF_{front}}{mg} \tag{2.74}$$

Next, the output for the yaw rate, lateral acceleration, and longitudinal acceleration is calibrated. Measurements are taken when the car is stationary and used to determine factors to subtract from raw data. These factors are shown in Table 2.3.

Table 2.3 Raw Data Calibration Factors

Calibration Factors	
Yaw Rate	0.027
Lateral Acceleration	-0.127
Longitudinal Acceleration	0.219

The cornering coefficient can be found using the calibrated output from an accelerometer and gyroscope. The car is taken out to a parking lot, and driven in circles at constant speed and constant steering angle. The steering angle and speed are varied as shown in Table 2.4.

Table 2.4 Experiment Steering Angles and Speeds

Steering Angle (degrees)	Speed (mph)
3	5
	10
5	5
	10
	15
	20
	25
10	5
	10
	15
	20
15	5
	10
	15
20	5
	10
	15
25	5
	10
	15
30	5
	10

In reality, it is difficult to keep a vehicle in a circular path in a parking lot given the fire hydrants, bumps, and parking dividers that may get in the way. It is important to keep the car in a circular path as much as possible. After the data is collected, the lateral acceleration is numerically integrated using the rectangular rule in a spreadsheet to calculate the lateral velocity from the lateral acceleration (Kreyszig, 2011).

The test vehicle in question was originally approximately neutrally-steered. Measurements were taken of the car to determine cornering stiffness before it was modified to make it oversteered. The beauty in using a neutrally-steered car to determine cornering stiffness is that the front and rear cornering stiffness can be assumed equal. This is due to the fact that the weight distributed to the front and rear of the vehicle is approximately the same. Using this assumption and the small angle assumption, substitute Eqns. 2.37 and 2.38 for the slip angles in Eqn. 2.41 to yield Eqn. 2.75.

$$C = \frac{-m\left(\frac{V^2}{R} + \dot{U}\right)}{\left(\frac{2U + r(a-b)}{V} - \delta\right)} \tag{2.75}$$

Equation 2.75 can be used to calculate the cornering stiffness of the front and rear tires. Note that many test vehicles will likely not be neutrally steered. In these cases, Eqns. 2.37 and 2.38 are substituted into Eqns. 2.41 and 2.42 to give values for the front and rear cornering stiffness as shown in Eqns. 2.76 and 2.77.

$$C_{\alpha f} = \frac{-I_z\dot{r} - \frac{mbV^2}{R} - mb\dot{U}}{L\left(\frac{U + ar}{V} - \delta\right)} \tag{2.76}$$

$$C_{\alpha r} = \frac{-\left(m\frac{V^2}{R} + m\dot{U} + C_{\alpha f}\alpha_f\right)}{\frac{U - br}{V}} \tag{2.77}$$

Note that Eqns. 2.76 and 2.77 use the small angle approximation. This means that the data collected for constant steering angle and constant speed needs to satisfy the condition. It is important to filter out the data that does not meet this approximation before calculating the cornering coefficient. Once the data has been filtered, a box plot of the cornering stiffness values for the different trials is calculated (see Fig. 2.23). Appendix A shows additional plots of raw data.

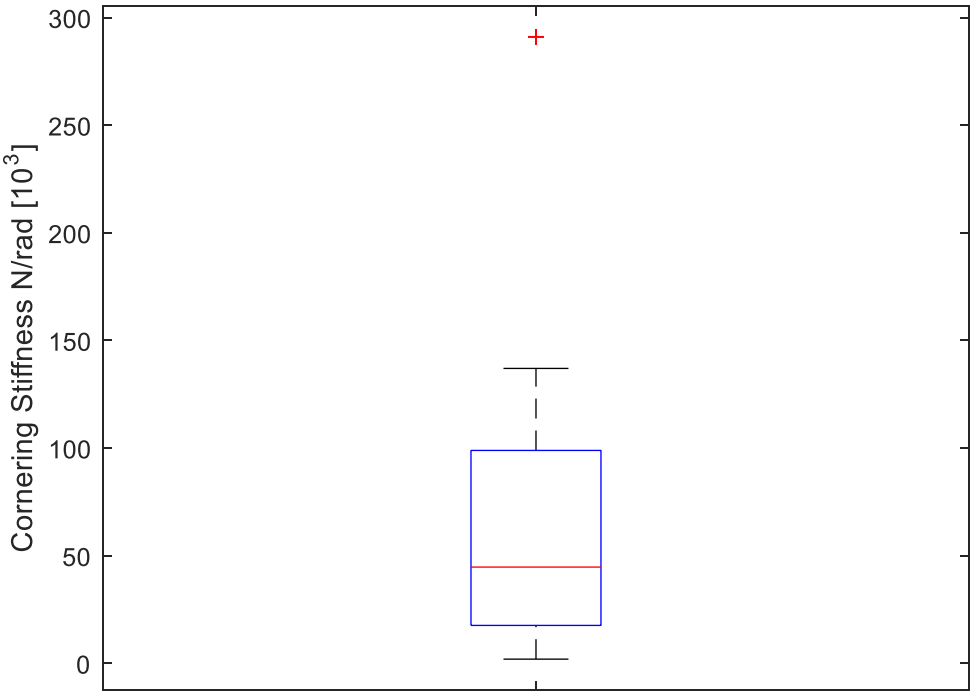

Figure 2.23 Experimental Cornering Coefficients

The average cornering coefficient is 65 kilo-Newtons per radian.

2.8.2 Theoretical Cornering Stiffness

There are many factors that affect the cornering stiffness of a tire. There is extensive research and material on modeling tires for vehicles. Even structures such as airplanes, which only use pneumatic wheels for short periods of time, have a wide range of information on their tire performance (Sleeper, 1980). Various factors affect how a tire will deform under load, including: age, type of tire (radial versus bias-ply), size, inflation pressure, load, rim width, tread, road surface, and temperature (Dixon, 1996). Out of all these factors, however, the inflation pressure and the load are the most important in determining tire deflection (Gillespie, 1992).

Besides having multiple factors that affect tire stiffness, there are also many models that describe the behavior of vehicle tires. The most widely known tire model is the Magic Formula tire model. There are also Dugoff's tire model, the dynamic tire model, and other models that focus

on the longitudinal slip of the tire (Rajamani, 2006). However, considering a linear relationship between the lateral force on the tire and slip angle is the easiest method. This is the method that will be used here to determine a theoretical value for stiffness. This assumption of a linear relationship is applicable for small slip angles. As the lateral force increases, the relationship becomes non-linear and the assumption is no longer valid (Dixon, 1996). See Fig. 2.24 for an approximation of this relationship.

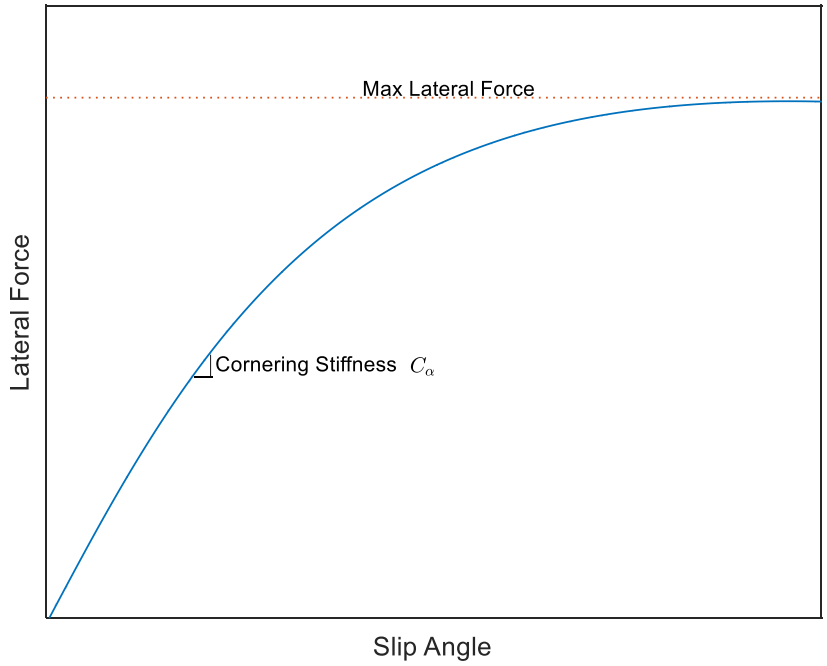

Figure 2.24 Relationship between Slip Angle and Lateral Force

For an approximately neutrally-steered car with a total mass of 1550 kilograms, a mass distribution in the front of 806 kilograms, a mass distribution in the rear of 744 kilograms, and a tire pressure of 36 pounds per square inch, using a graph of cornering coefficient versus inflation pressure, a theoretical estimate of cornering stiffness is 86 kilonewtons per radian in the front and 79 kilonewtons per radian in the rear. Note that the cornering coefficient is the cornering stiffness divided by the applied load. It is not a purely non-dimensional value, but it is extremely helpful in estimating stiffness of tires with different applied loads. In this case, for a tire with pressure equal

to 36 pounds per square inch, the cornering coefficient is 0.19 with units of degrees inverse. Multiplying by the acceleration due to gravity, the weight on the tire, and converting degrees to radians gives the approximation for the cornering stiffness (Wong, 2008). For comparison, consider Gillespie's work, which gives a graph of cornering stiffness versus inflation pressure. Using this graph, an estimate of the cornering stiffness would be 48 kilonewtons per radian after unit conversions (Gillespie, 1992). The method described by Wong's text will be used as an estimate in the following simulations because it applies changes in tire pressure and in tire load in the same calculation, while Gillespie's graphs do not.

2.8.3 Comparing Theoretical versus Experimental Results

The experimental result is on the same order of magnitude as the theoretical result for cornering stiffness, and is only about twenty percent less than the rear cornering stiffness. This indicates that there is agreement between the experimental results and the theoretical results. If the experiment is repeated in the future, measurements of the coefficient of friction between the road surface and the tire should be measured and factored into the result. The effect due to the coefficient of friction could be approximated by plotting data taken on a dry day and on a rainy day. Assuming that there is a linear relationship between cornering coefficient and the coefficient of friction, the coefficient of friction could be calculated by noting the relationship between the two test runs.

Also, the location of the accelerometer and gyroscope should be measured and recorded. It is likely that the sensors were not at the center of gravity of the vehicle, thus distorting the measurements taken. The problem should be remedied as follows. Consider sensor placement as shown in Fig. 2.25. When the sensor is moved to a new position relative to the center of gravity, the rotation of the vehicle as it moves through a turn will affect how the sensor gathers information.

Instead of just measuring the lateral and longitudinal speeds of the vehicle, the measured values are as shown in Eqns. 2.78 and 2.79.

$$V_{measured} = V + ry \tag{2.78}$$

$$U_{measured} = U + rx \tag{2.79}$$

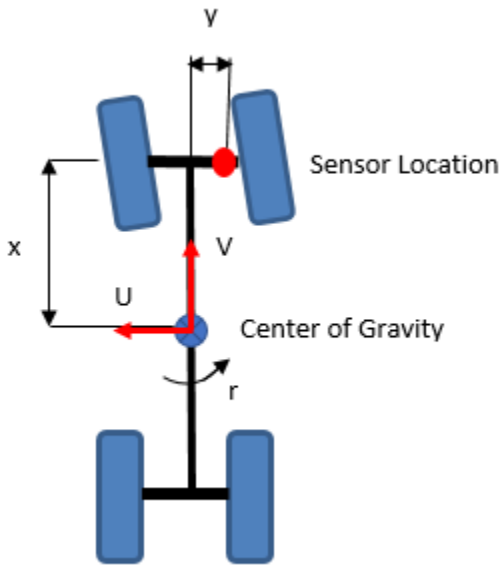

Figure 2.25 Accounting for Sensor Location

The sensor would also feel acceleration effects as described by Eqns. 2.80 and 2.81.

$$a_{longitudinal} = \dot{V} - rU \tag{2.80}$$

$$a_{lateral} = \dot{U} + rV \tag{2.81}$$

Equations 2.80 and 2.81 are derived using a more general acceleration equation used to find the acceleration as shown in Eqn. 2.82 (Karnopp and Margolis, 2008).

$$\frac{d\vec{V}}{dt} = \left(\frac{\partial \vec{V}}{\partial t}\right)_{relative} + \omega \times \vec{V} \tag{2.82}$$

Note that there is no term due to the change in yaw rate because in constant cornering the yaw rate is fixed by the radius of the turn and the longitudinal speed of the vehicle (see Eqn. 2.57).

Note that even if the acceleration effects and the coefficient of friction were accounted for, the cornering stiffness may still be far from theoretical results. Various tire manufacturers and vehicle designers have testing equipment devoted to tires in order to properly characterize road-tire friction, contact area, angle of the tire, and other configurations that cannot be easily described by the rough methods described in this section (Sakai, 1981).

2.8.4 Simulation Vehicles

The previous sections have shown that the experimental results for the cornering stiffness are questionable, so the method described by Wong will be used to find the stiffness values for the test vehicles. Three test vehicles will be simulated. One vehicle will have parameters based on the car described in Section 2.8.1. However, instead of being neutrally-steered, the vehicle will have increased weight in the rear. This is to simulate the effect of modifying a stock vehicle. A hypothetical neutrally-steered car and an understeered vehicle based on a Porsche 928 will also be simulated.

2.8.4.1 Oversteered Vehicle Parameters

The oversteered vehicle (called test vehicle one) has a mass of 1724 kilograms, total length of 2.77 meters, and width of 1.92 meters. The mass distributed towards the front of the car is equal to 784 kilograms and 940 kilograms to the rear. The length a of 1.51 meters and length b of 1.26 meters are calculated using Eqns. 2.73 and 2.74. The cornering stiffness of the front and rear tires are calculated in Eqns. 2.83 and 2.84.

$$C_{\alpha r} = \left(0.19\frac{1}{\text{deg}}\right) * \left(\frac{940kg}{2}\right) * \left(9.81\frac{m}{s^2}\right) * \left(\frac{180\ deg}{\pi\ radians}\right) = 100\ kN/rad \quad (2.83)$$

$$C_{\alpha f} = \left(0.19\frac{1}{deg}\right) * \left(\frac{784kg}{2}\right) * \left(9.81\frac{m}{s^2}\right) * \left(\frac{180\ deg}{\pi\ radians}\right) = 84\ kN/rad \quad (2.84)$$

The moment of inertia about the z-axis of the vehicle is calculated using the moment of inertia of a rectangle about its center and a factor to account for the rear-ward placement of center of gravity as shown in Eqn. 2.85 (Hibbeler, 2013).

$$I_z = \frac{1}{12}(mass) * ((length)^2 + (width)^2) + mass * (a-b)^2 \\ = 1.74 * 10^3\ kg * m^2 \tag{2.85}$$

The stability factor of the vehicle is found using Eqn. 2.63 to be -2.2*10^{-5} kilograms per meter. Note that stability factors are often small. Jazar gives an example in his text where the stability factor of an oversteered vehicle which is on the order of 10^{-4} (Jazar, 2008).

2.8.4.2 Neutral Steer Vehicle

In reality, no car is perfectly neutral steer. There is no agreed upon range that a vehicle must fall between in order to be considered neutrally-steered. In fact, a neutral steer car is a case that is best used to analyze the theoretical motion of a vehicle.

For the neutral steer test vehicle two, data based on a Porsche 928 will be modified to give a neutral steer car. Consider a car with mass equal to 1450 kilograms, a length of 2.5 meters, and a track width of 1.6 meters. Since the vehicle is neutral steer, a and b are equal to 1.25 meters. The cornering stiffness of the front and rear tires will be the same, and are calculated using the same procedure in the last section. The stiffness is 39 kilo-Newtons per radian. The moment of inertia is 1.06*10^3 kilograms times meters squared. The stability factor is zero, because of the set-up of the example (Campbell, 1981).

2.8.4.3 Understeered Vehicle

Vehicle three is more closely based on a Porsche 928. It has the same mass of vehicle two of 1450 kilograms and the same width of 1.6 meters and length of 2.5 meters. Although a real Porsche 928

has a forward-wheel drive configuration with the engine in the front of the vehicle, the car is oversteered. In this example, the weight ratio of an actual Porsche 49-to-51 will be reversed to 51-to-49 give an understeered vehicle. This gives a length a of 1.23 meters and a length b of 1.28 meters. The cornering stiffness of the front tire is 39 kilo-Newtons per radian and 38 kilo-Newtons per radian in the rear. The moment of inertia is $1.07*10^3$ kilograms times meters squared and the stability factor is $1.35*10^{-4}$ kilograms per meter (Campbell, 1981).

2.8.5 Simulation Results

Equations 2.41 and 2.42 can be rewritten in terms of the yaw rate r and the lateral velocity U using Eqns. 2.57 and 2.36 and put into a matrix form that is easier for coding shown in Eqn. 2.86.

$$\begin{bmatrix} \dot{r} \\ \dot{U} \end{bmatrix} = \begin{bmatrix} \frac{-C_{\alpha r}b^2}{IV} - \frac{C_{\alpha f}a^2}{IV} & \frac{-C_{\alpha f}a}{IV} + \frac{bC_{\alpha r}}{IV} \\ \frac{C_{\alpha r}b}{mV} - \frac{C_{\alpha f}a}{mV} - V & \frac{-C_{\alpha r}}{mV} - \frac{C_{\alpha f}}{mV} \end{bmatrix} \begin{bmatrix} r \\ U \end{bmatrix} + \begin{bmatrix} \frac{C_{\alpha f}a}{I} \\ \frac{C_{\alpha f}}{m} \end{bmatrix} \delta \qquad (2.86)$$

Holding the steering angle at five degrees, keeping the longitudinal velocity constant at 35 miles per hour, and using zero initial conditions gives the output shown in Figs. 2.26, 2.27, and 2.28 for the three vehicles. The constants shown for the three vehicles are shown in Table 2.5.

Table 2.5 Two-Wheel Simulation Constants

Constants	Oversteer	Neutral Steer	Understeer
mass (kg)	1724	1450	1450
length (m)	2.77	2.5	2.5
a (m)	1.51	1.25	1.23
b (m)	1.26	1.25	1.28
width (m)	1.92	1.6	1.6
Cr (kN/rad)	100	39	38
Cf (kN/rad)	84	39	39
Iz ($kg*m^2$)	$1.74*10^3$	$1.06*10^3$	$1.07*10^3$

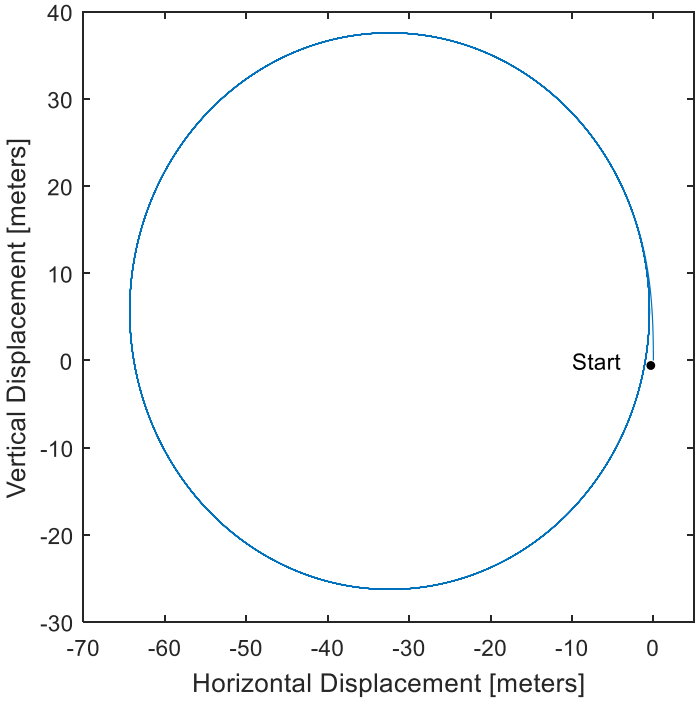

Figure 2.26 Oversteer Vehicle One Response to Constant Steering Angle and Longitudinal Velocity

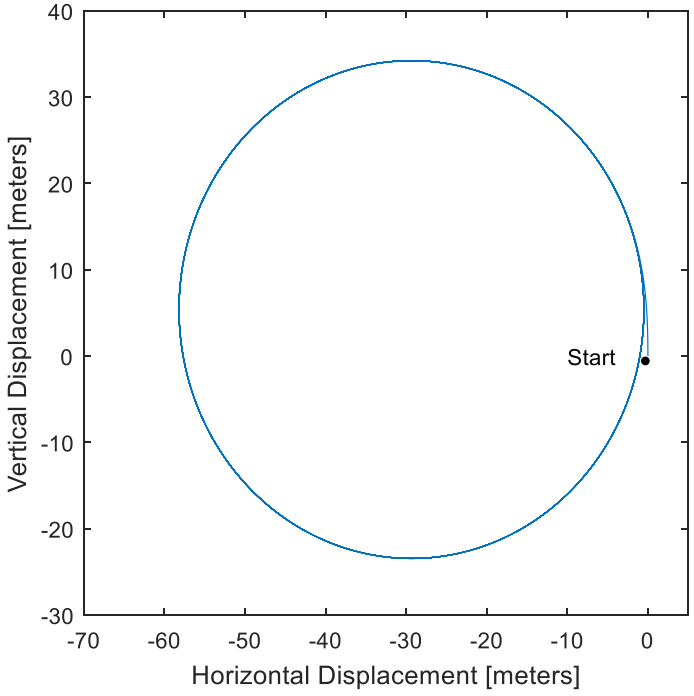

Figure 2.27 Neutral Steer Vehicle Two Response to Constant Steering Angle and Longitudinal Velocity

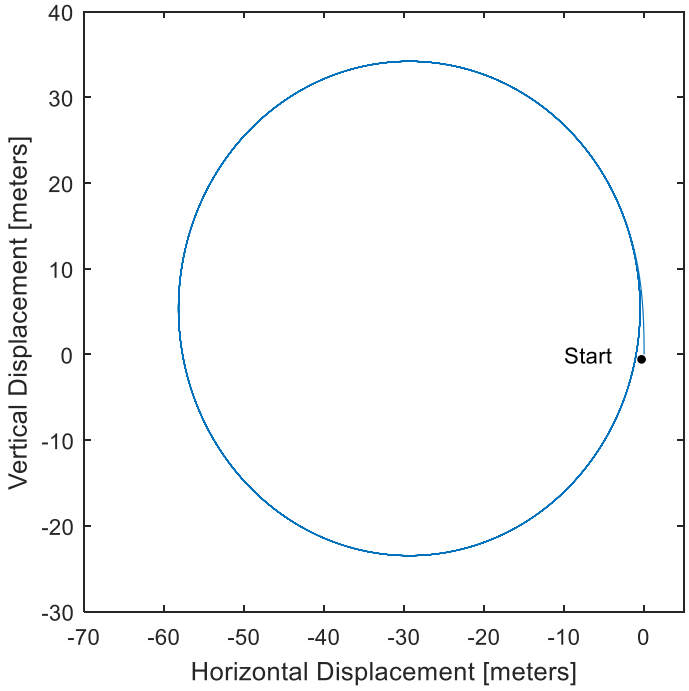

Figure 2.28 Understeer Vehicle Three Response to Constant Steering Angle and Longitudinal Velocity

It is interesting to note that the oversteered vehicle three travels in a wider circle than the understeered vehicle. This can be explained by looking at Eqns. 2.18 and 2.23. For a given steering angle, the understeered vehicle will have a steering angle and effect due to slip angles that gives it a larger overall Ackermann steering angle. The opposite is true for the oversteered vehicle, which will have a smaller Ackermann steering angle once slip angles are involved at greater speeds. According to Eqn. 2.10, the Ackermann steering angle is inversely proportional to the radius of the turn. Since the oversteered vehicle has a lower overall steering angle, it will move in a larger circular path than the understeered vehicle.

The yaw rate of the vehicles is important to analyze as well, because it gives insight to passenger comfort and stability of the car. If the yaw rate is too large, the car is likely to spin out of a turn. Also, the spinning sensation will be uncomfortable. Figures 2.29, 2.30, and 2.31 show the yaw rates of vehicle one, two, and three.

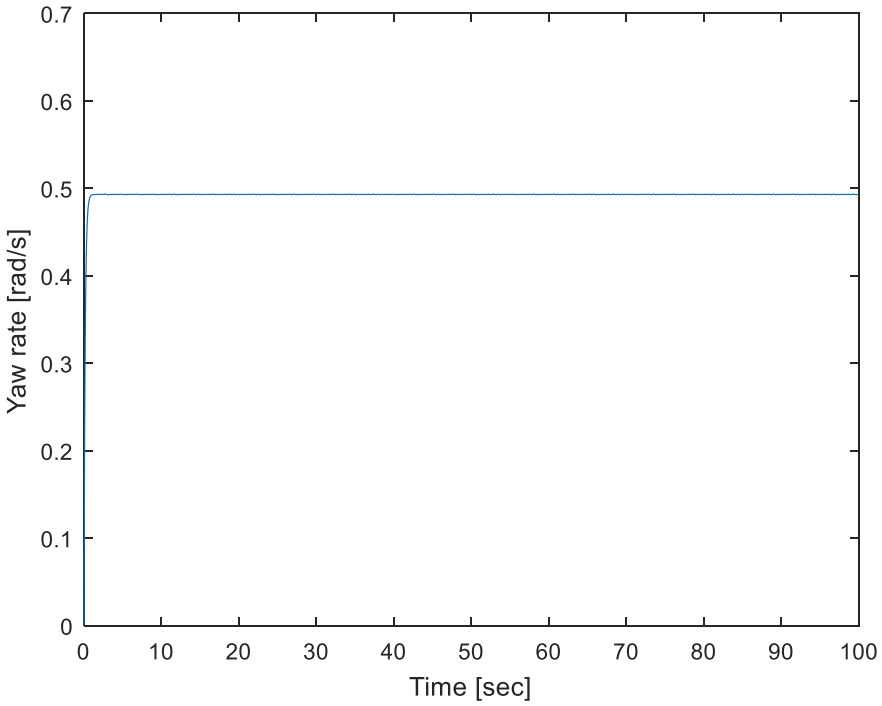

Figure 2.29 Vehicle One Yaw Rate

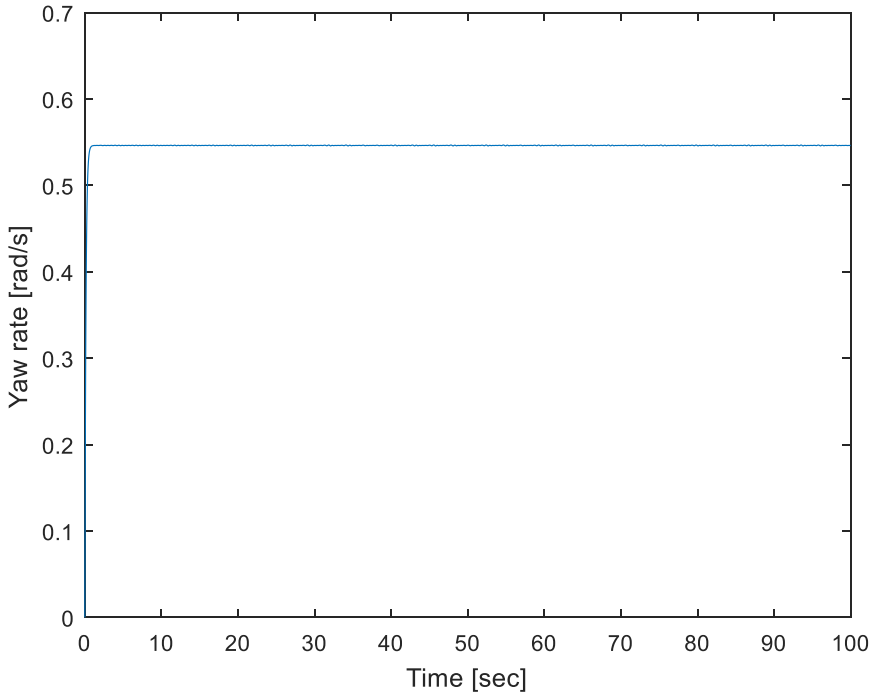

Figure 2.30 Vehicle Two Yaw Rate

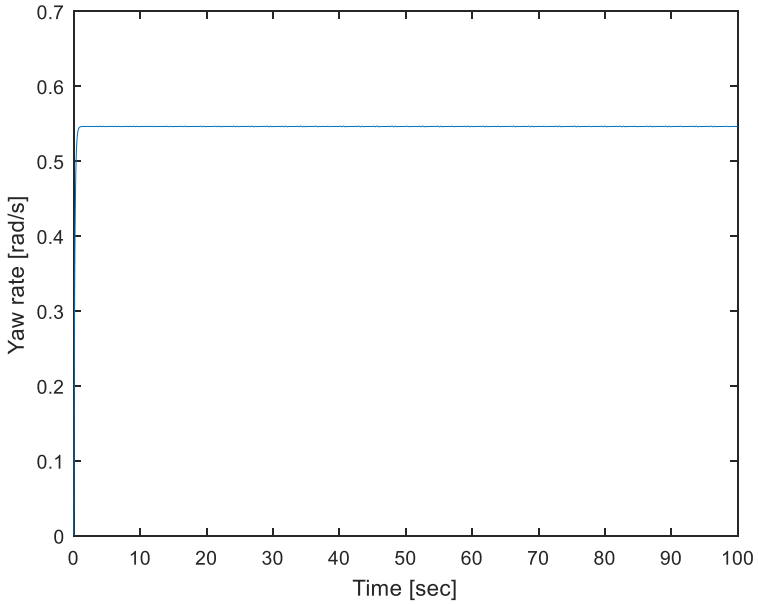

Figure 2.31 Vehicle Three Yaw Rate

The yaw rate stays constant, even after a few seconds due to the steady turning behavior of the vehicles. Note that the oversteer vehicle has a lower yaw rate than the other two vehicles. Equations 2.5, 2.18, 2.23, and 2.57 show that an understeered car with a larger Ackermann steering angle will have a smaller turn radius and thus a larger yaw rate. An oversteered vehicle will have a smaller Ackermann steering angle, larger turn radius, and smaller yaw rate. See Appendix B for additional simulations and Appendix D for a two-wheel model code.

Chapter 3. FOUR-WHEEL MODEL

The two-wheel model described in the last chapter is helpful for determining a rough estimate of the behavior of a vehicle. However, to develop a more accurate display of a car's path, a four-wheel model must be used. All of the parameters from the two-wheel model are valid, except there are added symbols for the slip angles at each tire. This model will also cover longitudinal dynamics from wind resistance and from climbing a hill. The added parameters are shown in Table 3.1.

Table 3.1 Additional Symbols

Term	Symbol
Front left slip angle	α_{11}
Front right slip angle	α_{12}
Rear left slip angle	α_{21}
Rear right slip angle	α_{22}
Torque applied to left rear wheel	T_{21}
Torque applied to right rear wheel	T_{22}
Longitudinal coefficient of friciton	μ
Front Area	A
Drag Coefficient	C_d
Air Density	ρ

This chapter will also discuss modeling the car without assuming a constant applied speed. Instead, models will use torque inputs to drive the rear wheels of the vehicle.

3.1 VEHICLE AERODYNAMICS

Vehicle aerodynamics are important to include in a complete model. The effect of air resistance on a vehicle is proportional to the area of the vehicle that pushes through the air, the density of the air, a drag coefficient, and the velocity squared of the vehicle (see Eqn. 3.1).

$$F_{drag} = \frac{1}{2}\rho A C_D V^2 \tag{3.1}$$

There are different values for the drag coefficient and area of a vehicle depending on the shape and size of the car. For a medium to large vehicle, typical values for the drag coefficient range from 0.30 to 0.42 and area that ranges from 1.90 to 2.16 square meters. Here, a median value of 0.36 will be used for the drag coefficient and 2.03 square meters will be used for the area. The density of air will vary depending on the elevation, humidity, and temperature. Here a value of 1.225 kilograms per meter cubed will be used. This corresponds to a temperature of fifteen degrees Celsius and a pressure of 101.32 kilo-Pascals.

Note that vehicle manufacturers will find more specialized values for the drag coefficient through testing. One test that is more feasible is the coast-down test. The test involves bringing the vehicle up to a known speed, and then letting it decelerate. As it decelerates, the speed of the vehicle is recorded and later used to determine the drag on the vehicle (Wong, 2008).

3.2 LONGITUDINAL DYNAMICS

Longitudinal dynamics, or travelling up a hill, affect the forces on the tires of a vehicle. See Fig. 3.1 for a diagram of a vehicle moving up an inclined surface. The forces on the front and rear wheels can be found by taking the sum of the forces in the z-direction and the sum of the moments in the y-direction (see Eqns. 3.2 and 3.3). The friction forces on the front and rear tires are approximated by the normal force on the tires times a coefficient of friction.

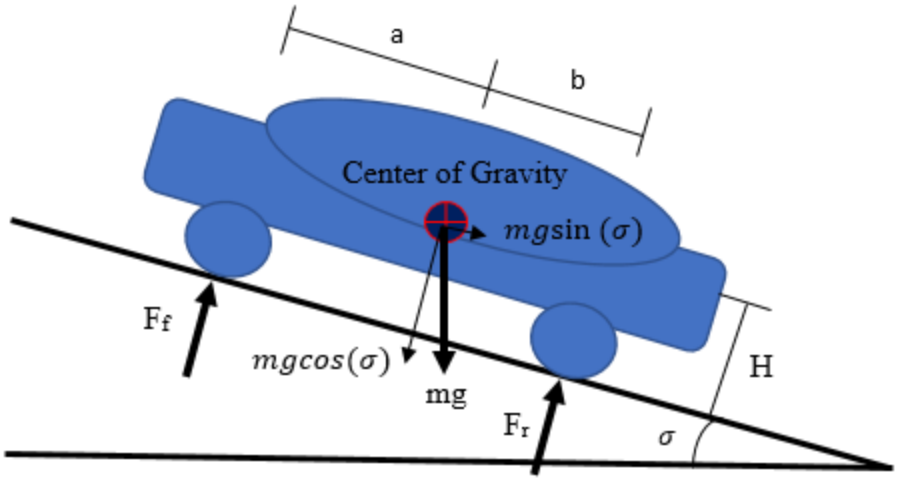

Figure 3.1 Vehicle Moving Up Inclined Surface

$$\sum F_z = 0: \quad F_f + F_r - mg\cos(\sigma) = 0 \tag{3.2}$$

$$\sum M_{y-axis} = 0: \quad F_f \mu H + F_r \mu H + F_r b - F_f a = 0 \tag{3.3}$$

Solving Eqns. 3.2 and 3.3 gives equations for the front and rear forces as shown in Eqns. 3.4 and 3.5 (Dixon, 1996).

$$F_r = \frac{amg\cos(\sigma) - \mu Hmg\cos(\sigma)}{L} \tag{3.4}$$

$$F_f = \frac{\mu Hmg\cos(\sigma) + bmg\cos(\sigma)}{L} \tag{3.5}$$

Values of coefficients of friction will vary depending on road conditions, but as a conservative estimate of rubber to concrete interaction, a value of 0.8 will be used (Serway and Jewett, 2010).

Note that the height of the center of gravity from the ground must be accounted for. This can be determined experimentally by using a car trailer to provide an inclined surface. Scales can be placed on the trailer, and the car placed on the scales. This will shift the weight on the front and rear tires. Equations 3.2 and 3.3 can then be used to determine the height of the center of gravity. Note that the vehicle will have to be constrained physically so that is does not roll off of the trailer.

This means that the friction forces are no longer keeping the vehicle in place, and they will be ignored when doing calculations (Milliken, 1995).

3.3 Four-Wheel Model Description

The four-wheel model is more complex than the two-wheel model because it involves slip angles and forces on each of the four tires. See Fig. 3.2 for a diagram of the model.

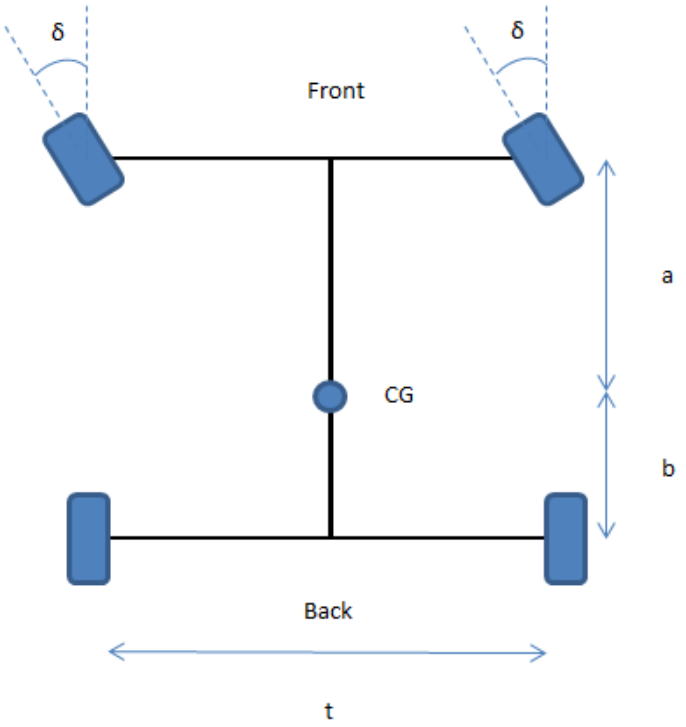

Figure 3.2 Four-Wheel Vehicle Diagram

Note that both front wheels have an applied steering angle δ. The width of the car is designated by t. As before, a and b are the lengths from the front and rear to the center of gravity. The forces on the tires that propel the vehicle forward are modeled as perpendicular to the tire length and width as shown in Fig. 3.3. The forces shown in Fig. 3.3 can be resolved into vectors pointing in the x- and y-directions as shown in Fig. 3.4. Figure 3.4 can be used to write the equations of motion.

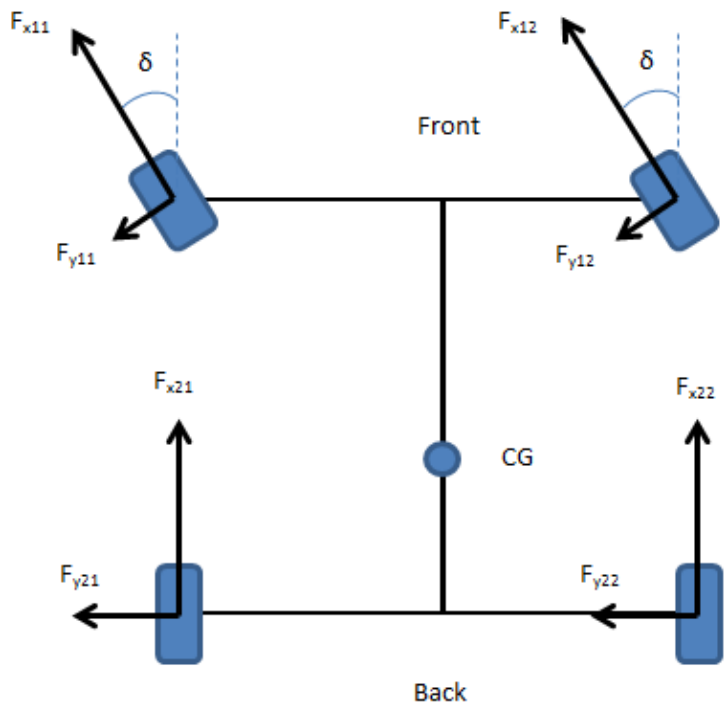

Figure 3.3 Four-Wheel Force Diagram

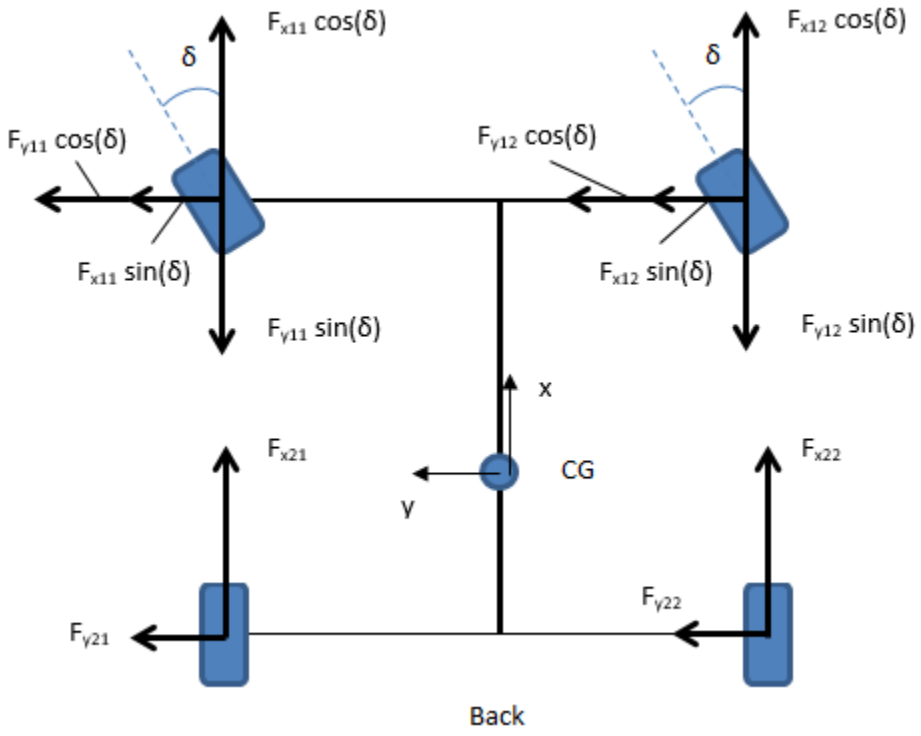

Figure 3.4 Four-Wheel Force Resolution Diagram

The sum of the moments, sum of the lateral forces, and sum of the longitudinal forces are shown in Eqns. 3.6, 3.7, and 3.8.

$$\sum M_z\colon I\dot{r} = (F_{x12}\cos\delta)\frac{t}{2} - \left(F_{y12}\sin\delta\right)\frac{t}{2} + (F_{x12}\sin\delta)a + \left(F_{y12}\cos\delta\right)a + \left(F_{y11}\cos\delta\right)a + (F_{x11}\sin\delta)a - (F_{x11}\cos\delta)\frac{t}{2} + \left(F_{y11}\sin\delta\right)\frac{t}{2} - F_{x21}\frac{t}{2} - F_{y21}b - F_{y22}b + F_{x22}\frac{t}{2} \tag{3.6}$$

$$\sum F_y\colon \left(F_{y21} + F_{y22}\right) + \cos\delta\left(F_{y11} + F_{y12}\right) + \sin\delta\left(F_{x11} + F_{x12}\right) = m(\dot{U} + Vr) \tag{87}$$

$$\sum F_x\colon F_{x21} + F_{x22} + \cos\delta\left(F_{x11} + F_{x12}\right) - \sin\delta\left(F_{y11} + F_{y12}\right) - \frac{1}{2}\rho C_d A V^2 = m(\dot{V} - Ur) \tag{88}$$

The tire forces in Eqns. 3.6, 3.7, and 3.8 can be written in terms of the tire slip angles. A diagram of the tire slip angles is shown in Fig. 3.5 and a diagram showing the velocity vector resolution at each tire is shown in Fig. 3.6. The velocity vector resolution shown in Fig. 3.6 is used to write the slip angles as shown in Eqns. 3.9, 3.10, 3.11, and 3.12.

$$tan(\delta + \alpha_{11}) = \frac{U + ra}{V - r\left(\frac{t}{2}\right)} \tag{3.9}$$

$$tan(\delta + \alpha_{12}) = \frac{U + ra}{V + r\left(\frac{t}{2}\right)} \tag{3.10}$$

$$tan(\alpha_{21}) = \frac{U - rb}{V - r\left(\frac{t}{2}\right)} \tag{3.11}$$

$$tan(\alpha_{22}) = \frac{U - rb}{V + r\left(\frac{t}{2}\right)} \tag{3.12}$$

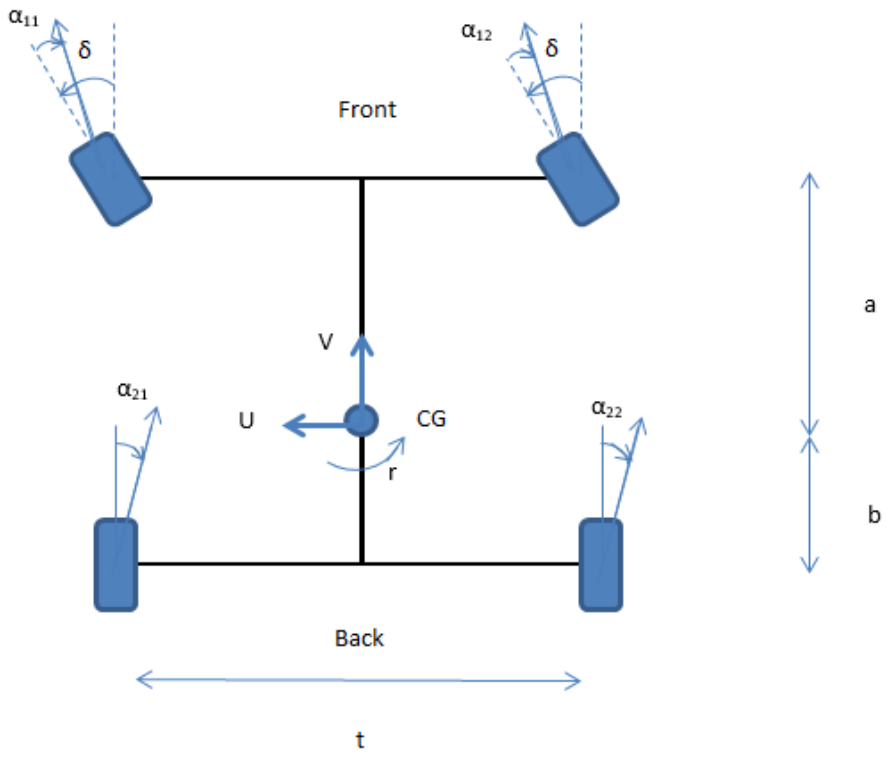

Figure 3.5 Slip Angle Diagram

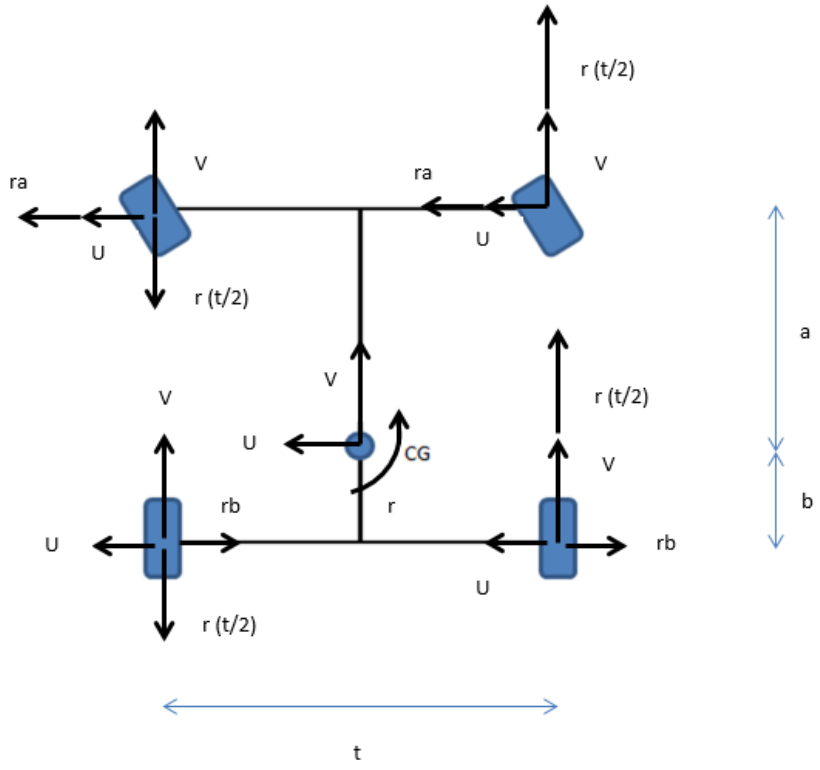

Figure 3.6 Four-Wheel Velocity Vector Diagram

Equations 3.6 through 3.12 can be linearized assuming small angles. Linearized equations for the sum of the moments in the z-direction, sum of the forces in the y-direction, and sum of the forces in the x-direction are shown in Eqns. 3.13, 3.14, and 3.15.

$$\sum M_z\colon I\dot{r} = (F_{x12})\frac{t}{2} - (\delta F_{y12})\frac{t}{2} + (\delta F_{x12})a + (F_{y12})a + (F_{y11})a + (\delta F_{x11})a - (F_{x11})\frac{t}{2} + (\delta F_{y11})\frac{t}{2} - F_{x21}\frac{t}{2} - F_{y21}b - F_{y22}b + F_{x22}\frac{t}{2} \tag{3.13}$$

$$\sum F_y\colon (F_{y21} + F_{y22}) + (F_{y11} + F_{y12}) + \delta(F_{x11} + F_{x12}) = m(\dot{U} + Vr) \tag{3.14}$$

$$\sum F_x\colon F_{x21} + F_{x22} + F_{x11} + F_{x12} - \delta(F_{y11} + F_{y12}) - \frac{1}{2}\rho C_d A V^2 = m(\dot{V} - Ur) \tag{3.15}$$

Each rear tire will be driven by applying a torque to the wheels. This is modeled using Eqns. 3.16 and 3.17.

$$I_w\dot{\omega}_{21} = T_{21} - RF_{x21} \tag{3.16}$$

$$I_w\dot{\omega}_{22} = T_{22} - RF_{x22} \tag{3.17}$$

Assuming that the moment of inertia of the tires is small, the rear tire force created by a torque input can be simplified as shown in Eqns. 3.18 and 3.19.

$$F_{x21} = \frac{T_{21}}{R} \tag{3.18}$$

$$F_{x22} = \frac{T_{22}}{R} \tag{3.19}$$

The slip angles of the tires can be linearized as shown in Eqns. 3.20 through 3.23.

$$\alpha_{11} = \frac{U + ra}{V - r\left(\frac{t}{2}\right)} - \delta \tag{3.20}$$

$$\alpha_{12} = \frac{U + ra}{V + r\left(\frac{t}{2}\right)} - \delta \tag{3.21}$$

$$\alpha_{21} = \frac{U - br}{V - r\left(\frac{t}{2}\right)} \tag{3.22}$$

$$\alpha_{22} = \frac{U - br}{V + r\left(\frac{t}{2}\right)} \tag{3.23}$$

The normal forces on both of the front and rear tires is shown in Eqns. 3.4 and 3.5. The friction force on each individual tire will oppose motion and will be proportional to the coefficient of friction times the normal force on the vehicle. The sign of the friction force can be calculated by dividing the longitudinal speed of the vehicle by the magnitude of the longitudinal speed and multiplying by a negative sign. See Eqns. 3.24 through 3.27 for the individual forces on each tire due to friction.

$$Friction_{x11} = -\mu \frac{V}{|V|}\left(\frac{\mu Hmgcos(\sigma) + bmgcos(\sigma)}{2L}\right) \tag{3.24}$$

$$Friction_{x12} = -\mu \frac{V}{|V|}\left(\frac{\mu Hmgcos(\sigma) + bmgcos(\sigma)}{2L}\right) \tag{3.25}$$

$$Friction_{x21} = -\mu \frac{V}{|V|}\left(\frac{amgcos(\sigma) - \mu Hmgcos(\sigma)}{2L}\right) \tag{3.26}$$

$$Friction_{x22} = -\mu \frac{V}{|V|}\left(\frac{amgcos(\sigma) - \mu Hmgcos(\sigma)}{2L}\right) \tag{3.27}$$

The friction forces and the slip angles are substituted into the equations of motion as shown in Eqns. 3.28, 3.29, and 3.30.

$$\sum M_z\colon I\dot{r} = (Friction_{x12})\frac{t}{2} - \delta\left(C_{\alpha f}\alpha_{12}\right)\frac{t}{2} + \delta(Friction_{x12})a + \left(C_{\alpha f}\alpha_{12}\right)a + \left(C_{\alpha f}\alpha_{11}\right)a + \delta(Friction_{x11})a - (Friction_{x11})\frac{t}{2} + \delta\left(C_{\alpha f}\alpha_{11}\right)\frac{t}{2} - (Friction_{x21} + \frac{T_{21}}{R})\frac{t}{2} - C_{\alpha r}\alpha_{21}b - C_{\alpha r}\alpha_{22}b + (Friction_{x22} + \frac{T_{22}}{R})\frac{t}{2} \tag{3.28}$$

$$\sum F_y\colon (C_{\alpha r}\alpha_{21} + C_{\alpha r}\alpha_{22}) + \left(C_{\alpha f}\alpha_{11} + C_{\alpha f}\alpha_{12}\right) + \delta(Friction_{x11} + Friction_{x12}) = m(\dot{U} + Vr) \tag{3.29}$$

$$\sum F_x\colon Friction_{x21} + \frac{T_{21}}{R} + Friction_{x22} + \frac{T_{22}}{R} + Friction_{x11} + Friction_{x12} - \delta C_{\alpha f}(\alpha_{11} + \alpha_{12}) - \frac{1}{2}\rho C_d A V^2 = m(\dot{V} - Ur) \tag{3.30}$$

The equations of motion are used to find the response of the vehicle to constant torque input in the next section (Martino, 2005).

3.4 Four-Wheel Simulation Results: Equal Torque to Rear Wheels

Simulation vehicle one (oversteered) will be used as a test case. Assume that the center of gravity is located at a height of 0.6 meters above the road surface. Note that the center of gravity for most passenger cars will be between 0.45 meters to 0.6 meters (Gillespie, 1992). A larger value for the center of gravity is used as a worst-case scenario for roll, which will be discussed later on in Chapter 4. Using the four-wheel equations of motion, the distance traveled by the vehicle is plotted while giving each rear wheel an equal torque of 1000 Newton-meters (approximately 733 pound-feet). To put this value into perspective, this would be the limit of a high-end sports car. Many cars, such as the Dodge Challenger SRT Hellcat, Tesla Model S, Chevrolet Corvette, Dodge Viper,

or Lamborghini Aventador, would not be able to output enough torque to meet 1000 Newton-meters (Hunting, 2015). This shows that the simulation is meant to describe the response of a powerful vehicle suited for racing, and not that of a commuter vehicle. The simulation output in Figs. 3.7 through 3.10 are for zero grade and 0.1 radians (5.7 degree) steering angle.

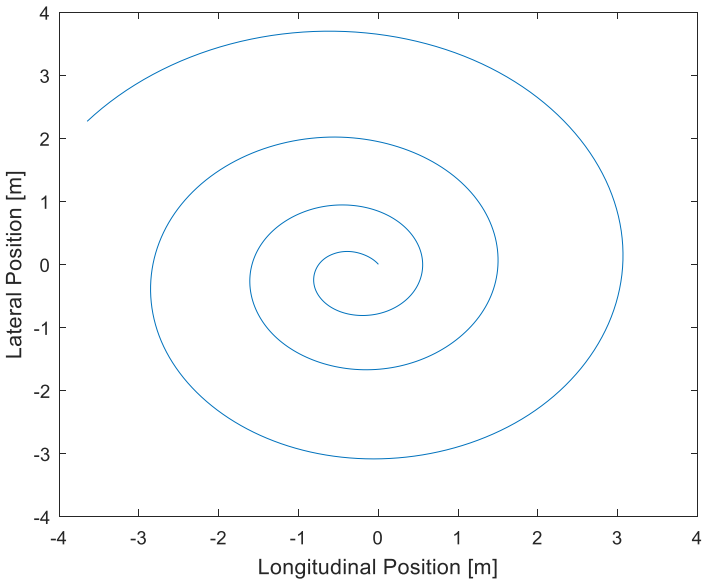

Figure 3.7 X-Y Plot for Constant Torque Output, Zero Grade

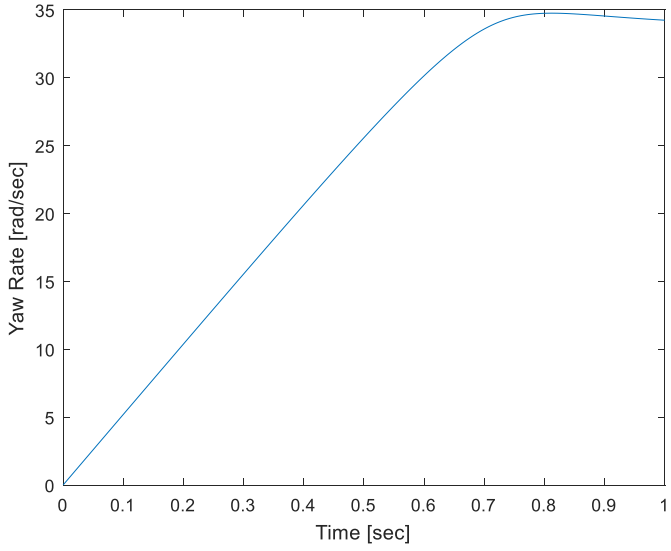

Figure 3.8 Yaw Rate for Constant Torque Output, Zero Grade

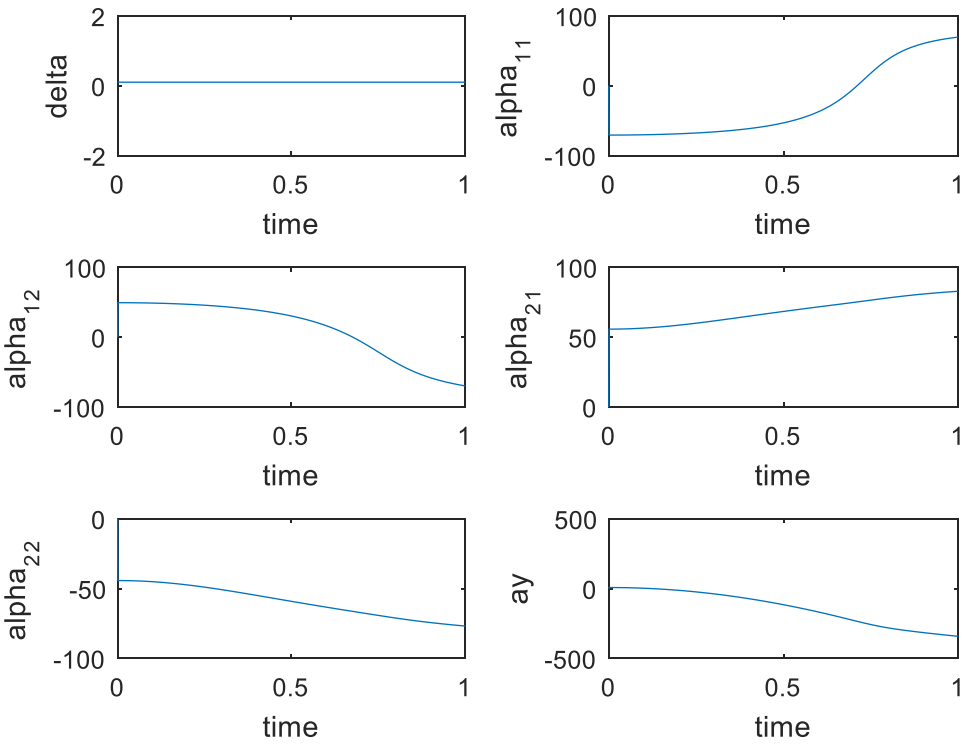

Figure 3.9 Angles for Constant Torque Output, Zero Grade

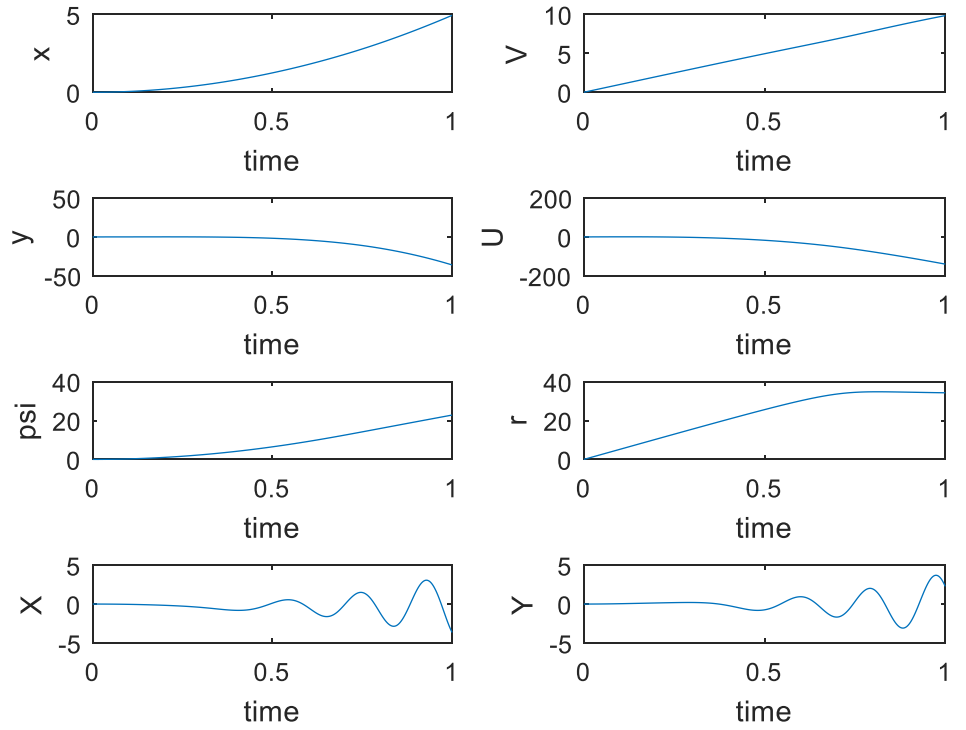

Figure 3.10 State Variables for Constant Torque Output, Zero Grade

Note that the vehicle will have slip angles develop as the speed of the vehicle increases. This occurs very rapidly, as seen in Fig. 3.9, which causes the slip angles to increase in magnitude very quickly. Once the slip angles become large, the small angle assumption is no longer valid. The small angle does not need to be employed, however, and the code used to generate the plots shown in Figs. 3.7 through 3.10 uses trigonometric functions instead of approximations. Although it is more accurate to use trigonometric functions, for longer running codes or real-time algorithms used to control vehicle speed, using trigonometric functions could make the code run longer than desired.

3.5 Four-Wheel Simulation: Different Torque to Rear Wheels

This simulation will use the same vehicle parameters as for Section 3.4. However, the right rear wheel will have 500 Newton-meters of torque applied and the left rear wheel will have 1000 Newton-meters of torque. There will be a 0.1 radian (5.7 degree) steering angle applied on the vehicle. The results are shown in Figs. 3.11 to 3.14.

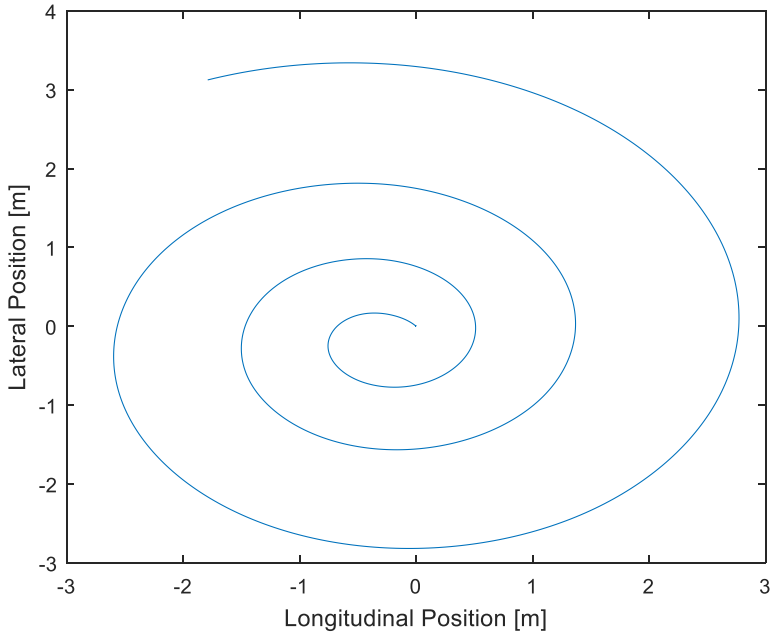

Figure 3.11 X-Y Plot for Differing Torque, Zero Grade

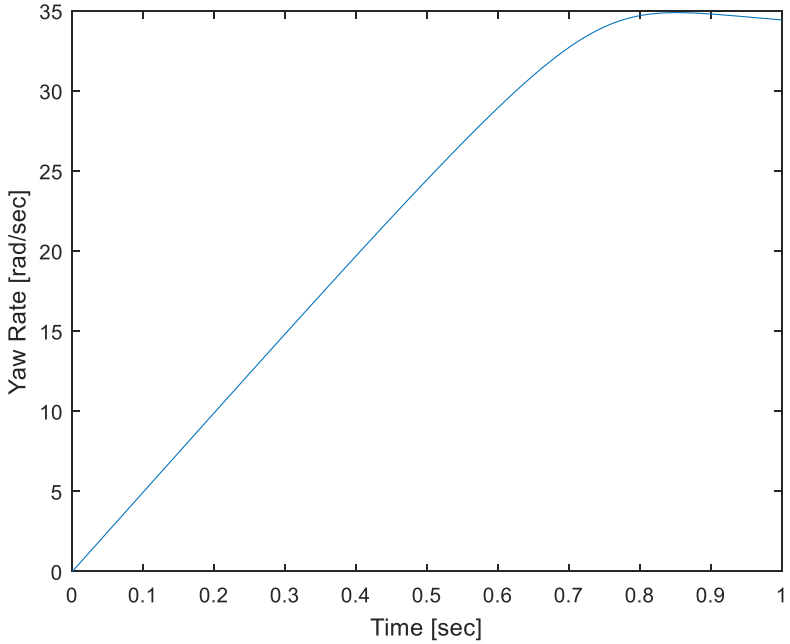

Figure 3.12 Yaw Rate Plot for Differing Torque, Zero Grade

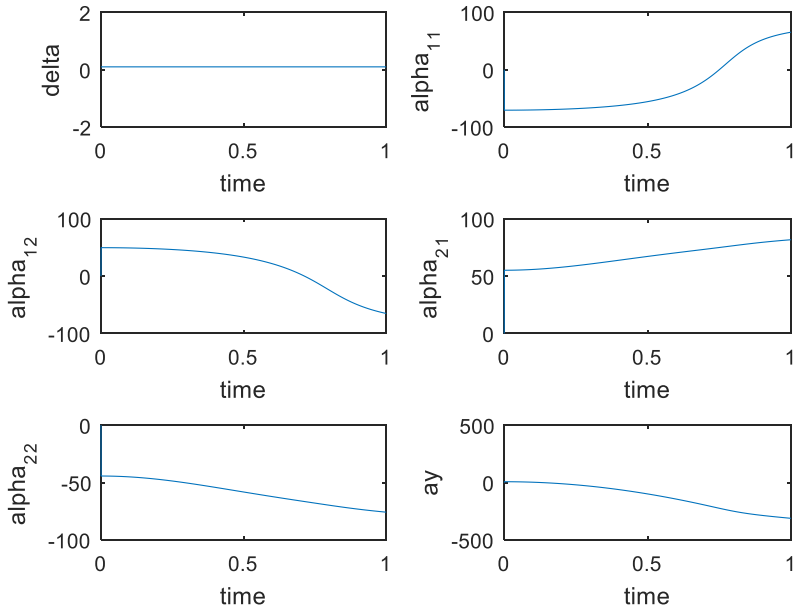

Figure 3.13 Angles Plot for Differing Torque, Zero Grade

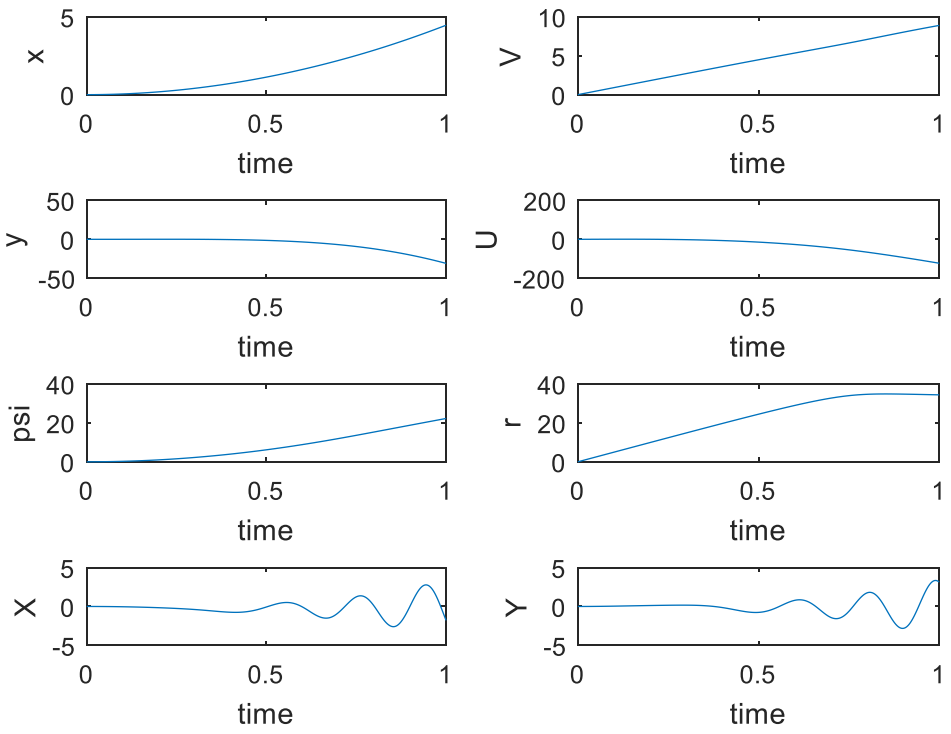

Figure 3.14 State Variables for Differing Torque, Zero Grade

The car has a very similar response as in the previous section. The slip angles are very similar to the values for equal torque to both rear wheels, as is the yaw rate graph. However, the trajectory shown in Fig. 3.11 is not as large as the trajectory shown in Fig. 3.7. This makes physical sense, because the tires are supplied with less torque which reduces the force of the tires on the pavement and slows down the vehicle.

3.6 Four-Wheel Model Simulation: Equal Torque and Grade

Consider the oversteered vehicle one as it enters a mountain road. As the vehicle moves up the spiraling road to the top of the mountain, more torque will need to be supplied or the vehicle will slow down and move less than it did on flat pavement. This simulation will use a 0.1 radian steering angle, 500 Newton-meter torque to the rear wheels, and a grade of 0.2 radians (about 11 degrees). The results are shown in Figs. 3.15 to 3.18.

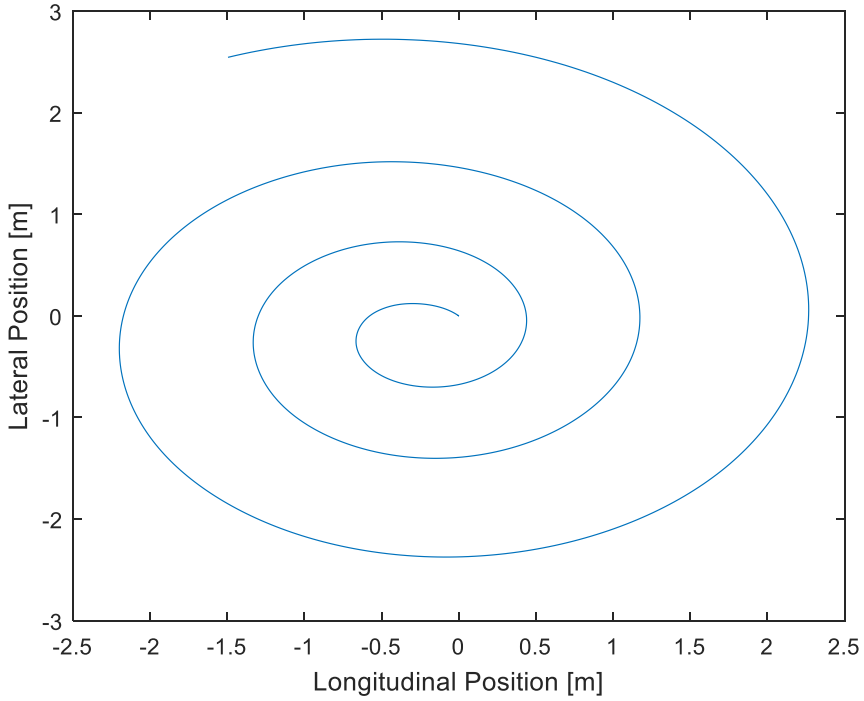

Figure 3.15 X-Y Plot for Equal Torque, Grade

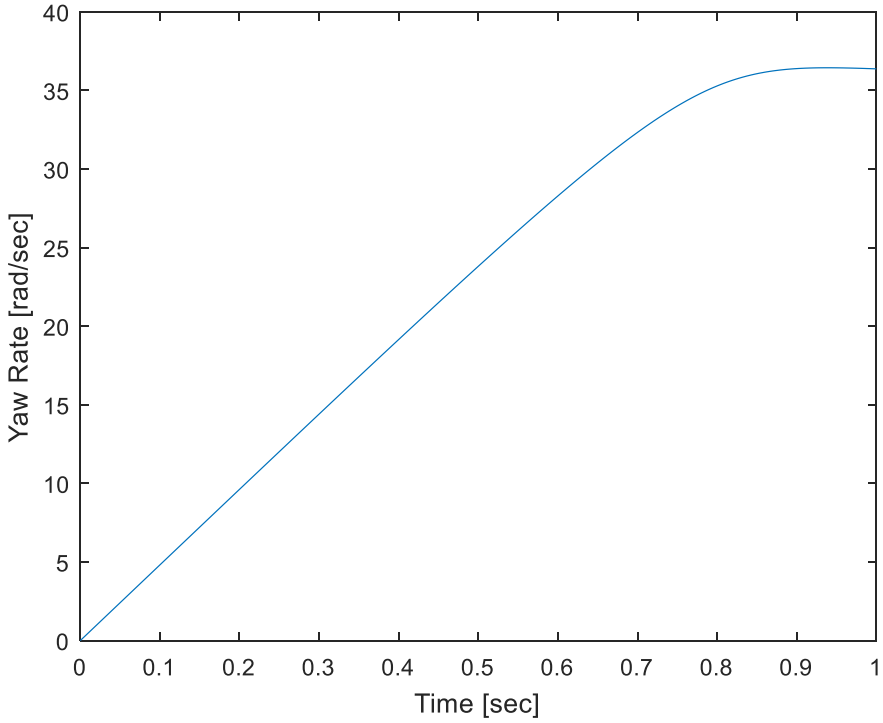

Figure 3.16 Yaw Rate Plot for Equal Torque, Grade

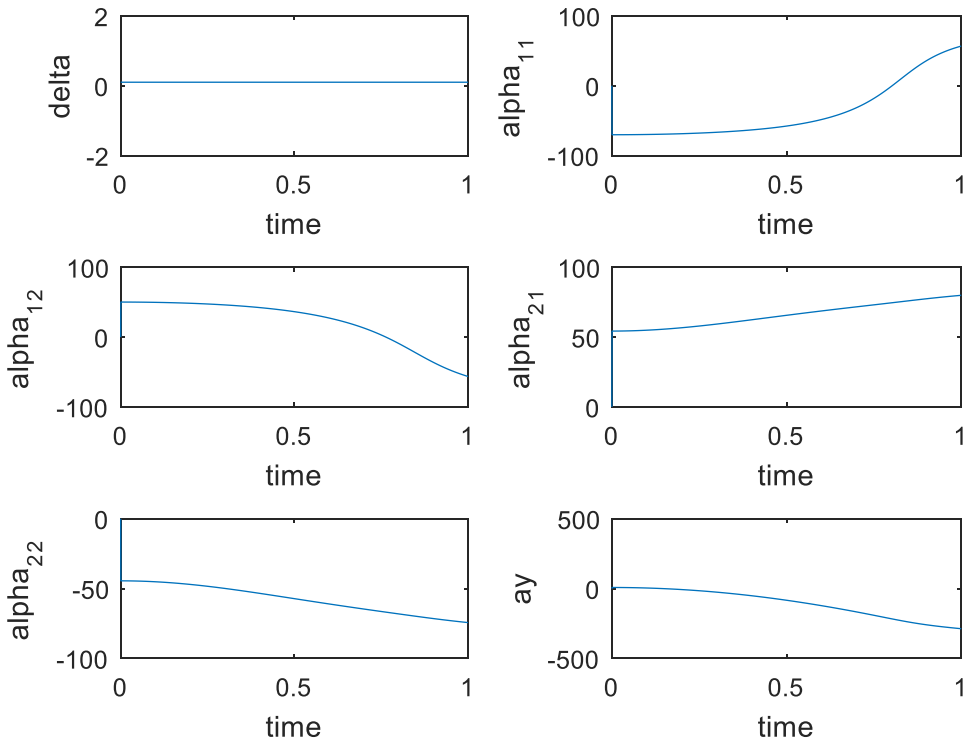

Figure 3.17 Angles Plot for Equal Torque, Grade

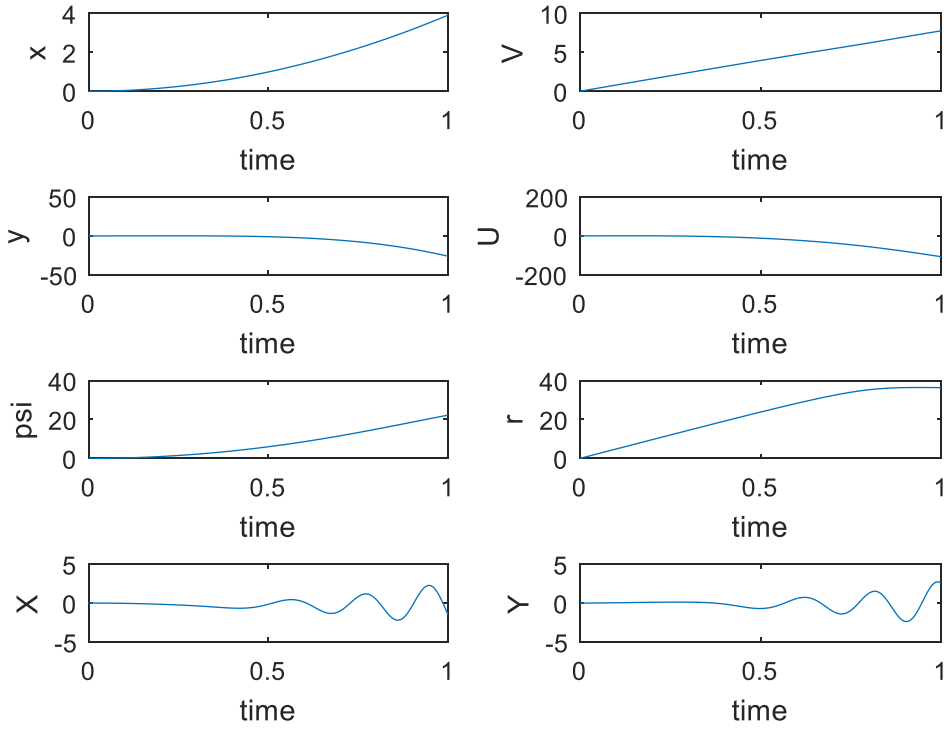

Figure 3.18 State Variables Plot for Equal Torque, Grade

The vehicle will move less longitudinally than the other simulated vehicles as it maneuvers up the grade because it is moving vertically as well. Note, however, that a 0.2 radian grade still allows the car to move up the hill quickly because a large 500 Newton-meter torque is applied to each of the rear wheels. It is also interesting to observe that the yaw rate is larger in this simulation than for other simulated scenarios. Recall that the yaw rate for an oversteered vehicle can increase to unstable quantities, but not in the case of an oversteered vehicle. An oversteered vehicle has greater loading on the rear tires than in the front tires. Maneuvering up an incline could exacerbate the oversteered characteristics of the vehicle by putting more weight on the rear tires and increasing the yaw rate. This simulation shows that if a control logic is implemented to reduce the yaw rate of a vehicle, care should be taken to include the effect of moving up an incline. For reference, additional four-wheel model simulations are given in Appendix C and code in Appendix E.

3.7 FOUR-WHEEL MODEL: LANE CHANGE

This simulation looks at the response of a vehicle moving into another lane of traffic. The goal is to keep the vehicle moving at 60 miles per hour (about 26 meters per second). Proportional controls are used to keep the difference between the actual longitudinal speed and the desired longitudinal speed close to one another (see Eqn. 3.31). The steering angle is also changed using proportional controls (see Eqn. 3.32). The value K (not to be confused with the stability factor) changes depending on the time of the simulation. At first, K is equal to one indicating that the vehicle should move over into another lane by one meter. Afterwards, the vehicle is moved back into the original lane by changing K to negative one to indicate that the car should move one meter laterally in the negative direction. The last step in the simulation for changing the steering angle sets K equal to zero to keep the car in one lane. The second half of the equation uses a term that controls

how far the vehicle moves relative to the centerline. This term is to give the vehicle added stability while maneuvering the lane change.

$$Motor\ torque = Gain * (V_{desired} - V_{actual}) \tag{3.31}$$

$$\delta = Gain_1 * (K - Lateral\ Position) + Gain_2 * (Lateral\ Position - Center\ line) \tag{3.32}$$

The vehicle properties used in the last section are carried over to this simulation, with the exception that no grade is induced. However, this simulation adds in a term for the rolling resistance of the tires. Rolling resistance partially accounts for the longitudinal deformation of the tires. Unlike many coefficients that describe tire deflection, rolling resistance is present as soon as the car begins to roll. Rolling resistance can be very difficult to measure experimentally, because it is dependent on many factors. Tire temperature, tire pressure, load, velocity, road surface, tire age, tire material, tire thickness, and other deflection caused by braking and cornering all have a part in determining the rolling resistance of a tire. An estimate of the rolling resistance of a passenger vehicle tire on a medium hard road is 0.08 (Gillespie, 1992). The rolling resistance is factored into the model for the four-wheel vehicle, and the results are shown in Figs. 3.19 to 3.22. Code is provided in Appendix F.

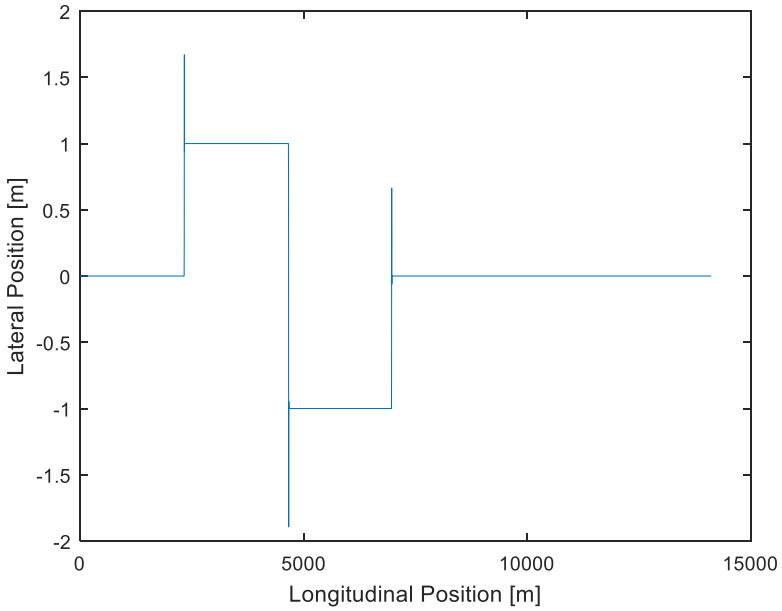

Figure 3.19 X-Y Plot for Lane Change

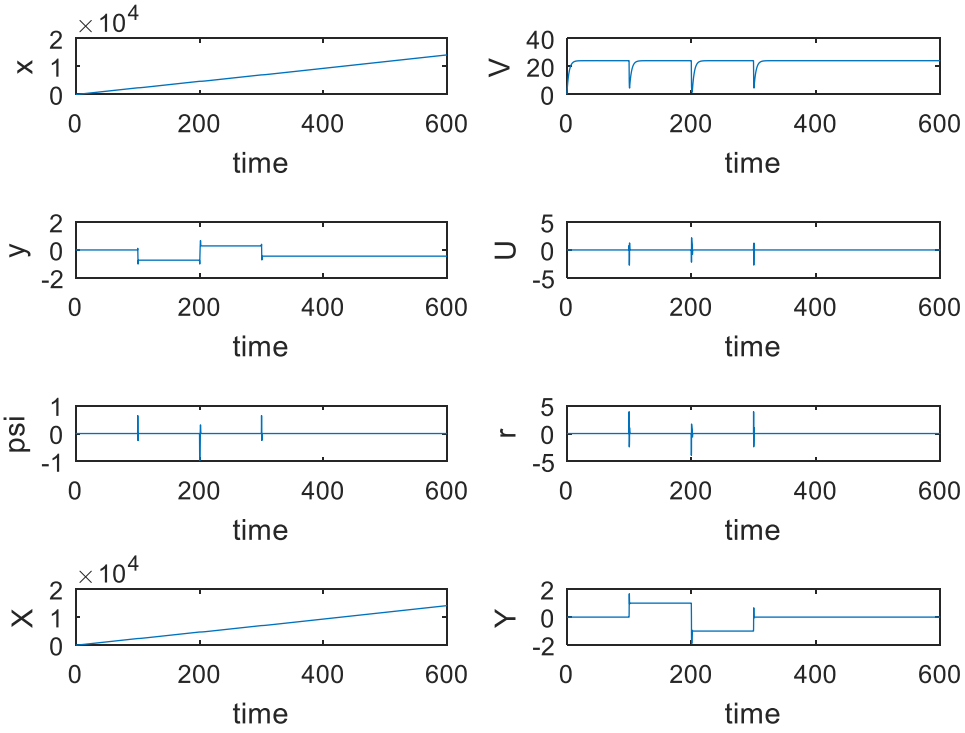

Figure 3.20 State Variables for Lane Change

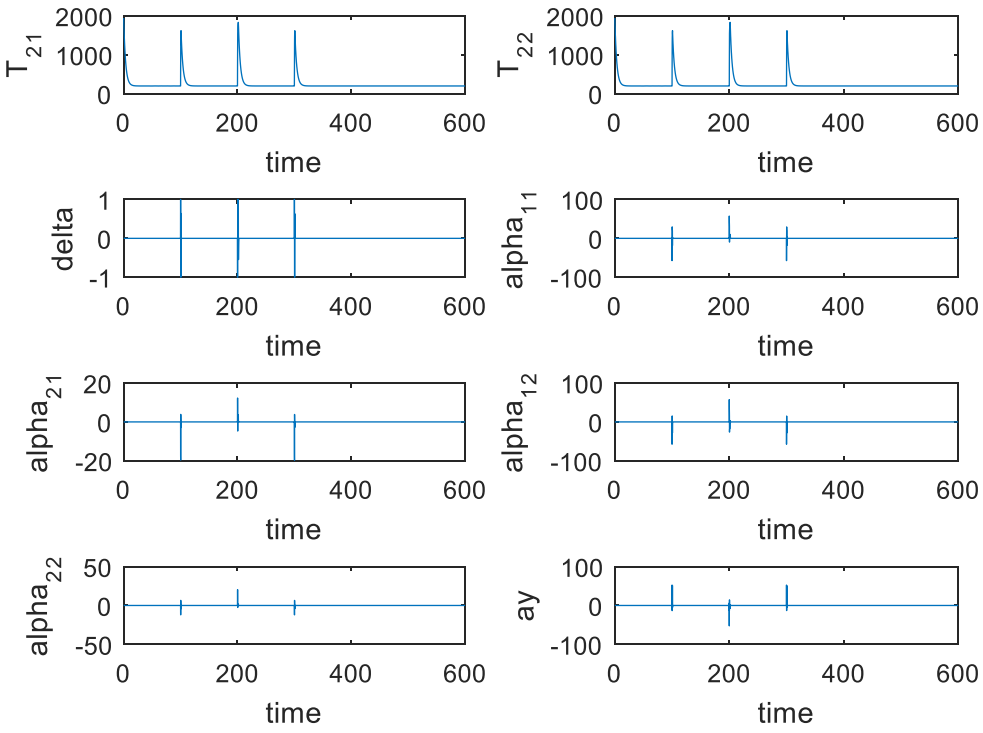

Figure 3.21 Additional State Variables for Lane Change

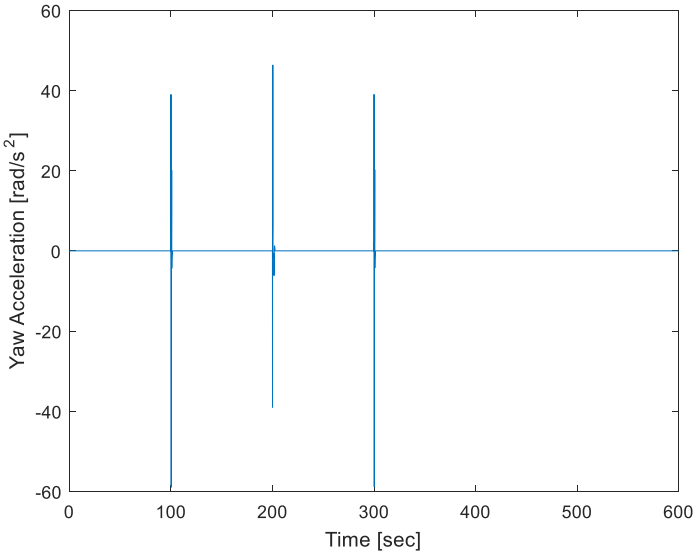

Figure 3.22 Yaw Acceleration for Lane Change

It is clear to see when the vehicle changes lanes, due to the spikes in the graph of torque seen in Fig. 3.21. If this program is used to create a controls algorithm to keep the car in a lane, different proportional gain constants should be chosen - this is a preliminary controls algorithm. Note that the torque to the rear wheels increases greatly to induce a lane change, but is fairly constant and

comparatively small for straight-line motion. Also note that the slip angles on the front of the car undergo a larger change in magnitude than the slip angles for the rear of the car (see Fig. 3.21). This is due to the quick step input of the steering angle given to the front wheels.

Although the vehicle does move around a lot, the yaw rate shown in Fig. 3.20 is within plus or minus five radians per second. However, the yaw acceleration shown in Fig. 2.22 reaches a magnitude of 60 radians per second. This is extremely unsafe. For minimum complaints about discomfort, yaw acceleration should be kept below 0.1 radian per second squared. From about 0.07 to 4 radians per second squared, passenger restraints become required to keep a person in place. Yaw accelerations greater than this will likely be very unsettling to passengers (Irwin, 1980). Improved controls algorithms will be needed to improve passenger comfort and safety.

Chapter 4. VEHICLE ROLL

Vehicle roll is important to consider to avoid unstable handling dynamics and even roll-over situations. This section will focus on the basics of vehicle roll and cover the determination of characteristic properties needed to build an accurate model. A two-wheel model will be used. Additional symbols needed for the roll model are shown in Table 4.1.

Table 4.1 Additional Symbols for Roll Model

Term	Symbol
Yaw	$r \; or \; \dot{\psi}$
Pitch	$q \; or \; \dot{\theta}$
Roll	$p \; or \; \dot{\varphi}$
Roll Center Coefficient	C_{β}
Roll Steer Coefficient	$C_{\delta\varphi}$
Roll Force Coefficient	$C_{\varphi r}, C_{\varphi f}$
Offset Coefficient	C_{Tf}, C_{Tr}

4.1 ROLL EQUATIONS OF MOTION

In the second chapter of this thesis, a two-wheel model without roll is considered. In this chapter, the two-wheel model will be expanded upon to consider the effect of roll. A diagram of a vehicle showing yaw, pitch, and roll is shown in Fig. 4.1. The model for vehicle roll is more complicated than the model introduced in Chapter 2 because it must be viewed as a three-dimensional problem, whereas before the two-wheel model could be viewed from the x-y plane. To cover vehicle roll thoroughly, the acceleration in the x, y, and z directions will be calculated. Consider the velocity vector given in Eqn. 4.1.

$$\vec{V} = \begin{bmatrix} V \\ U \\ T \end{bmatrix} \tag{4.1}$$

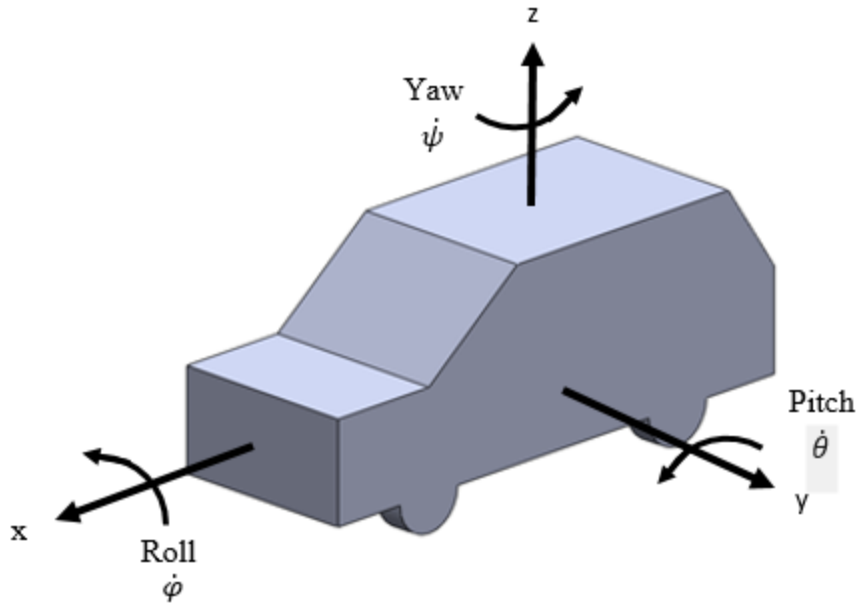

Figure 4.1 Vehicle Roll Model

Consider an angular velocity vector shown in Eqn. 4.2.

$$\vec{\omega} = \begin{bmatrix} \dot{\varphi} \\ \dot{\theta} \\ \dot{\psi} \end{bmatrix} \tag{4.2}$$

Since the body-centered coordinate system of the vehicle is rotating relative to the global coordinate system used to find the absolute motion of the car, the absolute acceleration of the vehicle must be calculated according to Eqn. 4.3.

$$\frac{d\vec{V}}{dt} = \left(\frac{\partial \vec{V}}{\partial t}\right)_{relative} + \omega \times \vec{V} \tag{4.3}$$

The first half of Eqn. 4.3 is evaluated in Eqn. 4.4 and the second half is evaluated in Eqn. 4.5.

$$\left(\frac{\partial \vec{V}}{\partial t}\right)_{relative} = \begin{bmatrix} \dot{V} \\ \dot{U} \\ \dot{T} \end{bmatrix} \tag{4.4}$$

$$\omega \times \vec{V} = \begin{vmatrix} \hat{\imath} & \hat{\jmath} & \hat{k} \\ \dot{\varphi} & \dot{\theta} & \dot{\psi} \\ V & U & T \end{vmatrix} = \hat{\imath}(\dot{\theta}T - \dot{\psi}U) - \hat{\jmath}(\dot{\varphi}T - \dot{\psi}V) + \hat{k}(\dot{\varphi}T - \dot{\theta}V) \tag{4.5}$$

Equations 4.3 through 4.5 are combined to give an equation for the acceleration in the x, y, and z directions as shown in Eqn. 4.6.

$$\vec{A} = \begin{bmatrix} \dot{V} + \dot{\theta}T - \psi U \\ \dot{U} + \psi V - \dot{\varphi}T \\ \dot{T} + \dot{\varphi}T - \dot{\theta}V \end{bmatrix} \tag{4.6}$$

The net moment applied to the vehicle's center of gravity can be calculated in a similar manner using the angular momentum. First, consider the moment of inertia applied about each axis of the vehicle shown in Eqn. 4.7.

$$I_{total} = \begin{bmatrix} I_{xx} & I_{xy} & I_{xz} \\ I_{yx} & I_{yy} & I_{yz} \\ I_{zx} & I_{zy} & I_{zz} \end{bmatrix} \tag{4.7}$$

The angular momentum of the vehicle is the total moment of inertia matrix (see Eqn. 4.7) times the angular velocity vector given in Eqn. 4.2. The result is shown in Eqn. 4.8.

$$\vec{\mathcal{L}} = \begin{bmatrix} I_{xx} & I_{xy} & I_{xz} \\ I_{yx} & I_{yy} & I_{yz} \\ I_{zx} & I_{zy} & I_{zz} \end{bmatrix} \begin{bmatrix} \dot{\varphi} \\ \dot{\theta} \\ \dot{\psi} \end{bmatrix} = \begin{bmatrix} \dot{\varphi} I_{xx} + \dot{\theta} I_{xy} + \dot{\psi} I_{xz} \\ \dot{\varphi} I_{yx} + \dot{\theta} I_{yy} + \dot{\psi} I_{yz} \\ \dot{\varphi} I_{zx} + \dot{\theta} I_{zy} + \dot{\psi} I_{zz} \end{bmatrix} = \begin{bmatrix} \mathcal{L}_i \\ \mathcal{L}_j \\ \mathcal{L}_k \end{bmatrix} \tag{4.8}$$

The moment about each axis can be found by taking the time derivative of the angular momentum according to Eqn. 4.3 (see Eqn. 4.9).

$$\frac{d\vec{\mathcal{L}}}{dt} = \left(\frac{\partial \vec{\mathcal{L}}}{\partial t}\right)_{relative} + \omega \times \vec{\mathcal{L}} \tag{89}$$

The first half of Eqn. 4.9 is evaluated in Eqn. 4.10 and the second half in Eqn. 4.11.

$$\left(\frac{\partial \vec{\mathcal{L}}}{\partial t}\right)_{relative} = \begin{bmatrix} \ddot{\varphi} I_{xx} + \ddot{\theta} I_{xy} + \ddot{\psi} I_{xz} \\ \ddot{\varphi} I_{yx} + \ddot{\theta} I_{yy} + \ddot{\psi} I_{yz} \\ \ddot{\varphi} I_{zx} + \ddot{\theta} I_{zy} + \ddot{\psi} I_{zz} \end{bmatrix} \tag{4.10}$$

$$\omega \times \vec{\mathcal{L}} = \begin{bmatrix} \dot{\varphi} \\ \dot{\theta} \\ \dot{\psi} \end{bmatrix} \times \begin{bmatrix} \mathcal{L}_i \\ \mathcal{L}_j \\ \mathcal{L}_k \end{bmatrix} = \begin{vmatrix} \hat{\imath} & \hat{\jmath} & \hat{k} \\ \dot{\varphi} & \dot{\theta} & \dot{\psi} \\ \mathcal{L}_i & \mathcal{L}_j & \mathcal{L}_k \end{vmatrix} \tag{4.11}$$

$$= \hat{\imath}\left(\dot{\theta}\mathcal{L}_k - \dot{\psi}\mathcal{L}_j\right) - \hat{\jmath}\left(\dot{\varphi}\mathcal{L}_k - \dot{\psi}\mathcal{L}_i\right) + \hat{k}(\dot{\varphi}\mathcal{L}_j - \dot{\theta}\mathcal{L}_i)$$

Combining Eqns. 4.10 and 4.11 and substituting in the angular moment of inertia terms from Eqn. 4.8 yields the moments about the center of gravity shown in Eqn. 4.12.

$$\frac{d\vec{\mathcal{L}}}{dt} = \vec{M} = \begin{bmatrix} \ddot{\varphi} I_{xx} + \ddot{\theta} I_{xy} + \ddot{\psi} I_{xz} \\ \ddot{\varphi} I_{yx} + \ddot{\theta} I_{yy} + \ddot{\psi} I_{yz} \\ \ddot{\varphi} I_{zx} + \ddot{\theta} I_{zy} + \ddot{\psi} I_{zz} \end{bmatrix} + \begin{bmatrix} \dot{\theta}(\dot{\varphi} I_{zx} + \dot{\theta} I_{zy} + \dot{\psi} I_{zz}) - \dot{\psi}(\dot{\varphi} I_{yx} + \dot{\theta} I_{yy} + \dot{\psi} I_{yz}) \\ \dot{\psi}(\dot{\varphi} I_{xx} + \dot{\theta} I_{xy} + \dot{\psi} I_{xz}) - \dot{\varphi}(\dot{\varphi} I_{zx} + \dot{\theta} I_{zy} + \dot{\psi} I_{zz}) \\ \dot{\varphi}(\dot{\varphi} I_{yx} + \dot{\theta} I_{yy} + \dot{\psi} I_{yz}) - \dot{\theta}(\dot{\varphi} I_{xx} + \dot{\theta} I_{xy} + \dot{\psi} I_{xz}) \end{bmatrix} \tag{4.12}$$

Equation 4.12 can be simplified greatly by assuming that the products of inertia (the terms of the moment of inertia matrix that are not along the main diagonal) are zero because the x, y, and z axes are assumed to align with the principal moment of inertia axes of the car. This means that Eqn. 4.12 can be simplified as shown in Eqn. 4.13 (Karnopp, 2008).

$$\frac{d\vec{\mathcal{L}}}{dt} = \vec{M} = \begin{bmatrix} \ddot{\varphi} I_{xx} \\ \ddot{\theta} I_{yy} \\ \ddot{\psi} I_{zz} \end{bmatrix} + \begin{bmatrix} \dot{\theta}\dot{\psi} I_{zz} - \dot{\psi}\dot{\theta} I_{yy} \\ \dot{\psi}\dot{\varphi} I_{xx} - \dot{\varphi}\dot{\psi} I_{zz} \\ \dot{\varphi}\dot{\theta} I_{yy} - \dot{\theta}\dot{\varphi} I_{xx} \end{bmatrix} \tag{4.13}$$

In this model, vertical movement in the z-direction and pitch rotation will not be analyzed. This makes the equations much easier to work with, as shown in Eqns. 4.14 and 4.15.

$$\vec{A} = \hat{\imath}\left(\dot{V} - \dot{\psi}U\right) + \hat{\jmath}(\dot{U} + \dot{\psi}V) \tag{4.14}$$

$$\frac{d\vec{\mathcal{L}}}{dt} = \vec{M} = \hat{\imath}(\ddot{\varphi} I_{xx}) + \hat{k}\left(\ddot{\psi} I_{zz}\right) \tag{4.15}$$

Equations 4.14 and 4.15 will be used to write the equations of motion. Recall Section 2.6 where the lateral forces were described by the slip angle. For a vehicle with roll, the slip angles will have

to include the effect of roll steer. Note that some vehicles will also have camber angles. Figure 4.2 shows how camber changes the inclination of a tire wheel.

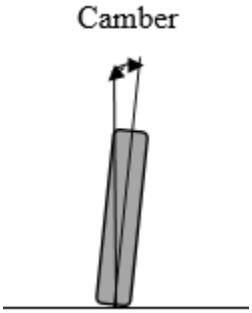

Figure 4.2 Vehicle Camber

According to SAE J670, camber angles of a tire are considered positive if the top of the tire is angled away from the body of the car. Camber is needed to create a more complete model of the vehicle, but it is not as important as the tire slip angles discussed in Chapter 2. For a radial tire, ten to fifteen degrees of camber are needed to create the same effect that one degree of tire slip would have (Gillespie, 1992). For this reason, camber will be left out of the vehicle roll model.

Besides camber, roll steer is also incorporated into the model. Roll steer involves the vehicle roll angle and the suspension geometry. When the vehicle rolls, the linkages that support the tire will deflect and cause deflection. This effect is called roll steer, and is an important topic for race car enthusiasts. Roll steer can be used to change the understeering tendencies of a vehicle through modifying the suspension or adding dampening features (Bastow, 1993). Specifically, if the vehicle roll axis is titled downwards in the front and upwards in the back when viewed from the left- or right-hand side of the car, the vehicle will have added understeer effects (Gillespie, 1992). The roll axis of a vehicle is found by connecting a line between the instant centers of two planes (such as the side view and rear view of a vehicle). The instant centers are locations about

which linkages rotate. These points may be off of the link, or on the link itself as shown in Fig. 4.3.

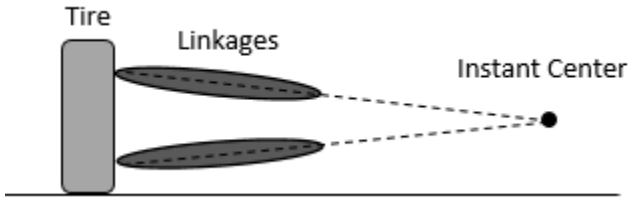

Figure 4.3 Instant Center

Besides knowing about the roll center axis, it is important to locate the roll center height. For an independent suspension vehicle, the roll center is the location where lateral force can be applied without creating a roll moment. To find the roll center of the car, the instant centers in each plane (side, front, rear) of the vehicle are located. Next, a line is extended from the bottom of the tire to the front instant center. This is repeated in all planes, and where these lines intersect gives the roll center. See Fig. 4.4 for a diagram of roll center location.

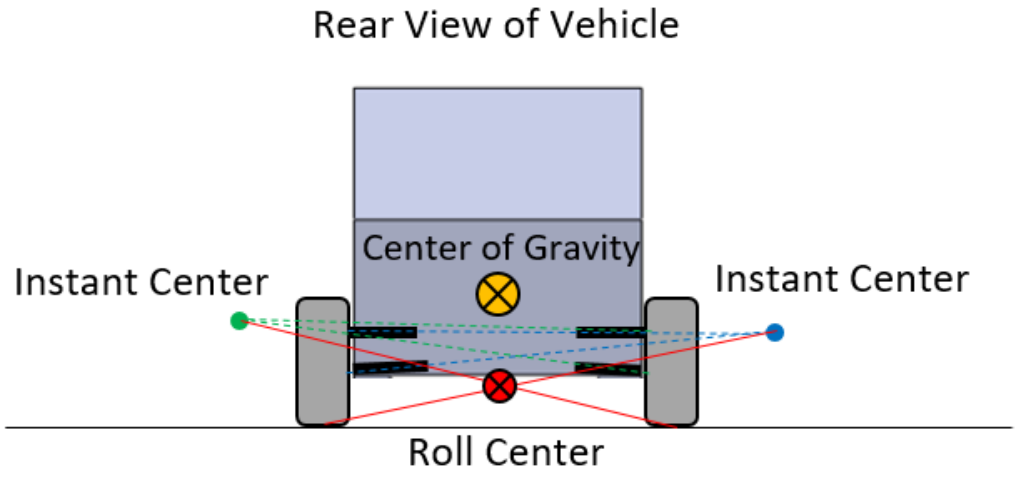

Figure 4.4 Roll Center

Designing a vehicle to have a lower roll center increases turning stability, because there is a larger moment that must be overcome in order to allow the vehicle to roll (Milliken, 1995). In this chapter, it will be assumed that the roll center of the vehicle is below the center of gravity.

The location of the roll center effects the body slip angle, which will now need to account for vehicle roll. Recall Fig. 2.19 where the body slip angles were defined using the velocity vectors at the rear tire, center of gravity, and front tire. The same method will be used in this chapter, as shown in Fig. 4.5.

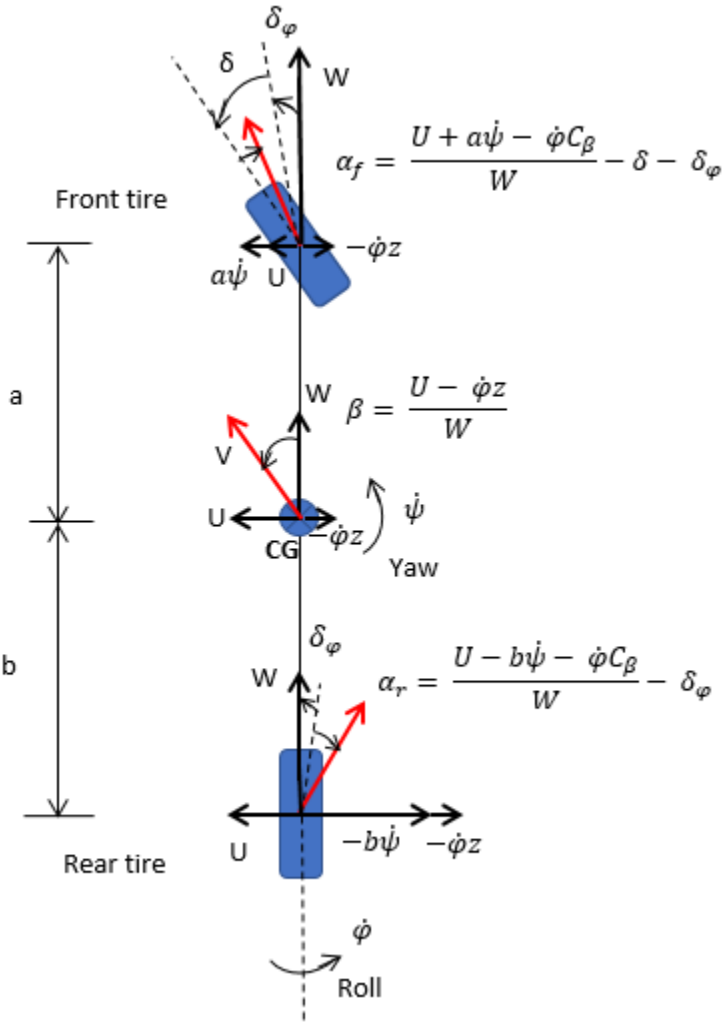

Figure 4.5 Roll Velocity Diagram

Since the roll center is assumed to be below the center of gravity by an amount labeled as z, there will be a roll moment produced by the cross product of $z\,\hat{k} \times \dot{\varphi}\,\hat{\imath}$ gives $-\dot{\varphi}z\,\hat{\jmath}$. Note, however, that the roll center is not a fixed point. As the linkages in the suspension system move as the vehicle turns and does other maneuvers, the instant centers will shift and so will the roll center. Since it is

difficult to determine the roll center from just one accelerometer, a roll center coefficient C_β is used to describe the average effect of roll center location on vehicle roll. To find this coefficient, accelerometers and gyroscopes would need to be placed on the linkages of the vehicle. While the car is driven through various turns, up hills, and at different speeds, data can be recorded and analyzed to find the varying positions of the roll center. Using the roll center data, a relationship between roll angle and roll center can be used to determine the constant C_β. Here, a value from Jazar's text will be used of -0.4 for the front tire and -0.1 for the rear.

Another difference between Fig. 4.5 and 2.19 is the addition of roll steer angle δ_φ. This angle is assumed to be linearly related to the roll angle by a roll steer coefficient $C_{\delta\varphi}$. This coefficient is based on the effect of roll on the direction that the tire rolls. This coefficient is not easy to determine experimentally because it involves many parameters. One approach would be to place accelerometers and gyroscopes in the center of the vehicle and at the tires. The roll angle would be measured by the gyroscope in the center of the car, and the direction that the tire velocity vector points in would be calculated from data recorded at the tire accelerometer. Using a plot of roll angle versus measured steering angle minus the driver-given steering angle, a relationship between the roll angle and induced steering angle due to roll can be determined. In Jazar's text, a value of 0 to 0.01 is used. This suggests that the effect is quite small. The roll steer and roll center coefficients which are used to write equations for the front and rear slip angles are shown in Eqns. 4.16 and 4.17. Note that the longitudinal velocity is assumed to be approximately equal to the total velocity V, an assumption also carried out in Chapter 2.

$$\alpha_f = \frac{U + a\psi - \dot{\varphi}C_\beta}{V} - \delta - \delta_\varphi = \frac{U + a\psi - \dot{\varphi}C_\beta}{V} - \delta - C_{\delta\varphi}\varphi \qquad (4.16)$$

$$\alpha_r = \frac{U - b\psi - \dot{\varphi}C_\beta}{V} - \delta_\varphi = \frac{U - b\psi - \dot{\varphi}C_\beta}{V} - C_{\delta\varphi}\varphi \tag{4.17}$$

The lateral forces on the front and rear tires will have an effect due to the slip angle as well as the roll angle. An additional roll force coefficient C_φ is used and is assumed to be linearly proportional to the roll angle. This coefficient can be experimentally determined by measuring the lateral acceleration of a vehicle during cornering. The roll angle of the car body can be measured by a gyroscope in the middle of the vehicle. A turn with very little roll can be compared to one with more roll to determine how the lateral force, or the lateral acceleration, increases with roll. This is more difficult than it may at first sound, because higher speeds would likely need to be used in order to make the vehicle roll more in the second case than in the first. This change in speed could affect the slip angle, and may cause erroneous results for the relationship between roll and lateral force. Jazar models a vehicle with roll using a roll force coefficient that is -3200 for the front tire and zero for the rear. This gives a general idea to the sensitivity that the front wheel must have to changes in roll. Equations 4.18 and 4.19 show the relationship between slip angle and roll angle on the lateral force of the front and rear tires (refer to Fig. 2.12 for background information on direction of lateral forces on the tires and a force diagram).

$$F_{yf} = -C_{\alpha f}\alpha_f - C_{\varphi f}\varphi \tag{4.18}$$

$$F_{yr} = -C_{\alpha r}\alpha_r - C_{\varphi r}\varphi \tag{4.19}$$

Equations 4.18 and 4.19 are used to write equations for the sum of the forces in the x- and y-directions (see Eqns. 4.20 and 4.21). Note that Eqn. 4.21 is based on Eqn. 2.80.

$$\sum F_y = -C_{\alpha r}\alpha_r - C_{\alpha f}\alpha_f - C_{\varphi f}\varphi - C_{\varphi r}\varphi = -C_{\alpha r}\left(\frac{U - b\psi - \dot{\varphi}C_\beta}{V} - C_{\delta\varphi}\varphi\right)$$

$$- C_{\alpha f}\left(\frac{U + a\psi - \dot{\varphi}C_\beta}{V} - \delta - C_{\delta\varphi}\varphi\right) - C_{\varphi f}\varphi - C_{\varphi r}\varphi \tag{4.20}$$

$$= \dot{U} + \psi V$$

$$\sum F_x = ma_x = m\left(\dot{V} - \psi U\right) = \frac{T}{R} \tag{4.21}$$

Now that the sum of the forces in the x- and y-directions has been written, the sum of the moments about the x- and z-axes will be discussed. The sum of the moments about the x-axis will include damping and stiffness effects due to the suspension. The roll stiffness is assumed to be directly related to the width of the vehicle and the stiffness of the front and rear suspension springs. Assume that the front suspension stiffness is 29 kilo-Newtons per meter, and the rear stiffness is 65 kilo-Newtons per meter as a rough estimation (Jameslk55, 2012). The vehicle that is simulated in this section is the oversteered vehicle discussed in Section 2.8.4.1 with a width of 1.92 meters, a front mass distribution of 784 kilograms, and a rear distribution of 940 kilograms. The mass distributions will be used in calculating the roll damping of the vehicle, which is related to the width of the vehicle and the front and rear dampers (Jazar, 2008). According to Wong, vehicles typically have damping ratios ζ between 0.2 to 0.4 (Wong, 2008). An intermediate damping ratio of 0.3 will be used. Equation 4.22 gives the relationship between the damping c and damping ratio (Rao, 2011).

$$\zeta = \frac{c}{2\sqrt{km}} \tag{4.22}$$

Equation 4.22 is used to calculate the front and rear damping, as shown in Eqns. 4.23 and 4.24. Note that the total mass in the front and rear is divided by two. This is because the front and rear axles have a damper at each wheel.

$$c_f = 2(0.3)\sqrt{\left(29 * 10^3 \frac{N}{m}\right)\left(\frac{784}{2}\ kg\right)} = 2.0 * 10^3\ kg/s \tag{4.23}$$

$$c_r = 2(0.3)\sqrt{\left(65 * 10^3 \frac{N}{m}\right)\left(\frac{940}{2}\ kg\right)} = 3.3 * 10^3\ kg/s \tag{4.24}$$

The damping and stiffness at the front and rear wheels are used to calculate the roll stiffness and roll damping (see Eqns. 4.25 and 4.26).

$$k_\varphi = width * \left(k_f + k_r\right) = 1.92\ m * \left(29\frac{kN}{m} + 65\frac{kN}{m}\right) = 180\ kN \tag{4.25}$$

$$c_\varphi = width * \left(c_f + c_r\right) = 1.92\ m * \left(2.0\frac{kg}{s} + 3.3\frac{kg}{s}\right) = 10\ \frac{m * kg}{s} \tag{4.26}$$

The last coefficient needed for the roll model involves the effect of slip angle on the x-axis roll moment. The slip angles cause a lateral force on the front and rear tires, and this in turn creates a moment about the x-axis. This moment is assumed to be linearly proportional to the lateral force on the tire according to the offset coefficient C_{Tf} or C_{Tr}. The offset coefficient takes into account the difference in height between the center of the wheel and the roll center. This difference in height is affected by changes in the suspension linkages, instantaneous changes in the spring length as the vehicle moves over bumps in a road, and the load on the wheel. Jazar gives a value of -0.2 to -0.4 for this coefficient. This value can be found experimentally by determining the average location of the roll center and the average distance from the roll center to the center of the wheel. Now that all of the coefficients have been discussed, the sum of the moments about the x- and z-axes can be written as shown in Eqns. 4.27 and 4.28 (see Eqn. 2.42 to compare the sum of the moments about the z-axis between the two-wheel model with and without roll).

$$\sum M_x = C_{Tf}F_{yf} + C_{Tr}F_{yr} - k_\varphi \varphi - c_\varphi \dot{\varphi} \tag{4.27}$$

$$\sum M_z = aF_{yf} - bF_{yr} \tag{4.28}$$

Note that the roll stiffness and roll damping work to oppose a positive roll moment. These terms work to keep the vehicle on the road. Equations 4.27 and 4.28 may be expanded using the equations of the lateral force (see Eqns. 4.29 and 4.30).

$$\begin{aligned}\sum M_x = & -C_{Tf}\left(C_{\alpha f}\left(\frac{U + a\psi - \dot{\varphi}C_\beta}{V} - \delta - C_{\delta\varphi}\varphi\right) + C_{\varphi f}\varphi\right) \\ & - C_{Tr}(C_{\alpha r}\left(\frac{U - b\psi - \dot{\varphi}C_\beta}{V} - C_{\delta\varphi}\varphi\right) + C_{\varphi r}\varphi) - k_\varphi\varphi - c_\varphi\dot{\varphi} \\ & = \ddot{\varphi}I_{xx}\end{aligned} \tag{4.29}$$

$$\begin{aligned}\sum M_z = & -a\left(C_{\alpha f}\left(\frac{U + a\psi - \dot{\varphi}C_\beta}{V} - \delta - C_{\delta\varphi}\varphi\right) + C_{\varphi f}\varphi\right) \\ & + b\left(C_{\alpha r}\left(\frac{U - b\psi - \dot{\varphi}C_\beta}{V} - C_{\delta\varphi}\varphi\right) + C_{\varphi r}\varphi\right) = \ddot{\psi}I_{zz}\end{aligned} \tag{4.30}$$

The equations of motion can be rewritten as shown in Eqns. 4.31 through 4.33.

$$\begin{aligned}\dot{U} = & U\left(\frac{-C_{\alpha r} - C_{\alpha f}}{V}\right) + \psi\left(\frac{C_{\alpha r}b - C_{\alpha f}a}{V} - V\right) + \dot{\varphi}\left(\frac{C_\beta C_{\alpha r} + C_\beta C_{\alpha f}}{V}\right) \\ & + \varphi(C_{\alpha r}C_{\delta\varphi} + C_{\alpha f}C_{\delta\varphi} - C_{\varphi f} - C_{\varphi r}) + \delta(C_f)\end{aligned} \tag{4.31}$$

$$\begin{aligned}\ddot{\varphi} = & \left(\frac{-C_{Tf}C_{\alpha f} - C_{Tr}C_{\alpha r}}{VI_{xx}}\right)U + \left(\frac{-aC_{Tf}C_{\alpha f} + bC_{Tr}C_{\alpha r}}{VI_{xx}}\right)\psi \\ & + \left(\frac{C_\beta C_{Tf}C_{\alpha f} + C_\beta C_{Tr}C_{\alpha r}}{VI_{xx}} - \frac{C_\varphi}{I_{xx}}\right)\dot{\varphi} \\ & + \left(\frac{C_{Tf}C_{\alpha f}C_{\delta\varphi} + C_{Tr}C_{\alpha r}C_{\delta\varphi} - C_{Tr}C_{\varphi r} - C_{Tf}C_{\varphi f} - k_\varphi}{I_{xx}}\right)\varphi \\ & + \left(\frac{C_{Tf}C_{\alpha f}}{I_{xx}}\right)\delta\end{aligned} \tag{4.32}$$

$$\ddot{\psi} = \left(\frac{bC_{\alpha r} - aC_{\alpha f}}{VI_{zz}}\right)U + \left(\frac{-a^2C_{\alpha f} - b^2C_{\alpha r}}{VI_{zz}}\right)\psi + \left(\frac{aC_{\alpha f}C_{\beta} - bC_{\alpha r}C_{\beta}}{VI_{zz}}\right)\dot{\varphi} + \left(\frac{aC_{\alpha f}C_{\delta\varphi} - aC_{\varphi f} - bC_{\alpha r}C_{\delta\varphi} + bC_{\varphi r}}{I_{zz}}\right)\varphi + \left(\frac{aC_{\alpha f}}{I_{zz}}\right)\delta \tag{4.33}$$

Terms are used to describe each of the equation's relationship with the state variables, as shown in Eqns. 4.34 through 4.36.

$$\dot{U} = \frac{Y_U U}{V} + \psi\left(\frac{Y_{\dot{\psi}}}{V} - V\right) + \frac{Y_{\dot{\varphi}}\dot{\varphi}}{V} + Y_{\varphi}\varphi + Y_{\delta}\delta \tag{4.34}$$

$$\ddot{\varphi} = \frac{\mathcal{R}_U U}{V} + \frac{\mathcal{R}_{\dot{\psi}}\psi}{V} + \dot{\varphi}\left(\frac{\mathcal{R}_{\dot{\varphi}1}}{V} - \mathcal{R}_{\dot{\varphi}2}\right) + \mathcal{R}_{\varphi}\varphi + \mathcal{R}_{\delta}\delta \tag{4.35}$$

$$\ddot{\psi} = \frac{\mathcal{W}_U U}{V} + \frac{\mathcal{W}_{\dot{\psi}}\psi}{V} + \frac{\mathcal{W}_{\dot{\varphi}}\dot{\varphi}}{V} + \mathcal{W}_{\varphi}\varphi + \mathcal{W}_{\delta}\delta \tag{4.36}$$

The terms used in Eqns. 4.34 through 4.36 are defined in Eqns. 4.37 through 4.51.

$$Y_U = -C_{\alpha r} - C_{\alpha f} \tag{4.37}$$

$$Y_{\dot{\psi}} = C_{\alpha r}b - C_{\alpha f}a \tag{4.38}$$

$$Y_{\dot{\varphi}} = C_{\beta}C_{\alpha r} + C_{\beta}C_{\alpha f} \tag{4.39}$$

$$Y_{\varphi} = C_{\alpha r}C_{\delta\varphi} + C_{\alpha f}C_{\delta\varphi} - C_{\varphi f} - C_{\varphi r} \tag{4.40}$$

$$Y_{\delta} = C_{\alpha f} \tag{4.41}$$

$$\mathcal{R}_U = \frac{-C_{Tf}C_{\alpha f} - C_{Tr}C_{\alpha r}}{I_{xx}} \tag{4.41}$$

$$\mathcal{R}_{\dot{\psi}} = \frac{-aC_{Tf}C_{\alpha f} + bC_{Tr}C_{\alpha r}}{I_{xx}} \tag{4.42}$$

$$\mathcal{R}_{\dot{\varphi}1} = \frac{C_{\beta}C_{Tf}C_{\alpha f} + C_{\beta}C_{Tr}C_{\alpha r}}{I_{xx}} \tag{4.43}$$

$$\mathcal{R}_{\dot{\varphi}2} = \frac{C_{\varphi}}{I_{xx}} \tag{4.44}$$

$$\mathcal{R}_{\varphi} = \frac{C_{Tf}C_{\alpha f}C_{\delta\varphi} + C_{Tr}C_{\alpha r}C_{\delta\varphi} - C_{Tr}C_{\varphi r} - C_{Tf}C_{\varphi f} - k_{\varphi}}{I_{xx}} \tag{4.45}$$

$$\mathcal{R}_{\delta} = \frac{C_{Tf}C_{\alpha f}}{I_{xx}} \tag{4.46}$$

$$\mathcal{W}_{U} = \frac{bC_{\alpha r} - aC_{\alpha f}}{I_{zz}} \tag{4.47}$$

$$\mathcal{W}_{\dot{\psi}} = \frac{-a^2C_{\alpha f} - b^2C_{\alpha r}}{I_{zz}} \tag{4.48}$$

$$\mathcal{W}_{\dot{\varphi}} = \frac{aC_{\alpha f}C_{\beta} - bC_{\alpha r}C_{\beta}}{I_{zz}} \tag{4.49}$$

$$\mathcal{W}_{\varphi} = \frac{aC_{\alpha f}C_{\delta\varphi} - aC_{\varphi f} - bC_{\alpha r}C_{\delta\varphi} + bC_{\varphi r}}{I_{zz}} \tag{4.50}$$

$$\mathcal{W}_{\delta} = \frac{aC_{\alpha f}}{I_{zz}} \tag{4.51}$$

These equations of motion can be written in matrix form as shown in Eqn. 4.52.

$$\begin{bmatrix} \dot{U} \\ \ddot{\varphi} \\ \dot{\varphi} \\ \dot{\psi} \end{bmatrix} = \begin{bmatrix} \frac{Y_U}{V} & \frac{Y_{\dot{\varphi}}}{V} & Y_{\varphi} & \frac{Y_{\dot{\psi}}}{V} - V \\ \frac{\mathcal{R}_U}{V} & \frac{\mathcal{R}_{\dot{\varphi}1}}{V} - \mathcal{R}_{\dot{\varphi}2} & \mathcal{R}_{\varphi} & \frac{\mathcal{R}_{\dot{\psi}}}{V} \\ 0 & 1 & 0 & 0 \\ \frac{\mathcal{W}_U}{V} & \frac{\mathcal{W}_{\dot{\varphi}}}{V} & \mathcal{W}_{\varphi} & \frac{\mathcal{W}_{\dot{\psi}}}{V} \end{bmatrix} \begin{bmatrix} U \\ \dot{\varphi} \\ \varphi \\ \psi \end{bmatrix} + \begin{bmatrix} Y_{\delta} \\ \mathcal{R}_{\delta} \\ 0 \\ \mathcal{W}_{\delta} \end{bmatrix} \delta \tag{4.52}$$

Equation 4.52 and Eqn. 4.21 fully describe the system (Jazar, 2008).

4.2 Steady-State Cornering With Roll

Roll is critical to analyze when turning. In this section, steady-state cornering will be discussed. For steady-state cornering, the lateral acceleration, longitudinal acceleration, angular accelerations, and roll rate are assumed to be zero. Note that in steady cornering, the yaw rate is

constant according to Eqn. 2.57. This means that the equations of motion reduce to the forms shown in Eqns. 4.53 to 4.55.

$$U\left(\frac{Y_U}{V}\right)+\frac{1}{R}\left(Y_{\dot{\psi}}-V^2\right)+\varphi\left(Y_\varphi\right)+\delta(Y_\delta)=0 \tag{4.53}$$

$$U\left(\frac{\mathcal{R}_U}{V}\right)+\frac{1}{R}\mathcal{R}_{\dot{\psi}}+\varphi\mathcal{R}_\varphi+\delta\mathcal{R}_\delta=0 \tag{4.54}$$

$$U\left(\frac{\mathcal{W}_U}{V}\right)+\frac{1}{\mathcal{R}}\mathcal{W}_{\dot{\psi}}+\varphi\mathcal{W}_\varphi+\delta\mathcal{W}_\delta=0 \tag{4.55}$$

Equations 4.53 through 4.55 can be rearranged to find relationships between the variables. The gain function for the inverse of the path radius versus the steering angle is shown in Eqn. 4.56.

$$\frac{1/R}{\delta}=\frac{K_1}{K_2} \tag{4.56}$$

The constants K_1 and K_2 are shown in Eqns. 4.57 and 4.58.

$$K_1=\frac{-Y_U\mathcal{W}_\delta\mathcal{R}_\varphi+Y_\delta\mathcal{W}_U\mathcal{R}_\varphi-Y_\varphi\mathcal{W}_U\mathcal{R}_\delta+Y_\varphi\mathcal{W}_\delta\mathcal{R}_U}{V\mathcal{W}_\varphi}+\frac{Y_U\mathcal{R}_\delta-Y_\delta\mathcal{R}_U}{V} \tag{4.57}$$

$$K_2=\frac{Y_U\mathcal{R}_{\dot{\psi}}-Y_{\dot{\psi}}\mathcal{R}_U}{V}-\mathcal{R}_U+\frac{\mathcal{R}_\varphi\mathcal{W}_U}{\mathcal{W}_\varphi}+\frac{Y_U\mathcal{R}_\varphi\mathcal{W}_{\dot{\psi}}+Y_\varphi\mathcal{R}_{\dot{\psi}}\mathcal{W}_U-Y_\varphi\mathcal{R}_U\mathcal{W}_{\dot{\psi}}-Y_{\dot{\psi}}\mathcal{R}_\varphi\mathcal{W}_U}{V\mathcal{W}_\varphi} \tag{4.58}$$

The parameters for the oversteered, neutral steer, and understeered vehicle discussed in Chapter 2 are used to produce a plot of Eqn. 4.56 as shown in Fig. 4.6. The steering angle starts at 0.1 radians. Here, the moment of inertia about the x-axis is approximated by Eqn. 4.59 (Hibbeler, 2013).

$$I_{xx}=\frac{1}{12}m(width)^2 \tag{4.59}$$

Figure 4.6 shows that the curvature response of the oversteered vehicle decreases much more quickly than the understeered or neutrally-steered vehicles. This means that as the path radius R

decreases, the oversteered vehicle needs a larger steering angle to maintain the path compared to the other two vehicles. This can be seen by referring back to Eqn. 2.23, where the oversteered vehicle's steering angle is greater than the Ackermann steering angle once the vehicle is brought up to a sufficient speed needed for slip angles to form. The neutrally-steered vehicle and the understeered vehicle have similar responses, which is likely because they both have the same mass. This gives the cars similar stiffness and moments of inertia, and similar gain functions.

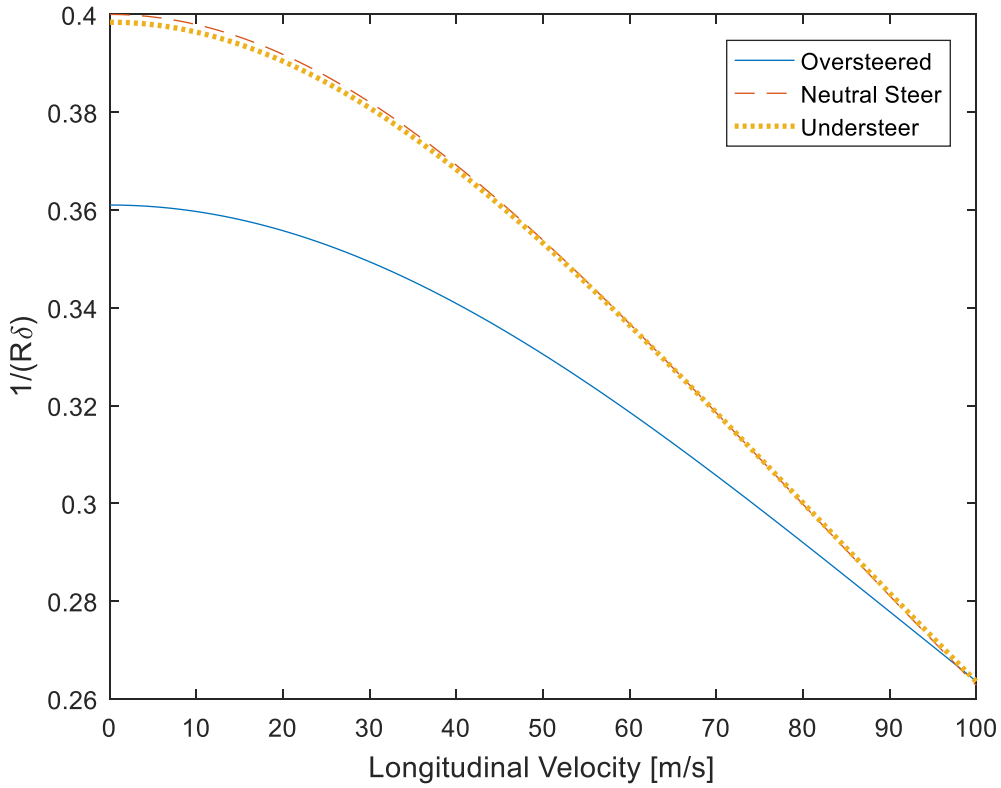

Figure 4.6 Curvature Response

The next gain function analyzed is the yaw rate gain (see Eqn. 4.60).

$$\frac{V/R}{\delta} = \frac{VK_1}{K_2} \tag{4.60}$$

Note that the yaw rate is constant, and equal to the longitudinal velocity divided by the path radius. This makes the yaw rate gain function directly related to the curvature gain function by a factor of V. The plot of the gain function is shown in Fig. 4.7. The steering angle starts at 0.1 radians. It is

interesting to note the differences between Fig. 4.7 and Fig. 2.21, the yaw rate gain function for a two-wheel model without roll. The two-wheel model without roll shows that the oversteered vehicle will have increasing yaw rate, but that the oversteered vehicle has a finite yaw rate limited by the characteristic speed. The two-wheel model with roll acts more as a neutrally-steered vehicle, because it does not show evidence of a critical speed nor a characteristic speed.

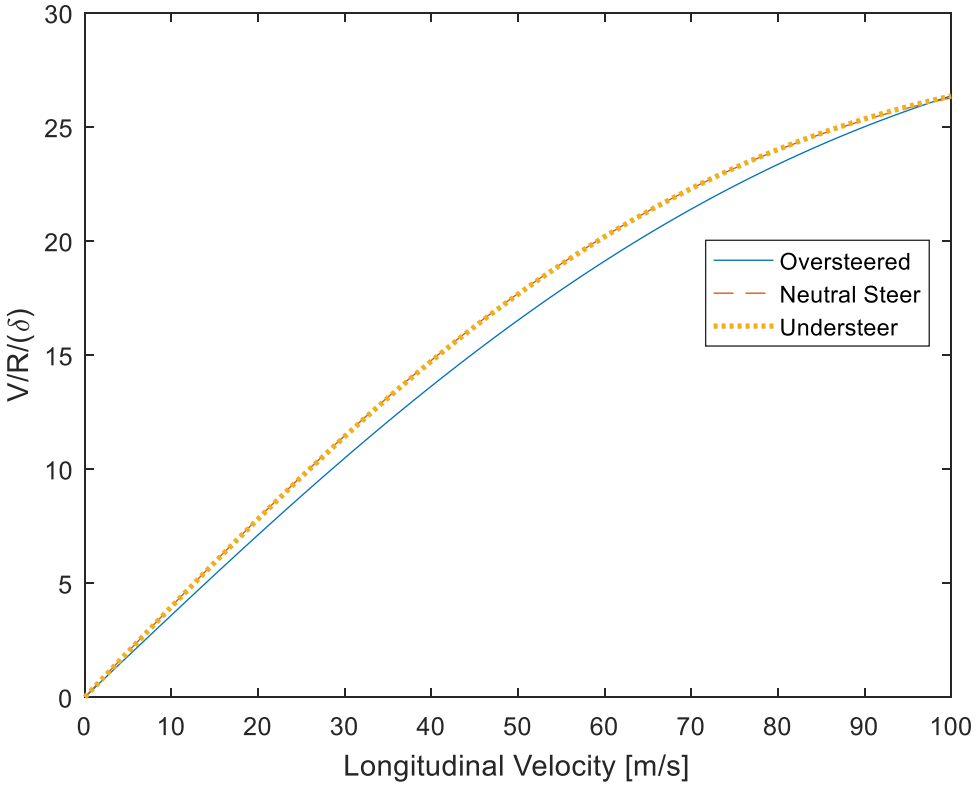

Figure 4.7 Yaw Rate Response

Another useful gain function is the lateral acceleration, which is found by multiplying the yaw rate gain equation by the longitudinal speed as shown in Eqn. 4.61.

$$\frac{V^2/_R}{\delta} = \frac{V^2 K_1}{K_2} \tag{4.61}$$

A plot of the response is shown in Fig. 4.8. Note that the starting steering angle is 0.1 radians. This dictates the starting point on the left-hand side of the graph. It is interesting to note that there is no indication of critical velocity or characteristic velocity. All three cars have similar responses, and

they have almost the same behavior for large values of longitudinal speed. This seems unusual, since the two-wheel model without roll showed large differences between the understeered and oversteered vehicles. This shows that it is worth investigating the roll coefficients more. Experimental values could be found instead of using the values in Jazar's text, or the values could be fitted to the two-wheel model without roll.

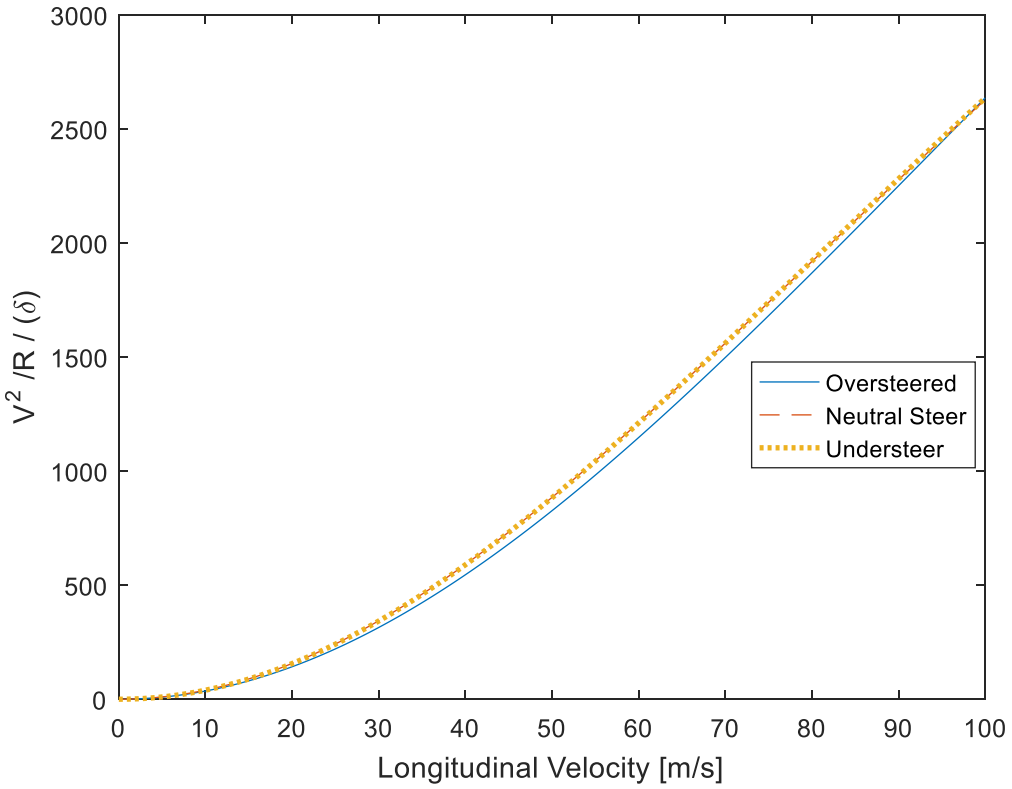

Figure 4.8 Lateral Acceleration Response

Next, the body slip angle gain function will be derived. The body slip angle is equal to the lateral velocity divided by the longitudinal velocity at the center of gravity of the vehicle. Equations 4.62 through 4.66 gives the body slip gain function.

$$\frac{U/V}{\delta} = \frac{L_3 L_1 + L_4}{1 - L_2 L_3} \tag{4.62}$$

$$L_1 = \frac{Y_\varphi W_\delta W_\varphi - Y_\delta {W_\varphi}^2}{Y_{\dot{\psi}} {W_\varphi}^2 - V{W_\varphi}^2 - Y_\varphi W_{\dot{\psi}} W_\varphi} \tag{4.63}$$

$$L_2 = \frac{Y_\varphi W_U W_\varphi - Y_U {W_\varphi}^2}{Y_{\dot{\psi}} {W_\varphi}^2 - V{W_\varphi}^2 - Y_\varphi W_\varphi W_{\dot{\psi}}} \tag{4.64}$$

$$L_3 = \frac{\mathcal{R}_\varphi W_{\dot{\psi}} W_\varphi - \mathcal{R}_{\dot{\psi}} {W_\varphi}^2}{\mathcal{R}_U {W_\varphi}^2 - W_U W_\varphi \mathcal{R}_\varphi} \tag{4.65}$$

$$L_4 = \frac{W_\delta \mathcal{R}_\varphi - \mathcal{R}_\delta W_\varphi}{\mathcal{R}_U W_\varphi - W_U \mathcal{R}_\varphi} \tag{4.66}$$

The body slip gain function is plotted in Fig. 4.9. An initial steering angle of 0.1 radians is used.

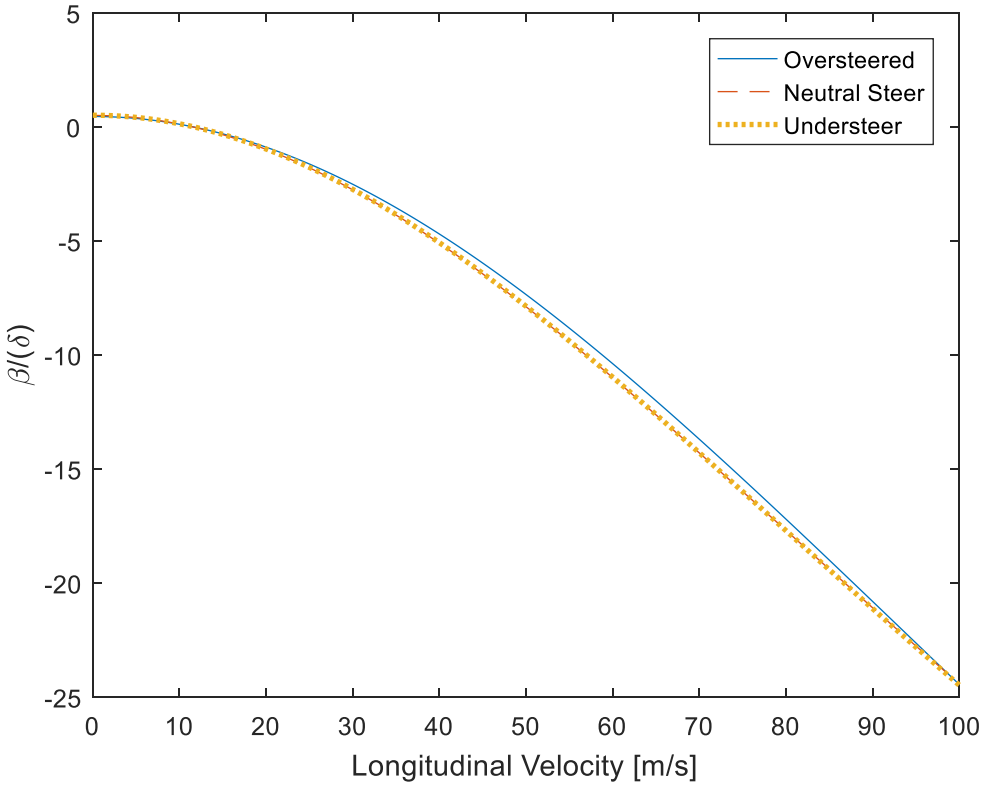

Figure 4.9 Body Slip Gain Response

Note that the body slip angle is positive for low speeds and then becomes negative for the rest of the graph. This means that initially the vehicle was angled into a left-hand turn, but as the longitudinal speed increased the lateral speed changed directions. This means that the vehicle

began to move in a negative y-direction, meaning that it changed the direction it was headed in. Again, the oversteered, neutrally-steered, and understeered vehicles have almost the same response.

The last gain function considered is the roll gain response, shown in Eqn. 4.67 through 4.73.

$$\frac{\varphi}{\delta} = \frac{N_1 N_2 + N_3}{N_4 N_5 + N_6} \tag{4.67}$$

$$N_1 = \frac{\mathcal{W}_\delta \mathcal{R}_U - \mathcal{R}_\delta \mathcal{W}_U}{\mathcal{W}_{\dot{\psi}} \mathcal{R}_U - \mathcal{R}_{\dot{\psi}} \mathcal{W}_U} \tag{4.68}$$

$$N_2 = \frac{\mathcal{R}_U Y_{\dot{\psi}} - \mathcal{R}_{\dot{\psi}} Y_U - V^2 \mathcal{R}_U}{\mathcal{R}_U} \tag{4.69}$$

$$N_3 = \frac{Y_U \mathcal{R}_\delta - Y_\delta \mathcal{R}_U}{\mathcal{R}_U} \tag{4.70}$$

$$N_4 = \frac{\mathcal{R}_\varphi \mathcal{W}_U - \mathcal{W}_\varphi \mathcal{R}_U}{\mathcal{W}_{\dot{\psi}} \mathcal{R}_U - \mathcal{R}_{\dot{\psi}} \mathcal{W}_U} \tag{4.71}$$

$$N_5 = \frac{\mathcal{R}_U Y_{\dot{\psi}} - \mathcal{R}_{\dot{\psi}} Y_U - V^2 \mathcal{R}_U}{\mathcal{R}_U} \tag{4.72}$$

$$N_6 = \frac{Y_\varphi \mathcal{R}_U - Y_U \mathcal{R}_\varphi}{\mathcal{R}_U} \tag{4.73}$$

The graph of the roll gain is shown in Fig. 4.10. Note that the graph for roll angle versus steering angle passes the small angle approximation. Only small angles of roll can be accurately represented by the model, and the fact that the gain becomes increasingly large is not necessarily physically accurate. However, it is useful to see the general trend as longitudinal speed increases. It shows that cars with increasing speed may be more likely to have large roll angles even if the vehicle only showed signs of small roll angles to begin with. Note that a negative roll angle means the

vehicle rolls to the left, and a positive roll angle would show the vehicle leaning out of a left-hand curve.

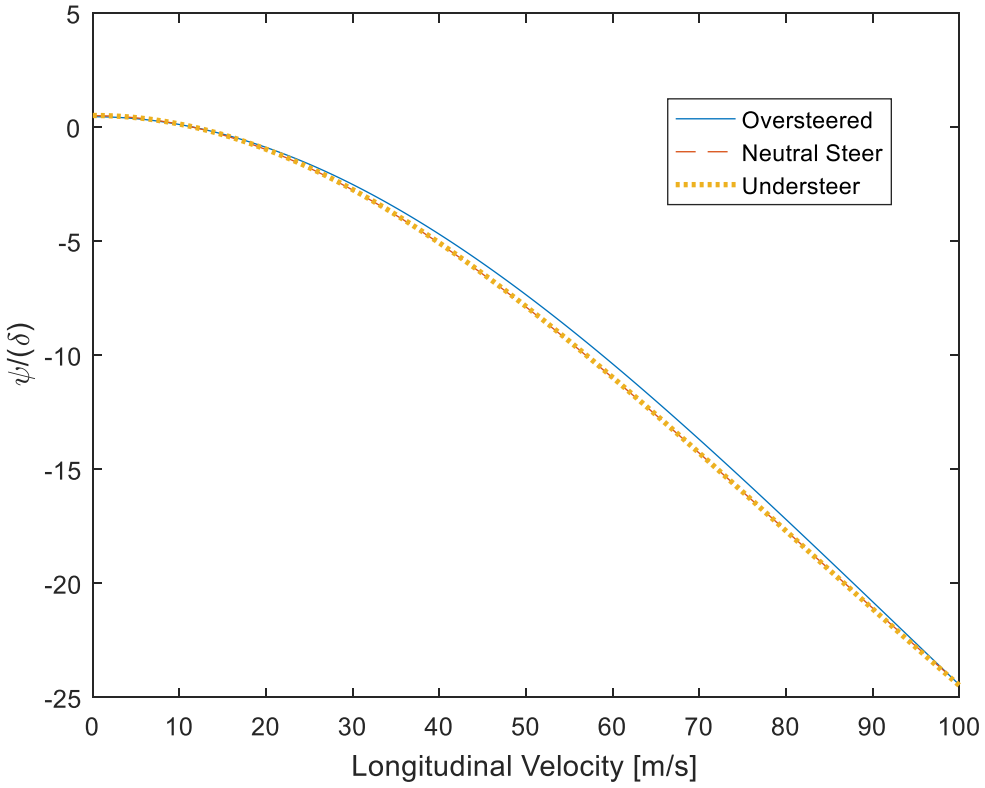

Figure 4.10 Roll Gain Response

Throughout these gain response curves, the three vehicles show similar responses. A better investigation of the parameters used in the model is needed if the simulations are to be used with confidence. For example, the critical speed could be found from the lateral acceleration equation for a vehicle with roll and the coefficients adjusted to match that of a two-wheel without roll. The same could also be done with the characteristic speed. The critical velocity for the vehicles can be found by setting the denominator of the curvature gain function equal to zero and solving for the velocity, just as in Chapter 2. The critical velocity equation for a vehicle with roll is given by Eqn. 4.74.

$$V_{critical}$$

$$= \frac{Y_\varphi\left(\mathcal{R}_U\mathcal{W}_{\dot{\psi}} - \mathcal{R}_{\dot{\psi}}\mathcal{W}_U\right) + Y_U\left(-\mathcal{R}_{\dot{\psi}}\mathcal{W}_\varphi - \mathcal{R}_\varphi\mathcal{W}_{\dot{\psi}}\right) + Y_{\dot{\psi}}(\mathcal{R}_U\mathcal{W}_\varphi + \mathcal{R}_\varphi\mathcal{W}_U)}{-\mathcal{R}_U\mathcal{W}_\varphi + \mathcal{R}_\varphi\mathcal{W}_U} \tag{4.74}$$

The characteristic velocity is found by taking the derivative of the yaw gain equation, taking the derivative, and setting it equal to zero. To make the gain equation easier to work with, it will be rewritten as shown in Eqns. 4.75 through 4.80.

$$\frac{V/_R}{\delta} = \frac{VK_1}{K_2} = \frac{(A+B)V}{C+DV+E} \tag{4.75}$$

$$A = \frac{-Y_U\mathcal{W}_\delta\mathcal{R}_\varphi + Y_\delta\mathcal{W}_U\mathcal{R}_\varphi - Y_\varphi\mathcal{W}_U\mathcal{R}_\delta + Y_\varphi\mathcal{W}_\delta\mathcal{R}_U}{\mathcal{W}_\varphi} \tag{4.76}$$

$$B = Y_U\mathcal{R}_\delta - Y_\delta\mathcal{R}_U \tag{4.77}$$

$$C = Y_U\mathcal{R}_{\dot{\psi}} - Y_{\dot{\psi}}\mathcal{R}_U \tag{4.78}$$

$$D = -\mathcal{R}_U + \frac{\mathcal{R}_\varphi\mathcal{W}_U}{\mathcal{W}_\varphi} \tag{4.79}$$

$$E = \frac{Y_U\mathcal{R}_\varphi\mathcal{W}_{\dot{\psi}} + Y_\varphi\mathcal{R}_{\dot{\psi}}\mathcal{W}_U - Y_\varphi\mathcal{R}_U\mathcal{W}_{\dot{\psi}} - Y_{\dot{\psi}}\mathcal{R}_\varphi\mathcal{W}_U}{\mathcal{W}_\varphi} \tag{4.80}$$

The derivative of Eqn. 4.75 is shown in Eqn. 4.81.

$$\frac{d}{dV}\left(\frac{(A+B)V}{C+DV+E}\right) = \frac{(C+DV+E)(A+B) - (A+B)VD}{(C+DV+E)^2} \tag{4.81}$$

Setting Eqn. 4.81 equal to zero and solving for the longitudinal velocity V gives Eqn. 4.82.

$$V_{characteristic} = \frac{-CA - EA - BC - BE}{DA + BD - AD - BD} \tag{4.82}$$

Note that the denominator of the characteristic velocity is equal to zero. This means that the understeered vehicle will not have a characteristic velocity or a maximum yaw rate. This is shown in Fig. 4.7 as the yaw rate increases without reaching a maximum value.

The critical velocity of the vehicles becomes the only parameter from the two-wheel model without roll that can be applied to the roll model to make the roll coefficients more accurate. Note, however, that there are eight additional constants used in the roll model that were not used in the two-wheel model discussed in Chapter 2. This makes fitting the roll model to a simple two-wheel model very difficult. If more accurate response curves are needed, experimental testing would be needed to determine the unique roll parameters of the oversteered, neutrally-steered, and understeered vehicles.

Chapter 5. CONCLUSIONS

In this thesis, three models are used to describe the motion of a vehicle. The two-wheel model is used to gain preliminary understanding of cornering. At low speeds, the Ackermann steering angle is used, and provides a useful reference point for higher speeds. For vehicles turning at greater speeds, a neutrally-steered vehicle has an Ackermann steering angle but an understeered vehicle has a larger Ackermann steering angle and an oversteered vehicle will have a smaller Ackermann steering angle. Besides cornering, the analysis of the acceleration of simplified understeer and oversteer vehicles shows that an oversteered vehicle will accelerate more quickly. The stability of three vehicles is considered, and the oversteered vehicle is found to have a yaw rate that can become unstable while the understeered vehicle remains stable. Simulations of the vehicles show that the oversteered vehicle will move in a larger circle than the understeered car.

The four-wheel model was used to better understand slip angles and body-slip angles. Simulations show that the vehicle moves in a spiraling manner away from the starting point. The response varies with torque and grade. Lane change simulations show that yaw acceleration is large, and that passengers would benefit from a more finely-tuned controls algorithm.

The last model used is a two-wheel model with roll. This model is limited by the lack of experimental data available on vehicle roll parameters. However, unlike the two-wheel model without roll, all vehicles showed similar behavior when roll angles are involved. Further testing is needed to determine parameters for the test vehicles to see if this relationship is valid.

Throughout the discussions of the different models, three vehicles are analyzed with differing centers of gravity to better capture the full range of possible responses. This thesis is intended to give students and faculty tools to use when working with vehicle dynamics and to make control algorithms for vehicles easier to develop.

BIBLIOGRAPHY

Bastow, Donald. "Car Suspension and Handling." Edited by Geoffrey P Howard, SAE, 1993.

Blundell, Mike and Damian Harty. "The Multibody Systems Approach to Vehicle Dynamics." SAE International, 2004.

Campbell, Colin. "New Directions in Suspension Design: Making the Fast Car Faster." Robert Bentley, Inc, 1981.

Dixon, John C. "Suspension Geometry and Computation." John Wiley and Sons, 2009.

Dixon, John C. "Tires, Suspension, and Handling, Second Edition." SAE International, 1996.

Gillespie, Thomas D. "Fundamentals of Vehicle Dynamics." SAE, 1992.

Hibbeler, R C. "Engineering Mechanics: Dynamics, Thirteenth Edition." Pearson Prentice Hall, 2013.

Hunting, Benjamin. "Top 10 Cars with the Most Torque for 2015." Autobytel, www.autobytel.com/car-buying-guides/features/top-10-cars-with-the-most-torque-for-2015-129395/. Accessed 16 April 2017.

Husain, Iqbal. "Electric and Hybrid Vehicles: Design Fundamentals." CRC Press, 2003.

Irwin, A W. "Perception, Comfort, and Performance Criteria for Human Beings Exposed to Whole Body Pure Yaw Vibration and Vibration Containing Yaw and Translational Components." Journal of Sound and Vibration, Volume 76, Number 4, 1981, pp. 481-497.

Jameslk55. "Spring Rates" *Camaro5,* 18 November 2012, camaro5.com/forums/showthread.php?t=234954. Accessed 16 April 2017.

Jazar, Reza N. "Vehicle Dynamics: Theory and Application." Springer, 2008.

Karnopp, Dean C and Donald L Margolis. "Engineering Applications of Dynamics." John Wiley and Sons, 2008.

Kato, Tomo and Kaoru Sawase. "Classification and Analysis of Electric-Powered Lateral Torque-Vectoring Differentials." Journal of Automobile Engineering, 2011.

Kreyszig, Erwin. "Advanced Engineering Mathematics, Tenth Edition." John Wiley and Sons, 2011.

Martino, Raffaele Di. "Modelling and Simulation of the Dynamic Behaviour of the Automobile." Université de Haute Alsace - Mulhouse, 2005. English.

Milliken, William F and Douglas L Milliken. "Race Car Vehicle Dynamics." SAE International, 1995.

Rajamani, Rajesh. "Vehicle Dynamics and Control." Springer, 2006.

Rao, Singiresu S. "Mechanical Vibrations, Fifth Edition." Pearson Prentice Hall, 2011.

Sakai, H. "Theoretical and Experimental Studies on the Dynamic Properties of Tyres Part 2: Experimental Investigation of Rubber Friction and Deformation of a Tyre." International Journal of Vehicle Design, Volume 2, Number 2, 1981, pp.182 - 226.

Serway, Raymond A and John W Jewett Jr. "Physics for Scientists and Engineers with Modern Physics, Eighth Edition." Brooks/Cole Cengage Learning, 2010.

Sleeper, Robert K. "Tire Stiffness and Damping Determined from Static and Free-Vibration Tests." NASA Scientific and Technical Information Office, 1980.

Society of Automotive Engineering. "Surface Vehicle Recommended Practice J670 R Vehicle Dynamics Terminology." SAE International, 2008.

Wong, J Y. "Theory of Ground Vehicles." John Wiley and Sons, 2008.

APPENDIX A

This appendix covers the experimental procedure to find the cornering coefficient in more detail. In calculating the cornering coefficient, data is collected using an accelerometer and gyroscope on a vehicle and driving it in circles in a parking lot. Sample data from an experiment where the wheel angle is intended to be about three degrees and the longitudinal velocity is around eight kilometers per hour are shown in Figs. A.1 to A.5. Note that there is a large change in the steering angle at two periods in the experiment. The parking lot used for the experiment had light posts and other obstructions that caused changes in the intended circular path.

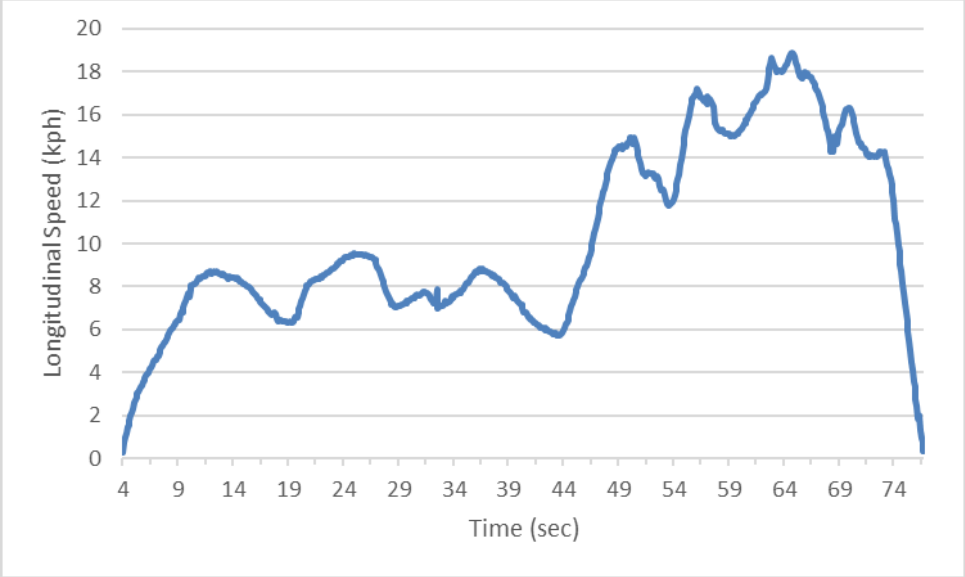

Figure A.1 Longitudinal Speed Versus Time

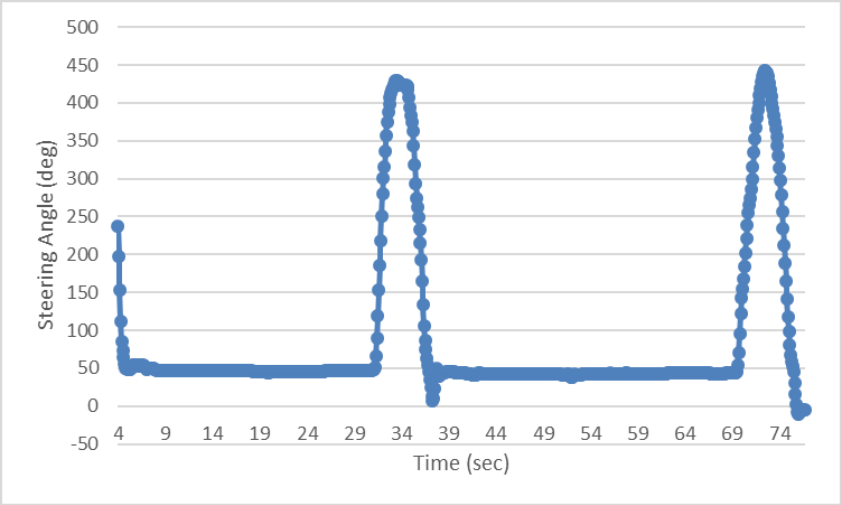

Figure A.2 Steering Angle Versus Time

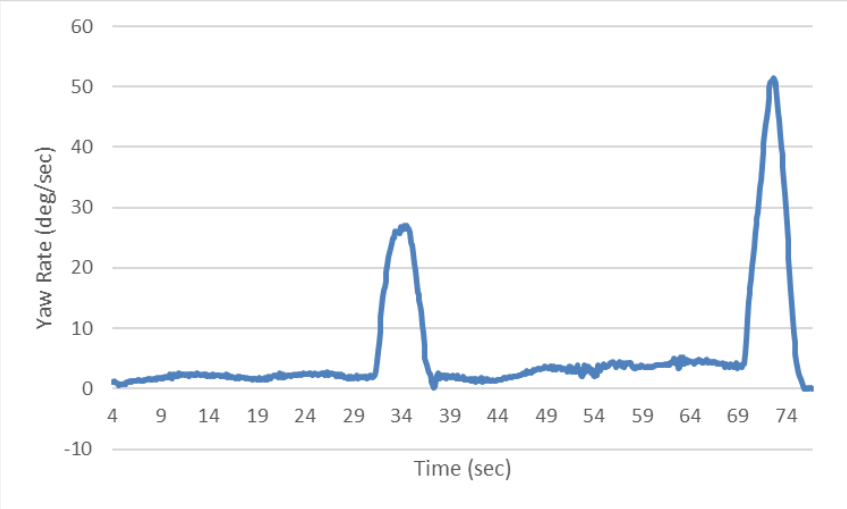

Figure A.3 Yaw Rate Versus Time

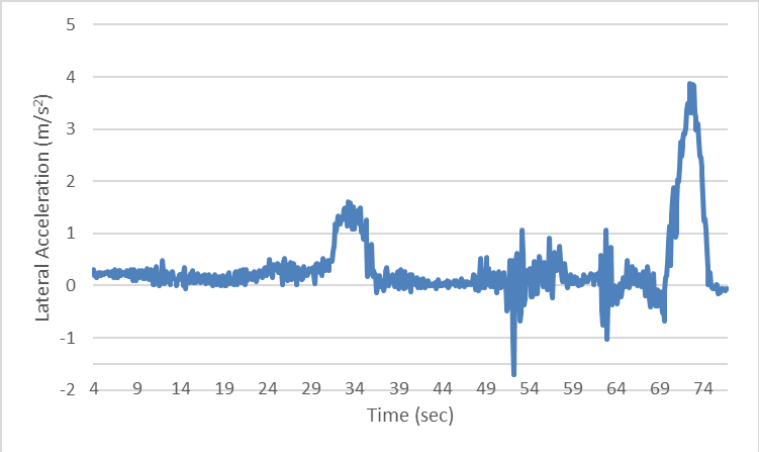

Figure A.4 Lateral Acceleration Versus Time

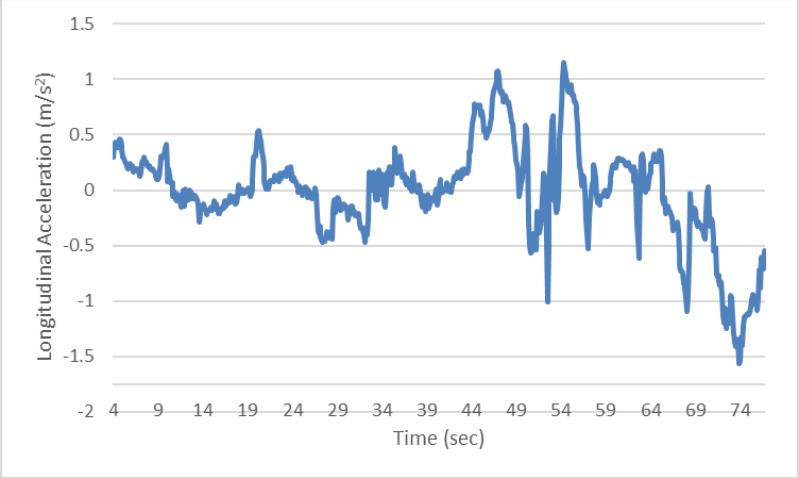

Figure A.5 Longitudinal Acceleration Versus Time

In calculating the average cornering stiffness, values of the slip angle greater than ten degrees are not used and are filtered out of the data. However, it is interesting to look at the change in cornering coefficient with front and rear slip angles (see Figs. A.6 to A.7).

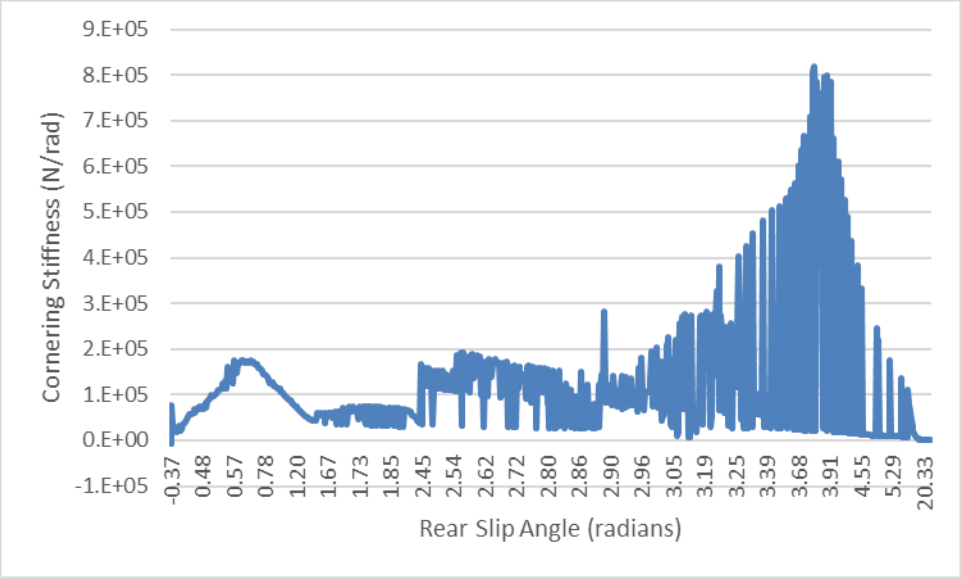

Figure A.6 Cornering Stiffness Versus Rear Slip Angle

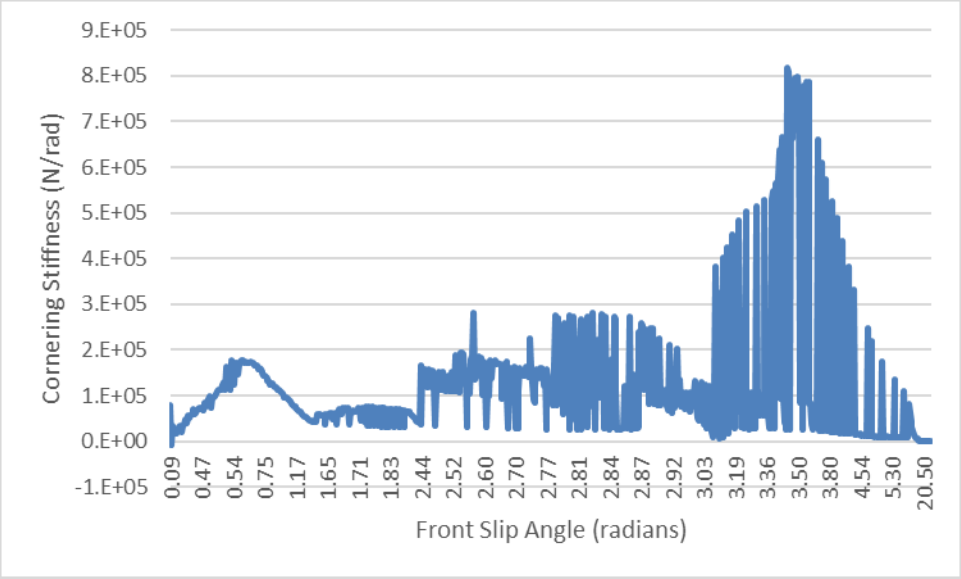

Figure A.7 Cornering Stiffness Versus Front Slip Angle

It is interesting to note in both Fig. A.6 and Fig. A.7 that neither show a trend similar to that of Fig. 2.24 where the cornering stiffness increases with slip angle in a smooth manner. It could be that the theoretical model only works for small slip angles, so Fig. 2.24 may not be the best representation of the cornering stiffness with increasing slip angles.

APPENDIX B

This appendix provides additional two-wheel simulations. Although it may seem trivial at first, it is important to test a code with a simple and intuitive example. Here, a zero steering angle and a speed of forty miles per hour will be used to test that the vehicle yaw rate is zero. When the steering angle is zero, Eqns. 2.2 and 2.3 show that the vehicle will move in a straight line, which is the expected result. Refer to Figs. B.1 and B.2, which show that the vehicles behaves as anticipated.

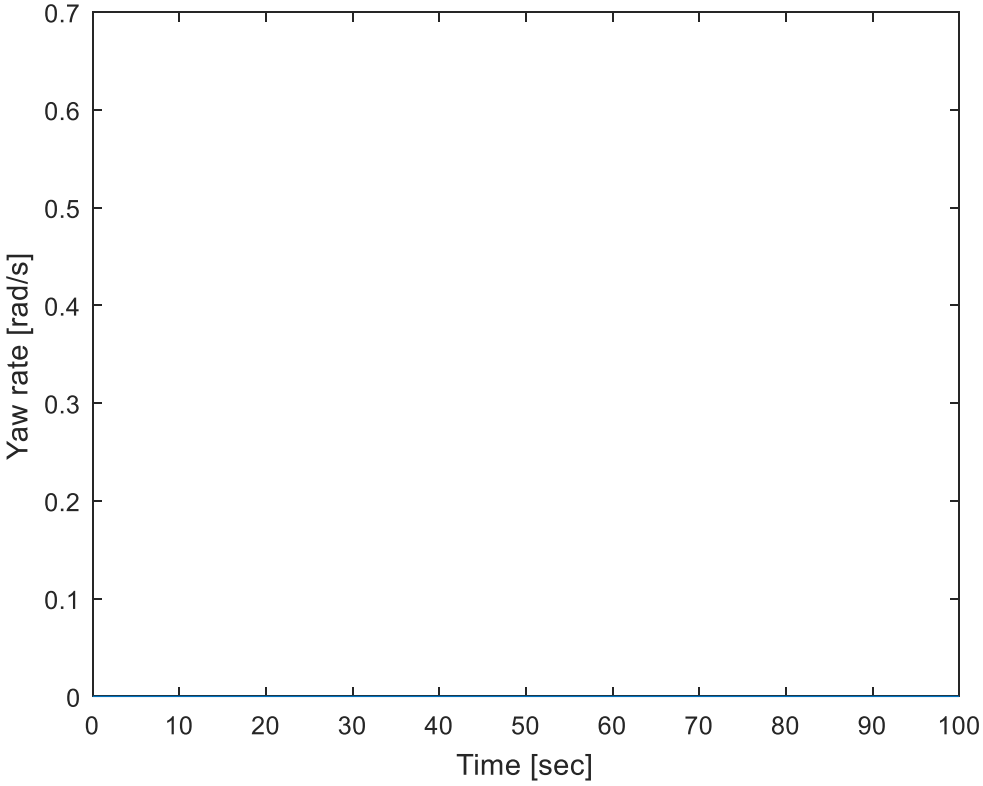

Figure B.1 Zero Steering Angle Yaw Rate

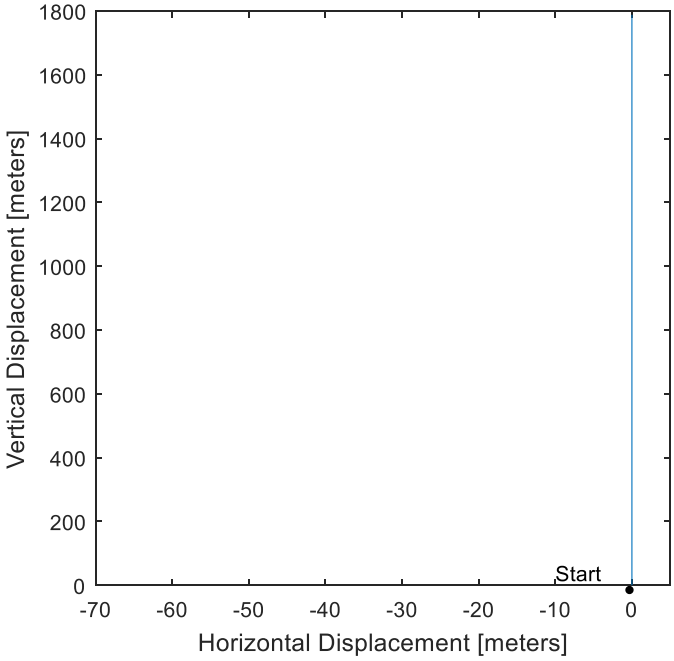

Figure B.2 X-Y Displacement for Zero Steering Angle

Next, consider a vehicle moving at twelve miles per hour with a very small steering angle of 5 degrees. See Figs. B.3 to B.8 for the simulations for the oversteered, neutrally-steered, and understeered vehicles.

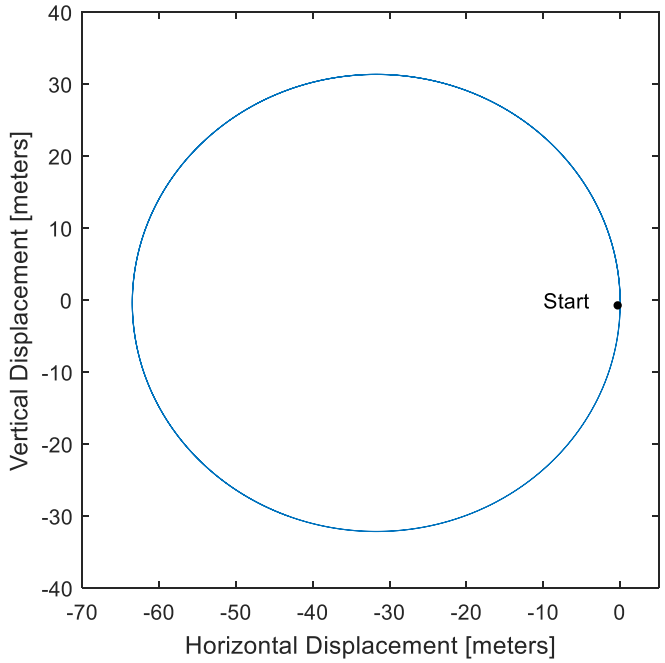

Figure B.3 Low-Speed Oversteer X-Y Trajectory

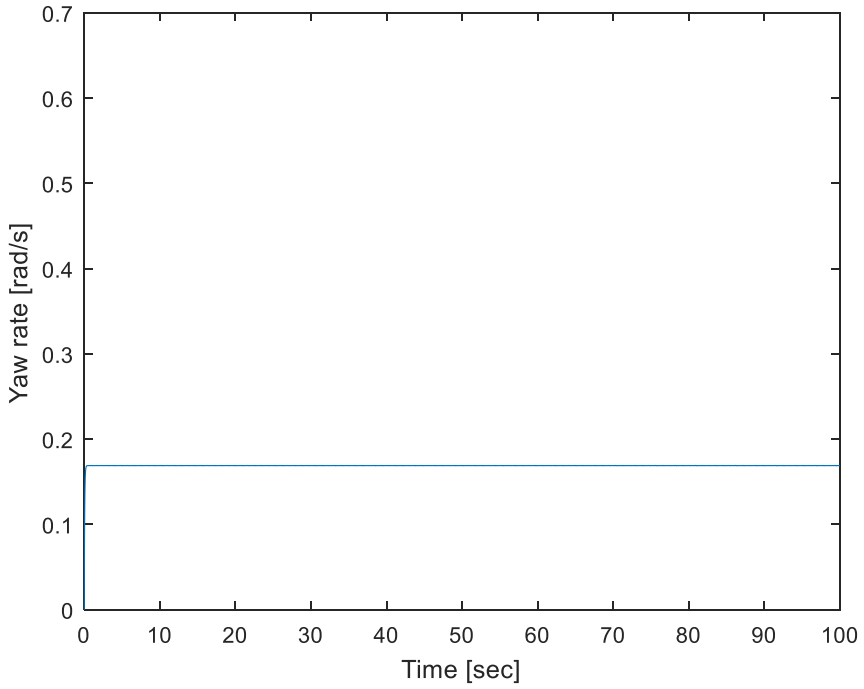

Figure B.4 Low-Speed Oversteered Vehicle Yaw Rate

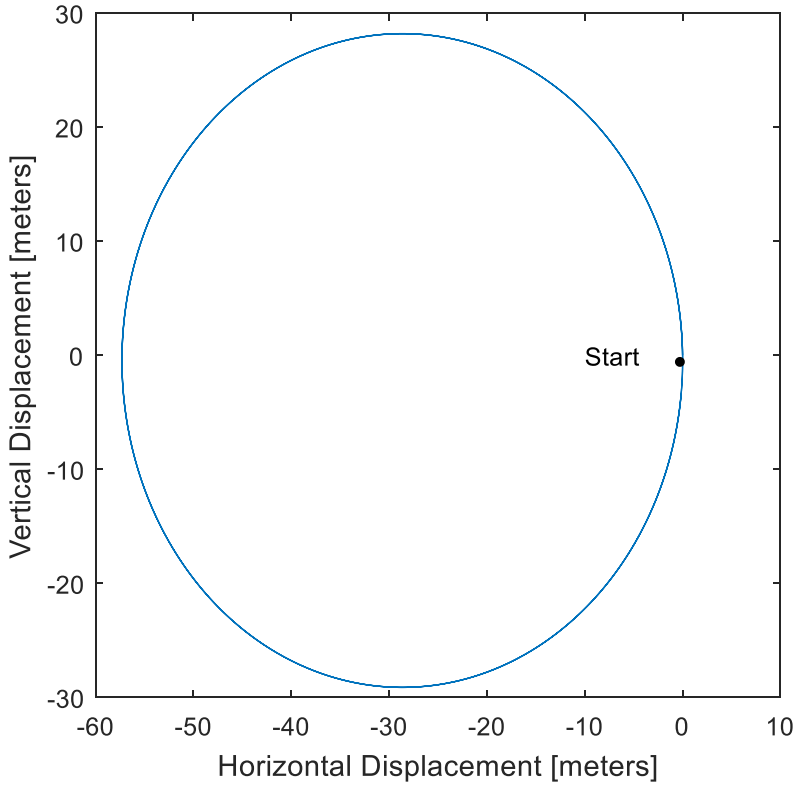

Figure B.5 Low-Speed Neutral Steer Vehicle X-Y Trajectory

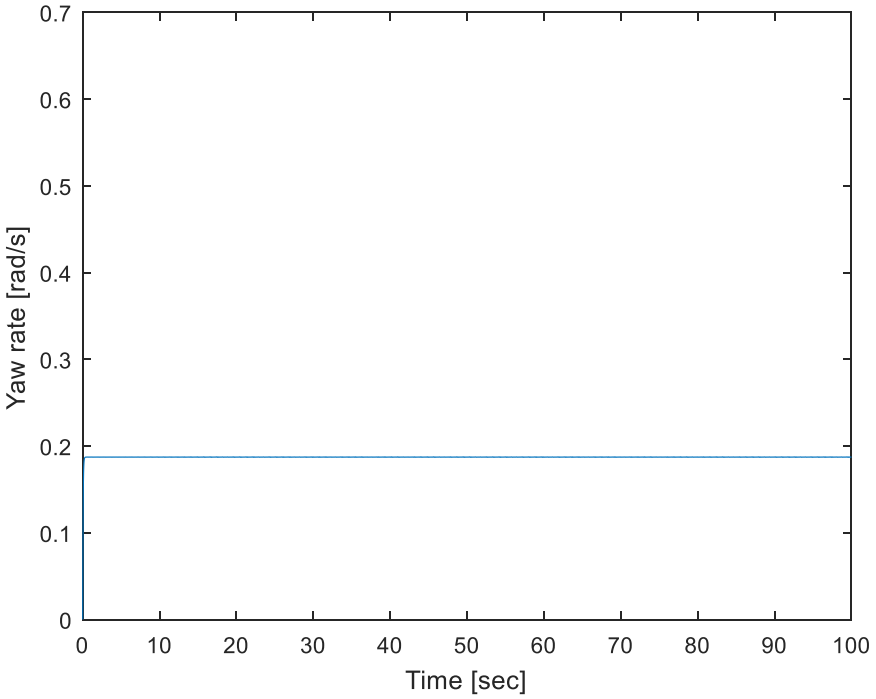

Figure B.6 Low-Speed Neutral Steer Yaw Rate

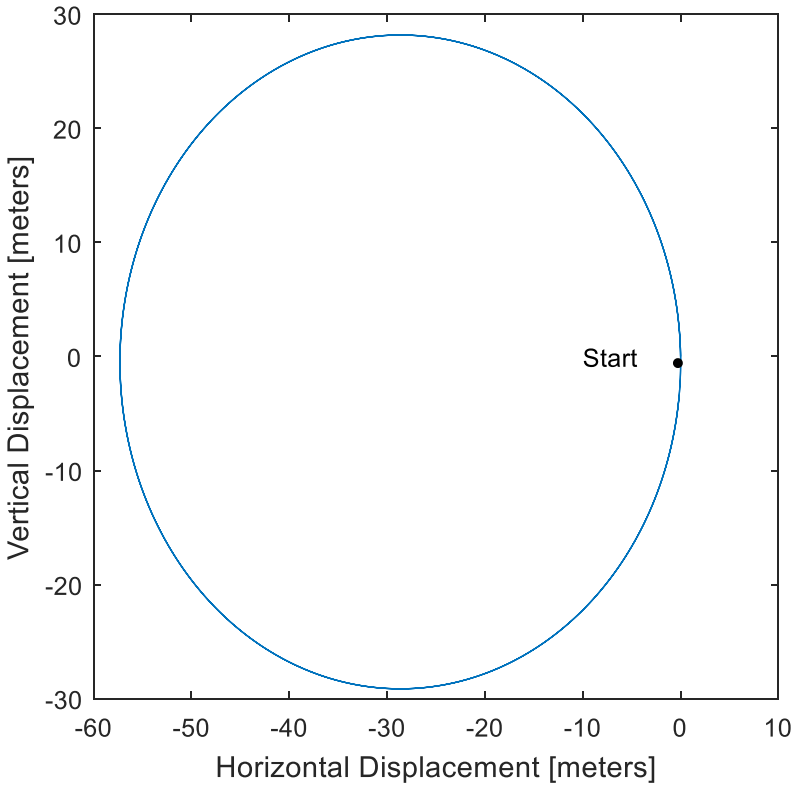

Figure B.7 Low-Speed Understeer X-Y Trajectory

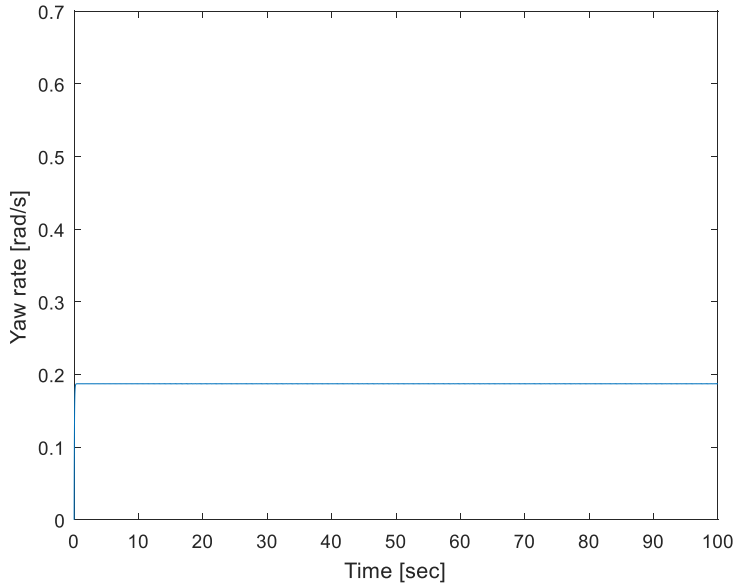

Figure B.8 Low-Speed Understeer Yaw Rate

Note that the yaw rate increases very quickly for each vehicle. This can be reduced using a controls algorithm.

The last additional case considered is for fifty-five miles per hour and a five degree steering angle (refer to Figs. B.9 to B.14).

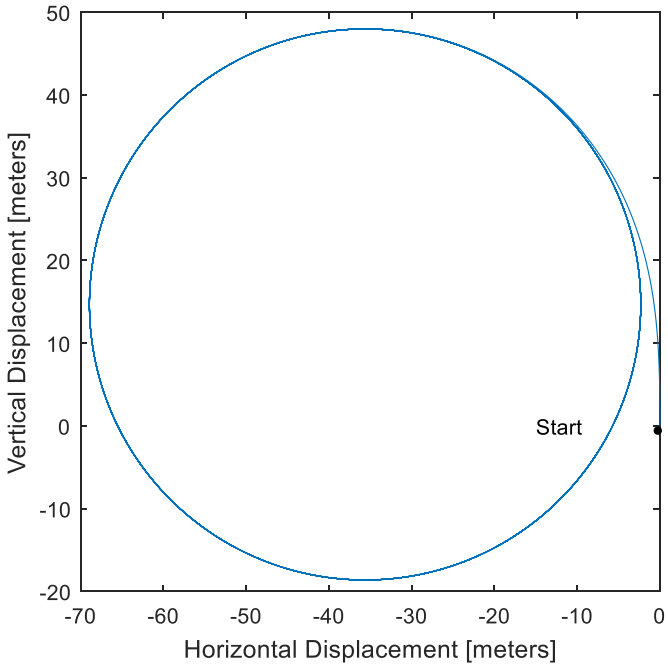

Figure B.9 High-Speed Oversteer X-Y Trajectory

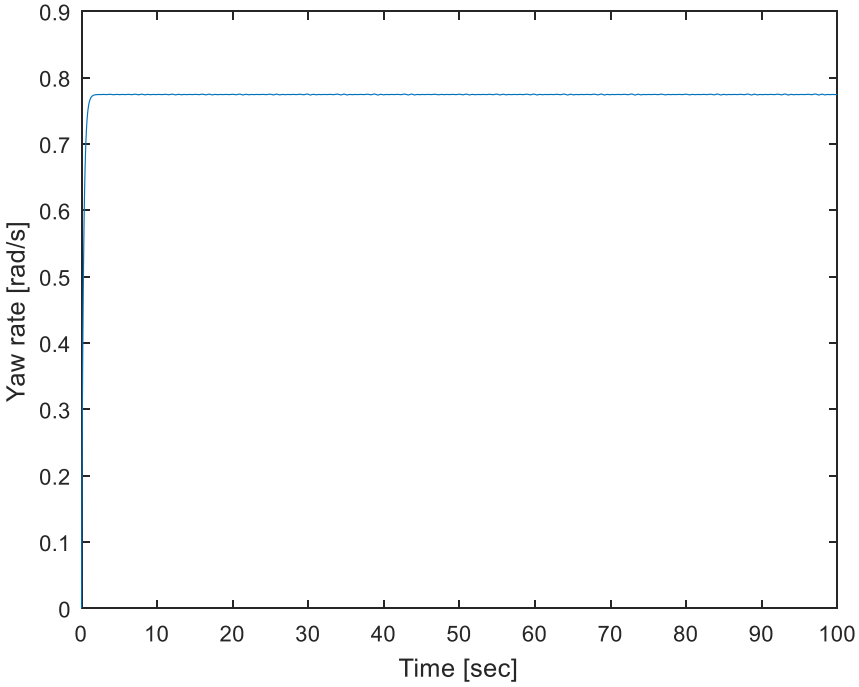

Figure B.10 High-Speed Oversteer Vehicle Yaw Rate

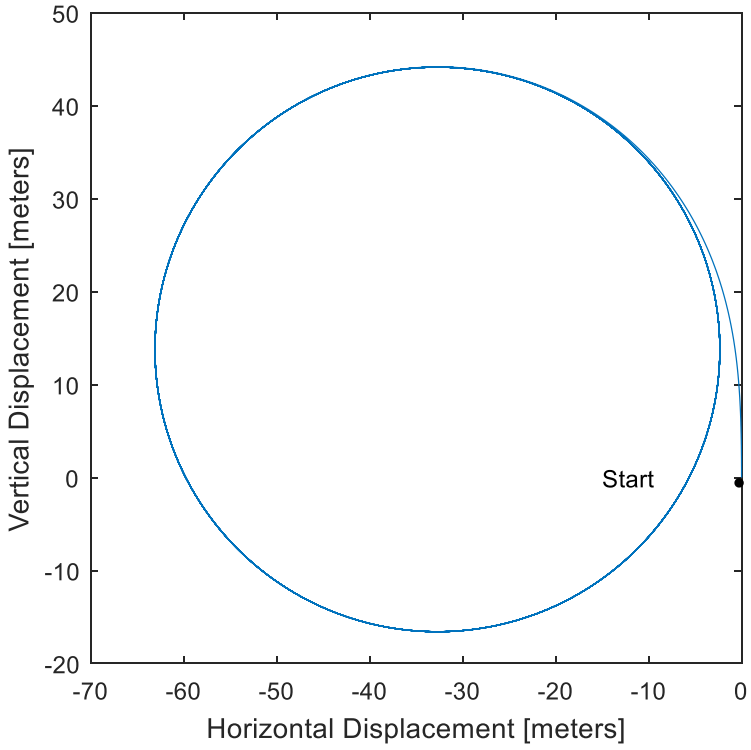

Figure B.11 High-Speed Neutral Steer Vehicle X-Y Trajectory

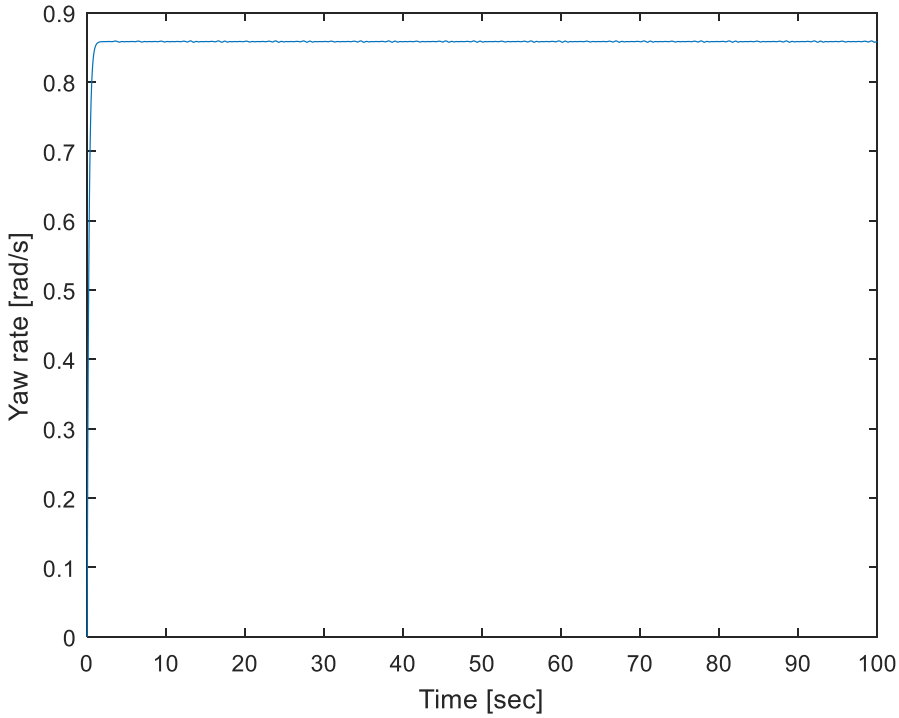

Figure B.12 High-Speed Neutral Steer Yaw Rate

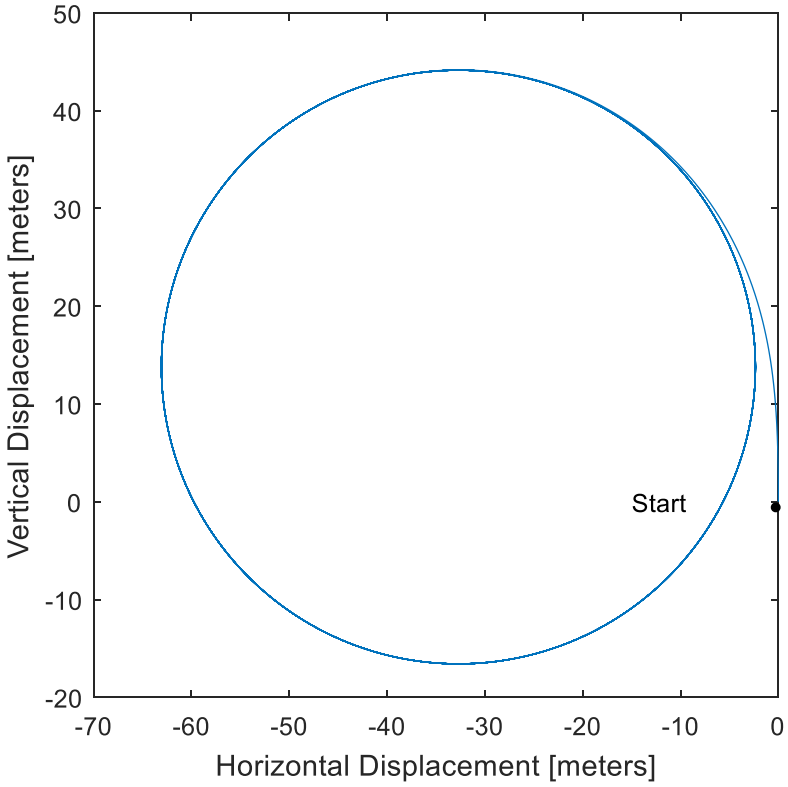

Figure B.13 High-Speed Understeer X-Y Trajectory

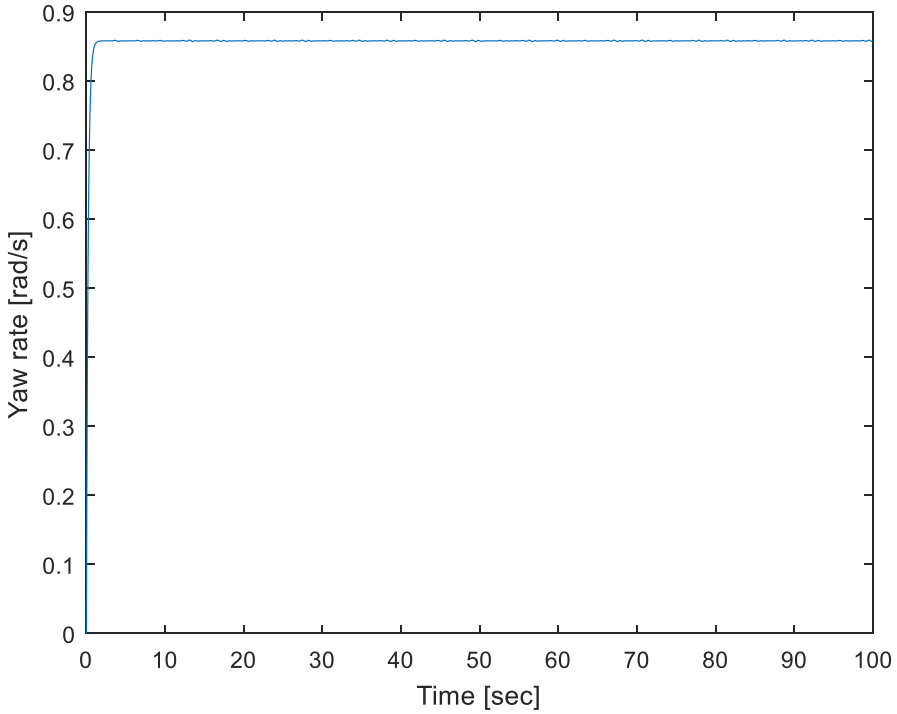

Figure B.14 High-Speed Understeer Yaw Rate

Note that the yaw rate for the high-speed case is greater than that of the high-speed case. This can be understood by considering the relationships between the steering angle, radius of the turn, and velocity as shown in Eqns. 2.5 and 2.57.

APPENDIX C

Appendix C gives an alternate four-wheel simulation with less torque. Consider a four-wheel car going around a corner with equal torque to the rear wheels of 100 Newton-meters (see Figs. C.1 to C.4).

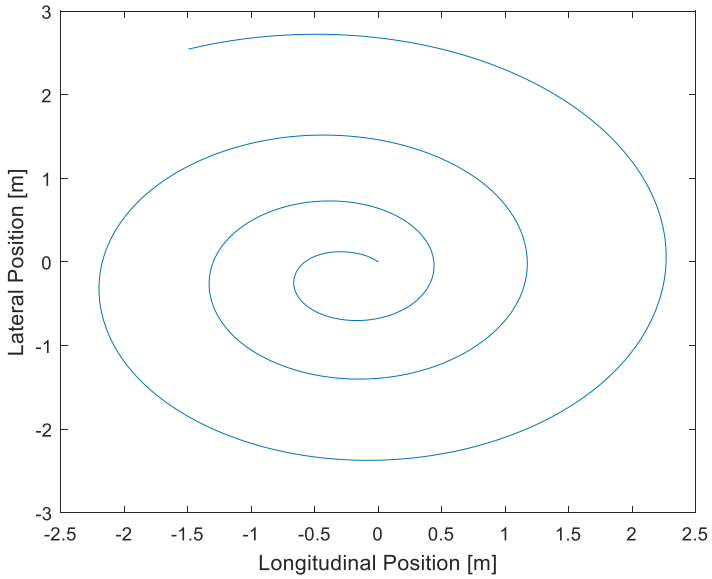

Figure C.1 Four-Wheel Model X-Y Trajectory for 100 Nm

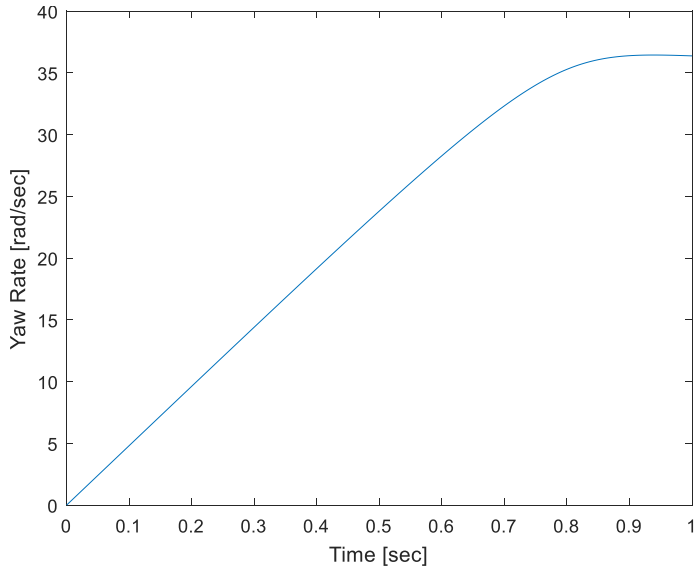

Figure C.2 Four-Wheel Model Yaw Rate for 100 Nm

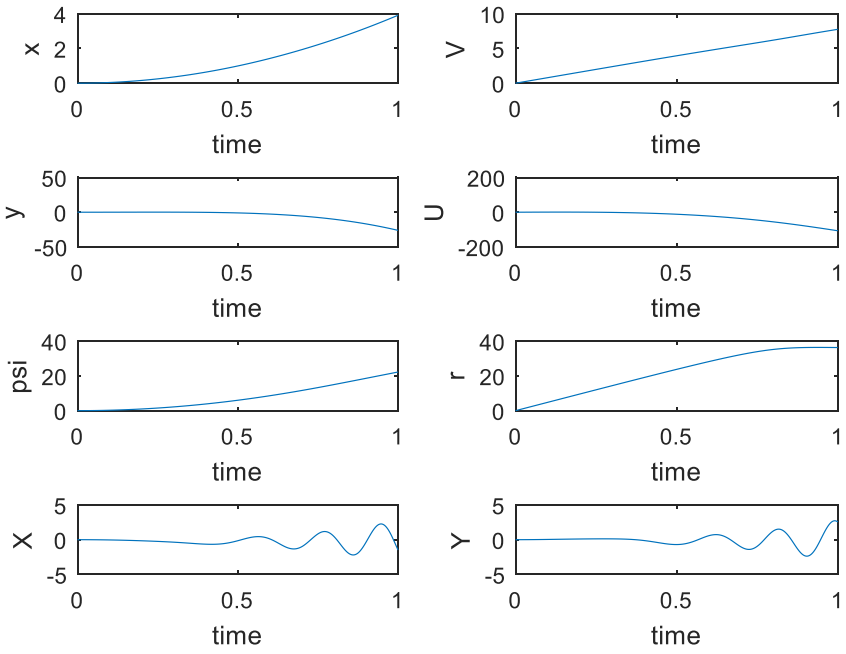

Figure C.3 Four-Wheel Model State Variables for 100 Nm

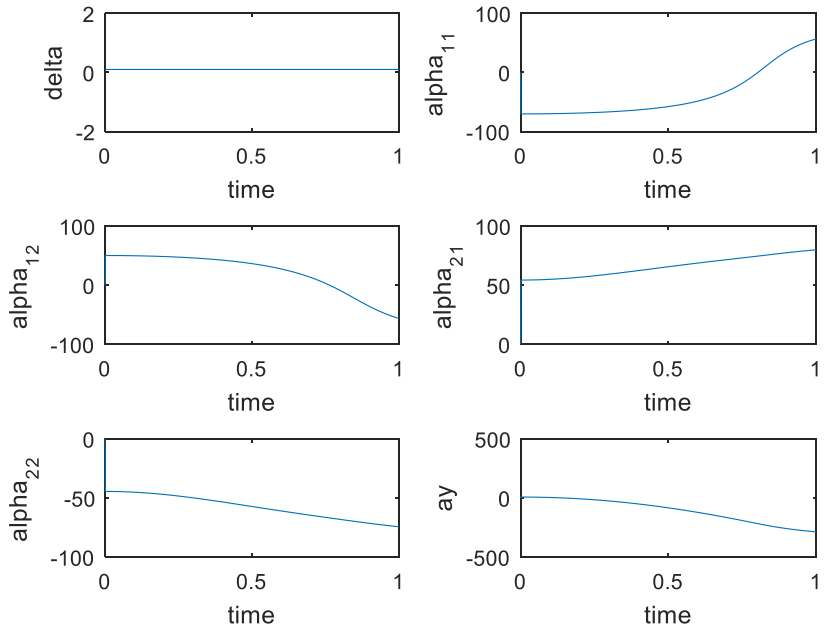

Figure C.4 Four-Wheel Model Angles for 100 Nm

It is interesting to note that the magnitude of the yaw rate and the radius of the trajectory of the vehicle are similar to the simulations in the four-wheel model section (refer to Figs. 3.11 to 3.14).

APPENDIX D

Appendix D provides the code for the two-wheel model written as a MATLAB script.

```
function two_wheel_model

%This code solves the lateral acceleration and yaw
%acceleration of a two-wheel vehicle.

%Divide time input into a vector
time = 100;
tstep = 0.01;
t = 0:tstep:time;

%Initial conditions for the model
theta0 = 0;
rdot0 = 0;
U0 = 0;
x0 = 0;
y0 = 0;

%Create vector of initial conditions
%y = zeros(5,1);
y_0(1) = theta0;
y_0(2) = rdot0;
```

```
y_0(3) = U0;

y_0(4) = x0;

y_0(5) = y0;


%Solving the ODEs

[~,y] = ode45(@(t,y)bikemodel(t,y),t,y_0);


X_dist = y(:,4);

Y_dist = y(:,5);


%Plotting

figure(1);

plot(X_dist,Y_dist);

axis square;

xlabel('Horizontal Displacement [meters]');

ylabel('Vertical Displacement [meters]');

%xlim([-70 5]);


str1 = '\bullet';

text(-1,0,str1);


str2 = 'Start';

text(-15,0,str2);
```

```
figure(2);
plot(t,y(:,2));
xlabel('Time  [sec]');
ylabel('Yaw  rate [rad/s]');
ylim([0  0.9]);

end

%-----------------------------------------------------------------

%create a function  for the ODE
%After  integrating  the following  vector dy, we get:
%y(1) = theta
%y(2) = r
%y(3) = U
%y(4) = x
%y(5) = y

function  dy = bikemodel(~,y)

degrees_to_radians  = pi / 180.0;
seconds_per_hour  = 60 * 60; % 60 sec/min  * 60 min/hr
```

```
meters_per_mile  = 1609.344;

meters_per_sec  = meters_per_mile  / seconds_per_hour;

g = 9.81;

L = 2.5;

a = 1.23;

b = L-a;

width = 1.6; %(m)

m = 1450; %mass of car, (kg)

I = (1/12)*m*( (L)^2 + width^2  ) + m*( a - b)^2; %Mass moment of inertia about z axis (kg*m^2)

mf = m * b / L; % mass on front axle

mr = m * a / L; % mass on rear axle

Cf = (0.19)*0.5*mf*g*(180/pi);  %Calculate front cornering coefficient;  see Wong pg.36 (N/rad)

Cr = (0.19)*0.5*mr*g*(180/pi);  %Rear cornering coefficient  (N/rad)


d = 5 * degrees_to_radians;  %convert from degrees to radians

V = 55 * meters_per_sec;  %convert from mph to m/s


%Define  yaw and lateral acceleration  equations

dy = zeros(size(y));

%define  theta.dot

dy(1) = y(2);

%define  rdot

dy(2) = (( -Cr*b^2 - Cf*a^2 )/(I*V))*y(2)  + (( -Cf*a + Cr*b)/(I*V))*y(3)  + ((Cf*a)/I)*d;
```

```
%define udot
dy(3) = (( Cr*b - Cf*a )/(m*V) - V)*y(2) + ((-Cr - Cf)/(m*V))*y(3) + (Cf/m)*d;
%Translate motion into inertial coordinates (this is why we need theta)
%define xdot
dy(4) = -V*sin(y(1)) - y(3)*cos(y(1));
%define ydot
dy(5) = -y(3)*sin(y(1)) + V*cos(y(1));


end
```

APPENDIX E

Appendix E gives the four-wheel model code as a MATLAB script.

```
function four_wheel_model


%Constants
m = 1724; % mass
Cd = 0.36; % coefficient of drag
A = 2.03; % car frontal area
g = 9.81; % acceleration due to gravity
sigma = 0.2; % grade
a = 1.51; % distance from center of mass to front axle
b = 1.26; % distance from center of mass to rear axle
c = 1.92; % track width;
w = 0.5*c; % half of the track width
H = 0.6; %height to center of gravity
L = a+b; % total length of the vehicle
mf = m * b / L; % mass on front axle
mr = m * a / L; % mass on rear axle
Cyr = 0.19*(mr)*g*(180/pi); % cornering stiffness rear tires (N/rad)
Cyf = 0.19*(mf)*g*(180/pi); % cornering stiffness front tires (N/rad)
rho = 1.225; % density of air
rtire = 0.29; % radius of tire (m)
mu = 0.8; % coefficient of friction
```

```
T21 = 500; % Torque to left rear tire (Nm)
T22 = 500; % Torque to right rear tire (Nm)

delta = 0.1; % Desired steering angle

q0 = [0;0;0;0;0;0;0;0;0]; % initial state
T = linspace(0,1,2000); % solution time mesh
[~,q] = ode45(@cartv, T, q0);

%x
figure(1)
subplot(4,2,1);
plot(T, q(:,1));
xlabel('time');
ylabel('x');

title('State Variables');

% xdot
subplot(4,2,2); plot(T, q(:,4)); xlabel('time'); ylabel('V');
% y
subplot(4,2,3); plot(T, q(:,2)); xlabel('time'); ylabel('y');
% ydot
```

```
subplot(4,2,4); plot(T, q(:,5)); xlabel('time'); ylabel('U');
% psi
subplot(4,2,5); plot(T, q(:,3)); xlabel('time'); ylabel('psi') ;
% psidot
subplot(4,2,6); plot(T, q(:,6)); xlabel('time'); ylabel('r');
% X
subplot(4,2,7); plot(T, q(:,7)); xlabel('time'); ylabel('X');
% Y
subplot(4,2,8); plot(T, q(:,8)); xlabel('time'); ylabel('Y');

figure(2);
plot(q(:,7),q(:,8));
title('X-Y Plot for Circular Path');
xlabel('Longitudinal Position [m]');
ylabel('Lateral Position [m]');

figure(3);
plot(T,q(:,6));
title('Yaw Rate vs. Time');
xlabel('Time [sec]');
ylabel('Yaw Rate [rad/sec]');

N = length(T);
```

```
steering  = zeros(N,1);
slip11  = zeros(N,1);
slip12  = zeros(N,1);
slip21  = zeros(N,1);
slip22  = zeros(N,1);
ay = zeros(N,1);
ax = zeros(N,1);

for i = 1:N
    % State variables
    %x = q(i,1);  % body fixed  x-axis
    %y = q(i,2);  % body fixed  y-axis
    %s = q(i,3);  % body yaw angle  (psi)
    xd = q(i,4);  % body fixed  x-axis  velocity
    yd = q(i,5);  % body fixed  y-axis  velocity
    sd = q(i,6);  % body yaw rate (psi_dot)
    %xx = q(i,7);  % global  x position  of car center of mass
    %yy = q(i,8);  % global  y position  of car center of mass

    % Drag force
    axd = abs(xd);
    fdrag = 0.5*rho*Cd*A*xd*axd;
```

```
% Tire  slip  angle
ad = xd - w*sd;
abs_ad = abs(ad);
alpha11  = 0;
if abs_ad > 0
   alpha11  = atan((yd  + a*sd)/ad)  - delta;
end

alpha21  = 0;
if abs_ad > 0
   alpha21  =atan((yd  - b*sd)/ad);
end

af = xd + w*sd;
abs_af = abs(af);
alpha12  = 0;
if abs_af > 0
   alpha12  = atan((yd  + a*sd)/af)  - delta;
end

alpha22  = 0;
if abs_af > 0
   alpha22  = atan((yd  - b*sd)/af);
```

```
end

% Tire  forces
fl1grade  = 0;
if axd > 0
   fl1grade  = -(mu*xd/axd)*(mu*H*m*g*cos(sigma)  + b*m*g*cos(sigma))/(2*L);
end
fl1x = -fl1grade;
fl1y = -Cyf*alpha11;

f21grade  = 0;
if axd > 0
   f21grade  = -(mu*xd/axd)*(a*m*g*cos(sigma)  - mu*H*m*g*cos(sigma))/(2*L);
end
f21x = -f21grade  + T21/rtire;
f21y = -Cyr*alpha21;

fl2grade  = 0;
if axd > 0
   fl2grade  = -(mu*xd/axd)*(mu*H*m*g*cos(sigma)  + b*m*g*cos(sigma))/(2*L);
end
fl2x = -fl2grade;
fl2y = -Cyf*alpha12;
```

```
    f22grade = 0;
    if axd > 0
        f22grade = -(mu*xd/axd)*(a*m*g*cos(sigma) - mu*H*m*g*cos(sigma))/(2*L);
    end
    f22x = -f22grade + T22/rtire;
    f22y = -Cyr*alpha22;

    steering(i) = delta;
    slip11(i) = alpha11*180/pi;
    slip12(i) = alpha12*180/pi;
    slip21(i) = alpha21*180/pi;
    slip22(i) = alpha22*180/pi;
    ay(i) = (-xd*sd + ( fl1x*sin(delta) +fl2x*sin(delta) + fl1y*cos(delta) + f21y + fl2y*cos(delta)
+ f22y )/m);
    ax(i) = (f21x + f22x + fl1x*cos(delta) + fl2x*cos(delta) - sin(delta)*(fl1y + fl2y)- fdrag +
sd*yd)/m;
end

figure(4);

title('Derived Parameters from State Variables');
```

```
subplot(3,2,1); plot(T, steering); xlabel('time'); ylabel('delta');
subplot(3,2,2); plot(T, slip11); xlabel('time'); ylabel('alpha_1_1');
subplot(3,2,3); plot(T, slip12); xlabel('time'); ylabel('alpha_1_2');
subplot(3,2,4); plot(T, slip21); xlabel('time'); ylabel('alpha_2_1');
subplot(3,2,5); plot(T, slip22); xlabel('time'); ylabel('alpha_2_2');
subplot(3,2,6); plot(T, ay); xlabel('time'); ylabel('ay');



end

%-----------------------------------------------------------------------
% assumes: linear cornering force proportional to tire slip angle
function qdot = cartv(~,q)

% State variables
%x = q(1,:); % body fixed x-axis
%y = q(2,:); % body fixed y-axis
s = q(3,:); % body yaw angle (psi)
xd = q(4,:); % body fixed x-axis velocity
yd = q(5,:); % body fixed y-axis velocity
sd = q(6,:); % body yaw rate (psi_dot)
%xx = q(7,:); % global x position of car center of mass
%yy = q(8,:); % global y position of car center of mass
```

```
%Pass the constant values back through here
%Constants
m = 1724; % mass
Cd = 0.36; % coefficient of drag
A = 2.03; % car frontal area
g = 9.81; % acceleration due to gravity
sigma = 0.2; % grade
a = 1.51; % distance from center of mass to front axle
b = 1.26; % distance from center of mass to rear axle
c = 1.92; % track width;
w = 0.5*c; % half of the track width
H = 0.6; %height to center of gravity
L = a+b; % total length of the vehicle
mf = m * b / L; % mass on front axle
mr = m * a / L; % mass on rear axle
Cyr = 0.19*(mr)*g*(180/pi); % cornering stiffness rear tires (N/rad)
Cyf = 0.19*(mf)*g*(180/pi); % cornering stiffness front tires (N/rad)
rho = 1.225; % density of air
rtire = 0.29; % radius of tire (m)
mu = 0.8; % coefficient of friction
T21 = 500; % Torque to left rear tire (Nm)
T22 = 500; % Torque to right rear tire (Nm)
```

```
Izz = (1/12)*m*(L^2 + c^2) + m*(a-b)^2; %Moment of intertia

delta = 0.1; % Desired steering angle

% Tire slip angle
ad = xd - w*sd;
abs_ad = abs(ad);
alpha11 = 0;
if abs_ad > 0
   alpha11 = atan((yd + a*sd)/ad) - delta;
end

alpha21 = 0;
if abs_ad > 0
   alpha21 = atan((yd - b*sd)/ad);
end

af = xd + w*sd;
abs_af = abs(af);
alpha12 = 0;
if abs_af > 0
   alpha12 = atan((yd + a*sd)/af) - delta;
```

```
end


alpha22 = 0;
if abs_af > 0
   alpha22 = atan((yd - b*sd)/af);
end


axd = abs(xd);


% Tire forces
fl1grade = 0;
if axd > 0
   fl1grade = -(mu*xd/axd)*(mu*H*m*g*cos(sigma) + b*m*g*cos(sigma))/(2*L);
end
fl1x = -fl1grade;
fl1y = -Cyf*alpha11;


f21grade = 0;
if axd > 0
   f21grade = -(mu*xd/axd)*(a*m*g*cos(sigma) - mu*H*m*g*cos(sigma))/(2*L);
end
f21x = -f21grade + T21/rtire;
f21y = -Cyr*alpha21;
```

```
f12grade = 0;
if axd > 0
   f12grade = -(mu*xd/axd)*(mu*H*m*g*cos(sigma) + b*m*g*cos(sigma))/(2*L);
end
f12x = -f12grade;
f12y = -Cyf*alpha12;

f22grade = 0;
if axd > 0
   f22grade = -(mu*xd/axd)*(a*m*g*cos(sigma) - mu*H*m*g*cos(sigma))/(2*L);
end
f22x = -f22grade + T22/rtire;
f22y = -Cyr*alpha22;

% Forces at center of mass
fdrag = 0.5*rho*Cd*A*xd*axd;   % Longitudinal drag force

qdot(1,:) = xd;
qdot(2,:) = yd;
qdot(3,:) = sd;
qdot(4,:) = (f21x + f22x + f11x*cos(delta) + f12x*cos(delta) - sin(delta)*(f11y + f12y)- fdrag +
sd*yd)/m; % Sum of Forces in x-direction/m
```

```
qdot(5,:) = (-xd*sd + ( fl1x*sin(delta) +fl2x*sin(delta) + fl1y*cos(delta) + f21y +
fl2y*cos(delta) + f22y )/m); %Sum of Forces in y-direction/m
qdot(6,:) = (-fl1x*cos(delta)*w + fl1y*a*cos(delta) + fl1x*a*sin(delta) + fl1y*w*sin(delta) +
fl2x*cos(delta)*w + fl2y*a*cos(delta) + fl2x*a*sin(delta) - fl2y*w*sin(delta) - f21x*w - f21y*b
- f22y*b + f22x*w)/Izz; %Sum of Moments/I
qdot(7,:) = -yd*cos(s) - xd*sin(s); % global x position of car center of mass
qdot(8,:) = -yd*sin(s) + xd*cos(s); % global y position of car center of mass

end
```

APPENDIX F

Appendix F gives the four-wheel lane change code as a MATLAB script.

```
function four_wheel_lane_change


m = 1724; % mass

I = 1.74*10^(3); % moment of inertia

Cd = 0.36; % coefficient of drag

A = 2.03; % car frontal area

Cr = 0.08; % rolling resistance coefficient rear tires

Cf = Cr; % rolling resistance coefficient front tires

g = 9.81; % acceleration due to gravity

theta = 0; % grade

Cyr = 1.00*10^(5);% cornering stiffness rear tires

Cyf = 8.37*10^(4);% cornering stiffness front tires

Cr = 0.008; % rolling resistance coefficient rear tires

Cf = Cr; % rolling resistance coefficient front tires

a = 1.51; % distance from center of mass to front axle

b = 1.26; % distance from center of mass to rear axle

c = 1.92; % track width;

L = a+b;

mf = m * b / L; % mass on front axle

mr = m * a / L; % mass on rear axle

rho = 1.225; % density of air
```

```
rtire = 0.29;   % radius of tire
Kmotor = 500;
KIdelta = 0;
xddesired = 26.8224; % => 60 mph
   %car_data.xddesired = 26.8224 * 0.5; % => 30 mph
   %car_data.xddesired = 26.8224 / 6.0; % => 10 mph
Kdelta = 10 * xddesired / 26;

q0 = [0;0;0;0;0;0;0;0;0;0];  % initial state

T = linspace(0,600,6001)';  % solution time mesh

TCRIT = [100,200,300,400,500]; % critical time points

%Q = ode45('car_tv', q0, T, TCRIT);
[~,q] = ode45(@cartv, T, q0, TCRIT);

figure(1)

%x
subplot(4,2,1); plot(T, q(:,1)); xlabel('time'); ylabel('x');

%title('State Variables');
```

```
% xdot
subplot(4,2,2); plot(T, q(:,4)); xlabel('time'); ylabel('V');
% y
subplot(4,2,3); plot(T, q(:,2)); xlabel('time'); ylabel('y');
% ydot
subplot(4,2,4); plot(T, q(:,5)); xlabel('time'); ylabel('U');
% psi
subplot(4,2,5); plot(T, q(:,3)); xlabel('time'); ylabel('psi') ;
% psidot
subplot(4,2,6); plot(T, q(:,6)); xlabel('time'); ylabel('r');
% X
subplot(4,2,7); plot(T, q(:,7)); xlabel('time'); ylabel('X');
% Y
subplot(4,2,8); plot(T, q(:,8)); xlabel('time'); ylabel('Y');

figure(2);
plot(q(:,7),q(:,8));
title('X-Y Plot for Lane Change');
xlabel('Longitudinal Position [m]');
ylabel('Lateral Position [m]');

figure(3);
```

```
yaw_accel = diff(q(:,6))/(0.1);
plot(T(1:length(yaw_accel),:),yaw_accel);
title('Yaw Acceleration');
xlabel('Time [sec]');
ylabel('Yaw Acceleration [rad/s^2]');



    % Model parameters
    w = 0.5*c;
    m1 = 0.5*mf;% mass on tire 1
    m3 = m1;    % mass on tire 3
    m2 = 0.5*mr;% mass on tire 2
    m4 = m2;    % mass on tire 4



N = length(T);
torque1 = zeros(N,1);
torque2 = zeros(N,1);
steering = zeros(N,1);
slip1 = zeros(N,1);
slip2 = zeros(N,1);
slip3 = zeros(N,1);
slip4 = zeros(N,1);
```

```
ay    = zeros(N,1);
yaw_accel  = zeros(N,1);


for i = 1:N
    t = T(i);
    % State variables
    x = q(i,1);  % body fixed  x-axis
    y = q(i,2);  % body fixed  y-axis
    s = q(i,3);  % body yaw angle  (psi)
    xd = q(i,4);  % body fixed  x-axis  velocity
    yd = q(i,5);  % body fixed  y-axis  velocity
    sd = q(i,6);  % body yaw rate (psi_dot)
    xx = q(i,7);  % global  x position  of car center  of mass
    yy = q(i,8);  % global  y position  of car center  of mass
    yyerr  = q(i,9); % YY-yy


    axd = abs(xd);


    % Drag force
    fdrag = 0.5*rho*Cd*A*xd*axd;


    % Grade force
    fgrade  = m*g*sin(theta);
```

```
% Motor force based on desired longitudinal velocity
Kxd = Kmotor; % proportional feedback gain
fmotor = Kxd * (xddesired - xd);

% Desired steering angle
delta = 0.0;
Kdelta = Kdelta;
KIdelta = KIdelta;
YY = 0;
if (t >= 100) && (t < 200)
   YY = 1;
   delta = Kdelta*(YY-yy) + KIdelta*yyerr;

end
if (t >= 200) && (t < 300)
   YY = -1;
   delta = Kdelta*(YY-yy)+ KIdelta*yyerr;

end
if (t >= 300)
   YY = 0;
   delta = Kdelta*(YY-yy) + KIdelta*yyerr;
```

```
end
if abs(delta) > 1
   delta = sign(delta);
end

cdelta = cos(delta);
sdelta = sin(delta);

% Tire slip angles

alpha1 = 0;
ad = abs(xd - w*sd);
if ad > 0
   alpha1 = atan((yd + a*sd)/ad) - delta; %alpha11
end

alpha2 = 0;
if ad > 0
   alpha2 = atan((yd - b*sd)/ad);%alpha21
end

alpha3 = 0;
```

```
ad = abs(xd + w*sd);
if ad > 0
   alpha3  = atan((yd  + a*sd)/ad)  - delta;%alpha12
end

alpha4  = 0;
if ad > 0
   alpha4  = atan((yd  - b*sd)/ad);%alpha22
end

% Tire  forces

f1roll  = 0;
if axd > 0
   f1roll  = Cf*0.8*m1*g*cos(theta)*xd/axd;
end
f1x = -f1roll;%f11x
f1y = -Cyf*alpha1;%f11y

f2roll  = 0;
if axd > 0
   f2roll  = Cr*0.8*m2*g*cos(theta)*xd/axd;
end
```

```
f2x = -f2roll + fmotor*0.5;%f21x

f2y = -Cyr*alpha2;%f21y


f3roll = 0;

if axd > 0

   f3roll = Cf*0.8*m3*g*cos(theta)*xd/axd;

end

f3x = -f3roll;  %f12x

f3y = -Cyf*alpha3;%f12x


f4roll = 0;

if axd > 0

   f4roll = Cr*0.8*m4*g*cos(theta)*xd/axd;

end

f4x = -f4roll + fmotor*0.5;%f22x

f4y = -Cyr*alpha4;%f22y


% Forces at center of mass


%f0x = -fdrag - fgrade;

%f0y = 0;


torque1(i) = 0.5*fmotor*rtire;
```

```
    torque2(i)  = 0.5*fmotor*rtire;
    steering(i)  = delta;
    slip1(i)  = alpha1*180/pi;
    slip2(i)  = alpha2*180/pi;
    slip3(i)  = alpha3*180/pi;
    slip4(i)  = alpha4*180/pi;
    ay(i)  = (-xd*sd + (f1x*sdelta  + f1y*cdelta  + f3x*sdelta  + f3y*cdelta  + f2y + f4y  )/m);

    %ct = 600/(6001-1); %based on T = linspace(0,600,6001)';  % solution  time  mesh
    %yaw_accel(i+1)  = ( sd(i+1)  - sd(i)  )/ct;

end

figure(4);

subplot(4,2,1);  plot(T,  torque1);  xlabel('time');  ylabel('T_2_1');

%title('Derived  Parameters  from  State Variables');

subplot(4,2,2);  plot(T,  torque2);  xlabel('time');  ylabel('T_2_2');
subplot(4,2,3);  plot(T,  steering);  xlabel('time');  ylabel('delta');
subplot(4,2,4);  plot(T,  slip1);  xlabel('time');  ylabel('alpha_1_1');
subplot(4,2,5);  plot(T,  slip2);  xlabel('time');  ylabel('alpha_2_1');
```

```
subplot(4,2,6); plot(T, slip3); xlabel('time'); ylabel('alpha_1_2');
subplot(4,2,7); plot(T, slip4); xlabel('time'); ylabel('alpha_2_2');
subplot(4,2,8); plot(T, ay); xlabel('time'); ylabel('ay');



end



%-----------------------------------------------------------------------

% assumes: linear cornering force proportional to tire slip angle
% proportional longitudinal speed control
% proportional steering control
function qdot = cartv(t,q)
   %global car_data

   %qdot = [0; 0; 0; 0; 0; 0; 0; 0; 0];

   % State variables
   x = q(1,:); % body fixed x-axis
   y = q(2,:); % body fixed y-axis
   s = q(3,:); % body yaw angle (psi)
```

```
xd = q(4,:); % body fixed x-axis velocity

yd = q(5,:); % body fixed y-axis velocity

sd = q(6,:); % body yaw rate (psi_dot)

xx = q(7,:); % global x position of car center of mass

yy = q(8,:); % global y position of car center of mass

yyerr = q(9,:); % err between the desired Y and the global y = YY-yy


%Pass the constant values back through here

m = 1724; % mass

I = 1.74*10^(3); % moment of inertia

Cd = 0.36; % coefficient of drag

A = 2.03; % car frontal area

Cr = 0.08; % rolling resistance coefficient rear tires

Cf = Cr; % rolling resistance coefficient front tires

g = 9.81; % acceleration due to gravity

theta = 0; % grade

Cyr = 1.00*10^(5);% cornering stiffness rear tires

Cyf = 8.37*10^(4);% cornering stiffness front tires

a = 1.51; % distance from center of mass to front axle

b = 1.26; % distance from center of mass to rear axle

c = 1.92; % track width;

L = a+b;

mf = m * b / L; % mass on front axle
```

```
mr = m * a / L; % mass on rear axle

rho = 1.225;    % density of air

rtire = 0.29;   % radius of tire

Kmotor = 500;

KIdelta = 0;

xddesired = 26.8224; % => 60 mph

%car_data.xddesired = 26.8224 * 0.5; % => 30 mph

%car_data.xddesired = 26.8224 / 6.0; % => 10 mph

Kdelta = 10 * xddesired / 26;



% Model parameters

w = 0.5*c;

m1 = 0.5*mf;% mass on tire 1

m3 = m1;    % mass on tire 3

m2 = 0.5*mr;% mass on tire 2

m4 = m2;    % mass on tire 4


% Motor force based on desired longitudinal velocity

Kxd = Kmotor; % proportional feedback gain

fmotor = Kxd * (xddesired - xd);

% motors have equal torque control

f2motor = 0.5*fmotor;
```

```
f4motor  = 0.5*fmotor;


% Desired  steering  angle
delta = 0;
Kdelta = Kdelta;
KIdelta = KIdelta;
YY = 0;
if (t >= 100) && (t < 200)
   YY = 1;
   delta = Kdelta*(YY-yy)  + KIdelta*yyerr;

end
if (t >= 200) && (t < 300)
   YY = -1;
   delta = Kdelta*(YY-yy)+  KIdelta*yyerr;

end
if (t >= 300)
   YY = 0;
   delta = Kdelta*(YY-yy)  + KIdelta*yyerr;

end
if abs(delta) > 1
```

```
    delta = sign(delta);
end

cdelta = cos(delta);
sdelta = sin(delta);

axd = abs(xd);
stheta = sin(theta);
ctheta = cos(theta);

% Tire slip angles

dd = xd - w*sd;
ad = abs(dd);

alpha1 = 0;
if ad > 0
    alpha1 = atan((yd + a*sd)/dd) - delta;
end

alpha2 = 0;
if ad > 0
    alpha2 = atan((yd - b*sd)/dd);
```

```
end

dd = xd + w*sd;
ad = abs(dd);

alpha3  = 0;
if ad > 0
   alpha3  = atan((yd  + a*sd)/dd)  - delta;
end

alpha4  = 0;
if ad > 0
   alpha4  = atan((yd  - b*sd)/dd);
end

% Tire  forces

f1roll  = 0;
if axd > 0
   f1roll  = Cf*0.8*m1*g*ctheta*xd/axd;
end
f1x = -f1roll;
f1y = -Cyf*alpha1;
```

```
f2roll  = 0;
if axd > 0
   f2roll  = Cf*0.8*m2*g*ctheta*xd/axd;
end
f2x = -f2roll  + f2motor;
f2y = -Cyr*alpha2;

f3roll  = 0;
if axd > 0
   f3roll  = Cr*0.8*m3*g*ctheta*xd/axd;
end
f3x = -f3roll;
f3y = -Cyf*alpha3;

f4roll  = 0;
if axd > 0
   f4roll  = Cr*0.8*m4*g*ctheta*xd/axd;
end
f4x = -f4roll  + f4motor;
f4y = -Cyr*alpha4;

% Forces at center of mass
```

```
    fdrag  = 0.5*rho*Cd*A*xd*axd;    % Longitudinal drag force
    fgrade = m*g*stheta;             % Longitudinal grade force

    f0x = -fdrag - fgrade;
    f0y = 0;

    qdot(1,:) = xd;
    qdot(2,:) = yd;
    qdot(3,:) = sd;
    qdot(4,:) = (f2x + f4x + f1x*cos(delta) + f3x*cos(delta) - sin(delta)*(f1y + f3y)- fdrag +
sd*yd)/m; % Sum of Forces in x-direction/m
    qdot(5,:) = (-xd*sd + (f1x*sdelta + f1y*cdelta + f3x*sdelta + f3y*cdelta + f2y + f4y )/m);
    qdot(6,:) = (-f1x*cos(delta)*w + f1y*a*cos(delta) + f1x*a*sin(delta) + f1y*w*sin(delta) +
f3x*cos(delta)*w + f3y*a*cos(delta) + f3x*a*sin(delta) - f3y*w*sin(delta) - f2x*w - f2y*b -
f4y*b + f4x*w)/I; %Sum of Moments/I
    ss = sin(s);
    cs = cos(s);
    qdot(7,:) = xd*cs - yd*ss;
    qdot(8,:) = xd*ss + yd*cs;
    qdot(9,:) = YY - yy;
end
```